SEDIMENTARY STRUCTURES, TEXTURE, AND PALEOENVIRONMENT OF THE HINUERA FORMATION

Thesis submitted as a partial requirement
for the degree of Bachelor of Philosophy
in Earth Sciences

Alan M. Sherwood,
University of Waikato
February, 1972.

CONTENTS

ABSTRACT

The Hinuera Formation is an extensive Upper Pleistocene terrestrial deposit of alluvial origin, underlying the plains of the Hamilton Basin and the Hauraki Lowland. The textures and sedimentary structures of ten stratigraphic sections are studied in detail, and indicate uniformity of the Hinuera Formation on a regional scale. Four dominant lithotypes occur: rhyolitic and pumiceous gravelly sands, quartz sands, pumice silt, and rhyolitic sandy gravels. A variety of primary and post-depositional structures is present, and four types of cross-stratification (Rho, Nu, Epsilon and Sigma) and three types of horizontal stratification are described. Textures indicate rapid deposition in an environment of fluctuating high turbulent energy. Relative energies of the different sedimentary structures are suggested from the relations of structures to texture. Sedimentary structures are also related to flow regime. Six facies are erected for the Hinuera Formation on the basis of lithology, texture, sedimentary structures, and flow regime, which indicate deposition by a braided river system. Deposition was contemporaneous with intense volcanic activity in the Central Volcanic Region, which combined with the cold, wet climate of a glacial period, led to the supply of large amounts of sediment to the river systems of the region, and aggradational fans were constructed in the Hauraki Lowland and the Hamilton Basin. The six facies are incorporated into a suggested physiographic model of the Hinuera Formation.

CHAPTER ONE

I N T R O D U C T I O N

1.1 THE HINUERA FORMATION

The Hinuera Formation is a terrestrial deposit of alluvial origin and underlies the extensive plains of the Hamilton Basin and the southern half of the Hauraki Lowland. Less extensive deposits are mapped along the present course of the Waikato River between Karapiro and Whakamarumaru, and in the vicinity of Reporoa (Fig. 1.1). The formation is approximately 1950 square kilometres in areal extent (estimated area from four mile geological maps) and is up to 90 metres thick (Kear and Schofield, 1964).

Numerous well exposed quarry and road-cut sections show rapid lateral and vertical changes in texture, lithology, and sedimentary structures within the formation. Cross stratification is almost always present, although variable in scale and other characteristics. Lithologies range from pure pumice gravelly sands, sands, and silts, through rhyolitic and pumiceous gravelly quartz sands to clean quartz sands containing abundant feldspar and ferromagnesian minerals, with interbedded peats.

1.2 GEOLOGICAL HISTORY

The stratigraphic terminology, lithologic character, and ages of the rocks in the Hamilton Basin are summarised in Table 1.1 (after Kear and Schofield, 1964); formational nomenclature is presented for the post-Miocene rocks only.

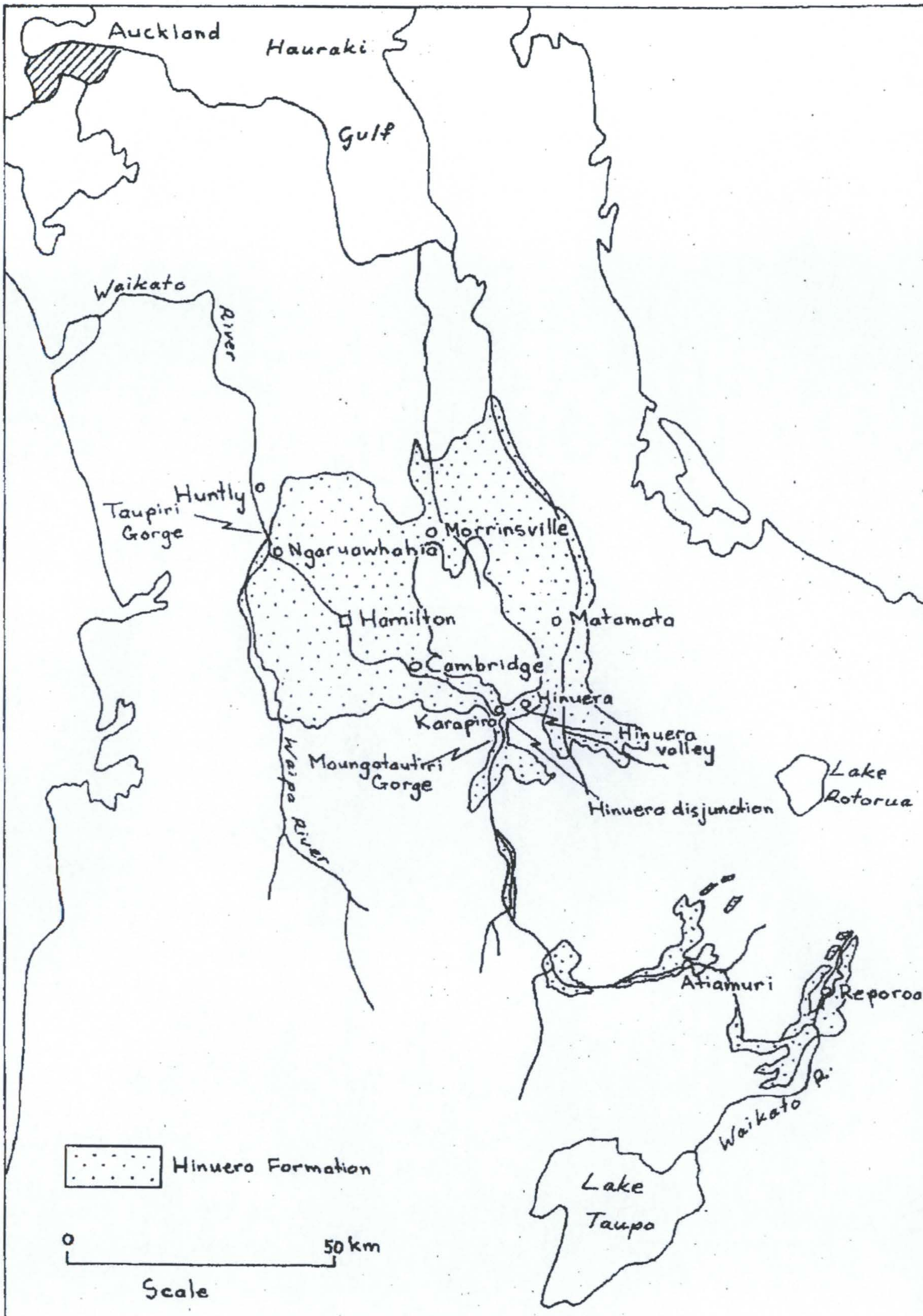

Fig. 1.1 Locality map showing areal distribution of the Hinuera Formation.

Table 1.1 Summary of the Stratigraphic Sequence in the Hamilton Basin (after Kear and Schofield, 1964).

GROUP	SUBGROUP	FORMATION	LITHOLOGY	AGE	VOLCANIC FORMATIONS	
TAURANGA GROUP (300 metres)	PIAKO	Taupo Pumice Alluvium	Pumice sand and silt and current bedded rhyolitic coarse sand.	A.D. 130		HOLOCENE
		Hauraki Clay	Estuarine clay	Holocene		
		Hinuera Formation	Current bedded pumiceous and rhyolitic gravelly sands interbedded with pumice silts and peat.	Last Glaciation		PLEISTOCENE
	WALTON	Karapiro Formation	Highly weathered rhyolitic sands (c.f. Hinuera Formation)	Wc-Hawera	Franklin Basalts	
		Waeranga Gravels	Locally derived, weathered gravels, mainly greywacke pebbles.	Wc-Hawera		
		Puketoka Formation	Pumice sands, silts, clays and peats.	Wn-Wc	Interbedded with Pakaumanu Ignimbrite	
	FRANKTON	Whangamarino Formation	Clays, lignites and gravels; some pure pumice silts and sands	Wo-Wn		PLIOCENE
		Koromatua Blacksand	Non-marine blacksand, minor clays	Ww	Alexandra Volcanics	
		Aberfoyle Siltstone	Moderately consolidated non-marine siltstones, minor sandstones	Ww		
		Kaawa Formation	Moderately consolidated shallow marine sandstones	Wo-Ww		
REGIONAL UNCONFORMITY (Kaikoura Orogeny)					Kiwitahi Volcanics	
WAITEMATA GROUP (600 metres)			Moderately hard, marine calcareous and non calcareous silstones and sandstones	Po		L. MIO.
UNCONFORMITY						
TE KUITI GROUP (400 metres)			Limestones and calcareous siltstones overlying non-calcareous marine siltstones and sandstones with basal non-calcareous estuarine mudstones and coal seams	Ab-Lw		M.EO.-OLIG.
REGIONAL UNCONFORMITY (Post-Hokonui Orogeny)						
MAHAIA HILL, KIRIKIRI, KENGARENGA, and NEWCASTLE GROUPS (12000 metres +)			Indurated sandstones and siltstones ("greywackes and argillites")			MESOZOIC

The Upper Tertiary Kaikoura Orogeny was characterised by widespread block-faulting of the pre-Tauranga Group rocks, forming basins of Upper Cainozoic sedimentation between the bounding ranges. The climax of the orogeny is marked by a regional unconformity between the Waitemata and Tauranga Groups.

The general similarity of lithologies and paucity of auterops in the Tauranga Group make it difficult to unravel a complex history of Tuaternary sedimentation influenced by climatic changes, fluctuating volcanic activity and oscillating base levels. All Upper Cainozoic deposits are included in the Tauranga Group, which is dominated by terrestrial sedimentation derived from rhyolitic provenances, mainly the Rotorua-Taupo region. The Tauranga Group is divided into three subgroups (Table 1.1). The Franklin Subgroup is of Opoition to Nukumaruan age and is non-marine except for the basal sandstones of the Kaawa Formation. The dominant members of the overlying Walton Subgroup are the Puketoka Formation and the Karapiro Formation. The basal Puketoka Formation, of Nukumaruan to Castlecliffian age, consists of pumice gravels and soft, unconsolidated ignimbritic material (McCraw, 1967) and is interfingered with the Pakaumanu Ignimbrite, possibly the earliest of the ignimbrites erupted from the Central Volcanic Region. The Puketoka Formation may be largely the result of sheet wash from the Pakaumanu Ignimbrite and is possibly partly colluvial and partly alluvial in origin. The Karapiro Formation, of Castlecliffian to Hawera age, is of alluvial origin, consisting of clays, sands, and gravels which include fragments of volcanic rocks and greywacke (Kear and Schofield, in press), and, apart from red weathering, is very similar to the Hinuera Formation. Interfingered with the Karapiro Formation are weathered greywacke gravels, the Waeranga Gravels (Kear and Schofield, 1964), locally derived from the nearby ranges.

Overlying the erosional topography of the sediments of the Walton Subgroup is a mantle of volcanic ash. Three groups of ash can be recognised (McCraw, 1967): Kauroa ash, the eroded remnants of a deeply red weathered ash, Hamilton ash, and Wairoa ash.

The Hinuera Formation is the basal and volumetrically most important members of the Piako Subgroup. Deposition of the Hinuera Formation began during the Last Glaciation, about 20,000 years B.P., and probably continued until about 10-12,000 years B.P., during which time extensive aggradation partly buried the underlying ash mantled topography of the lowlands. The ancestral Waikato River initially flowed through the Hinuera Valley towards Matamata and the Hauraki Gulf. This course was abandoned, resulting in the present unusual configuration of the Waikato River at the head of the Hinuera Valley, known as the "Hinuera disjunction" (Schofield, 1965). The river then flowed through the Maungatautiri Gorge and Karapiro to the Hamilton Basin where an aggradational fan began to build up. The subsequent history of the river was one of continuing deposition and shifting river courses, the most recent of which can be identified from surface morphology. The present micro-topography of the Hamilton Basin is largely the result of this migratory alluvial activity (McCraw, 1967). The latest phase in the evolution of the

Waikato River and its floodplain is entrenchment into its own deposits. This was interrupted by deposition of the Taupo Pumice alluvium from the Taupo eruption of 130 A.D. The present river probably carries less sediment load and is more sluggish than at any time in its history.

1.3 PREVIOUS WORK

Hochstetter (1867) noted the unusual morphology of the Waikato River near Maungatautiri, and Cussen (1889, 1894) discussed the changes in the courses of the Waikato River, particularly with reference to the old course of the Hinuera Valley, and noted that the plains of the Hamilton Basin consisted of pumiceous and rhyolitic sands deposited by the Waikato River. Henderson (1913) also discussed the abandonment of the Hinuera Valley and observed that the Waikato Basin was a plain formed by the "smothering of an old land-surface with loose pumice sands of fluviatile origin". Henderson and Grange (1926) elaborated only slightly on this, noting that "the Older Pleistocene land surface" is covered by a fan built up of loosely consolidated pumiceous gravels, sands and silts of fluviatile origin.

Healy (1946) proposed the name Hinuera Formation for the coarse sands and gravels that built up the aggradational fan of the Waikato River, noting their current bedded nature, and that they showed a "fair degree of sorting". The history of shifting river courses was further elaborated on and a maximum thickness of 75 metres was recorded from Healy's borehole data. Thompson (1958) recorded the lithology of the Hinuera Formation in the vicinity of the Atiamuri Dam site and correlated this with the Hinuera Formation at Karapiro, described by Healy (1946). The Hinuera Formation has since been mapped as current bedded fluviatile pumice, rhyolite and ignimbrite sands and gravels (Grindly, 1960; Kear, 1960; Healy, Schofield and Thompson, 1964; Schofield, 1967).

Schofield (1965) described the lithology and texture of the Hinuera Formation in slightly more detail, and elaborated extensively on the surface form and the effect of climatic, volcanic, and base level controls on the deposition of the sediments. Schofield (1965) also chose the type section (N66/193336) from the implied type locality in the Hinuera Valley (Healy, 1946). The surface form and its relation to old river courses was also discussed by McCraw (1967) who extended the concept of the Hinuera Formation forming a large low-angle fan by recognising the common three-part fan pattern, with decreasing grain size away from the fan apex.

To date the texture, lithology, mineralogy and sedimentary structures of the Hinuera Formation have not been described in any detail.

1.4 PURPOSE OF STUDY

The aim of this study was to obtain information about the texture of the sediments of the Hinuera Formation and to relate this to particular depositional facies within the alluvial environment. A secondary aim was to determine whether or not any relationship exists between texture and sedimentary structures, and if possible to incorporate this information into an alluvial facies model.

1.5 METHODS OF STUDY

A total of 71 samples were taken from eight exposures in the Hamilton Basin, the Maungatautiri Gorge and the Hinuera Valley. At each exposure, detailed stratigraphic columns were erected incorporating information on thickness, composition, texture, and sedimentary structures. All samples were treated by standard techniques of washing and splitting and were sieved at $\frac{1}{2}\phi$ sieve intervals. Samples containing significant amounts of material smaller than 4ϕ were analysed by standard pipette methods. Size parameters of mean grain size, sorting, skewness and kurtosis were calculated for all samples by graphical methods.

Localities are indicated by one-mile sheet numbers (NZMS1) and grid references. All sample numbers refer to those in the collection of the Department of Earth Sciences, University of Waikato.

1.6 ACKNOWLEDGEMENTS

The writer would like to thank Mr. Campbell S. Nelson for generous advice and criticism given during this study, and for reading and suggesting improvements in the manuscript. Thanks are also due to Professor J.D. McCraw, Dr. M.J. Selby and Mr. Terry Hume for fruitful discussion and advice, Mr. Rex Julian for developing and printing the photographs, and to Mrs. Judy Boyle for the typing of the manuscript. Thanks are also expressed to Mr. Tim Oliver for permission to use unpublished density data.

CHAPTER TWO

STRATIGRAPHIC SECTIONS

Ten sections of the Hinuera Formation (Figs. 2.3-2.12) were studied in detail at eight exposures (A-H). The grid references of these are given in Table 2.1 and the localities shown in Fig. 2.1.

Stratigraphic Section	Fig. No.	Grid Reference (NZMS 1)
A_1	2.3	N65/676427
A_2	2.4	"
A_3	2.5	"
B	2.6	N56/795525
C	2.7	N65/812437
D	2.8	N65/956435
E	2.9	N66/001337
F	2.10	N66/103275
G	2.11	N66/164273
H	2.12	N66/193336

Table 2.1. Grid references of stratigraphic sections.

Three sections (Figs. 2.3-2.5) were studied at one exposure (N65/676427) to compare the degree of textural, lithological and structural variability between sections a few metres apart with the variability of sections up to 48km apart. The sediments of the type section (Section H, N66/193336), deposited within the confines of the Hinuera Valley, were compared with sediments deposited in the less

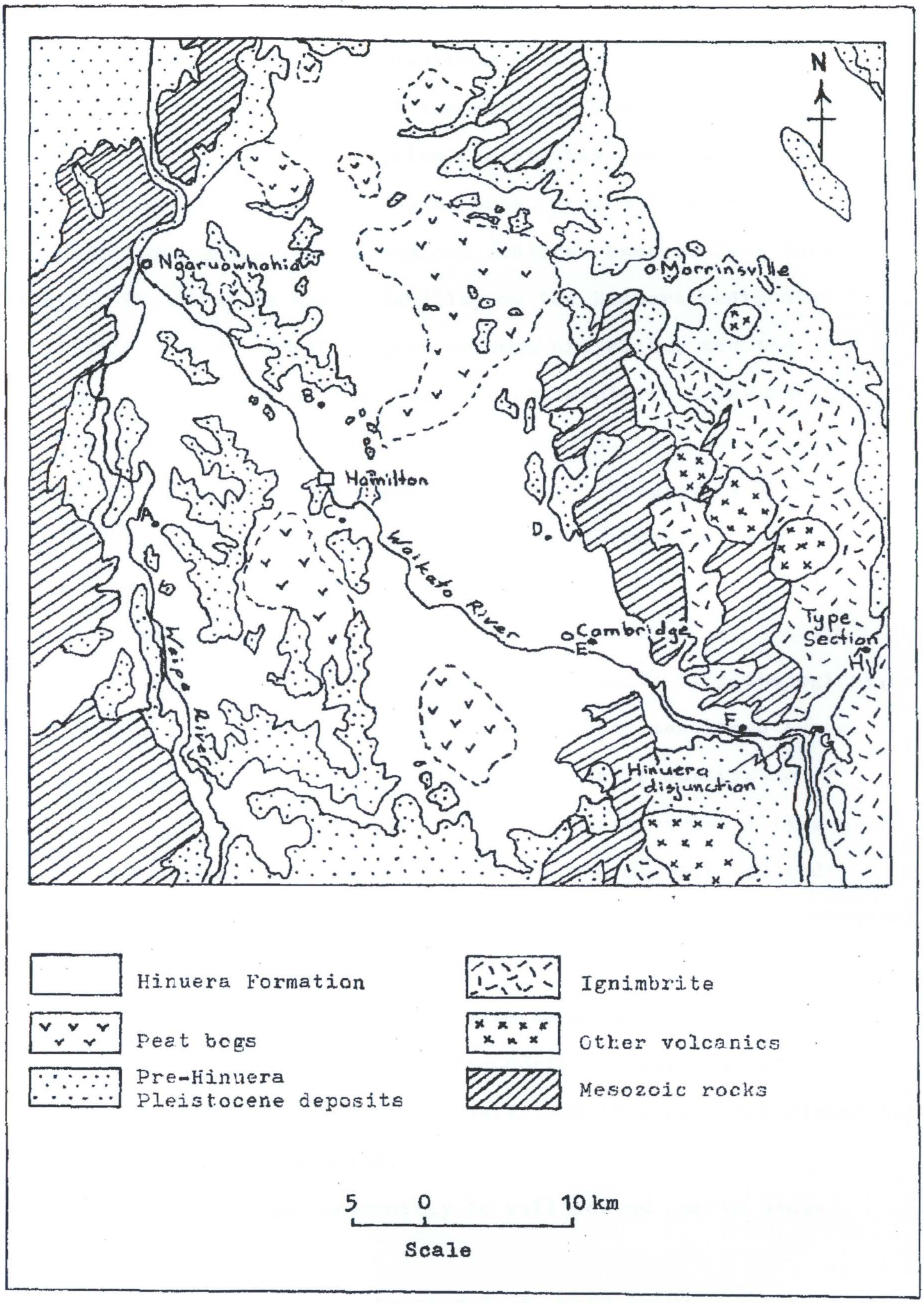

Fig. 2.1 Localities of stratigraphic sections (A-H)

restricted environment of the Hamilton Basin.

Several characteristics of the Hinuera Formation emerge from the mass of detail comprising the stratigraphic sections, and are summarised in the following broad generalisations.

(1) Two apparently paradoxical features emerged from this study. The first is the variability of the Hinuera sediments in detail. No two stratigraphic columns are alike, and the sequence of lithologies, textures, and sedimentary structures is as different in the three adjacent sections (A_1, A_2, and A_3, N65/676427) as between any other sections. The Hinuera Formation is characterised by rapid lateral and vertical changes in these properties.

The second feature is the uniform appearance of the Hinuera Formation on a regional scale. Within the limits of lithological, textural, and sedimentary structural variability mentioned above, the characteristic appearance of the formation in outcrop as unconsolidated, coarse, current-bedded sediments varies little over its very wide areal extent. Exposures in the Hauraki Lowland appear very similar to those in the Hinuera Valley, the Maungatautiri Gorge, and the Hamilton Basin.

(2) The Hinuera Formation is made up of four dominant lithotypes:

(i) Cross-stratified, moderately to poorly sorted, rhyolitic and pumiceous gravelly and slightly gravelly quartz sands, comprising the bulk of the Hinuera sediments.

(ii) Cross-stratified, moderately to well sorted quartz sands.

(iii) Pumice silt.

(iv) Poorly stratified or structureless, very poorly sorted, dominantly rhyolitic sandy gravels or gravelly sands.

(3) The morphology of the cross-stratification displayed at each section enabled current directions to be ascertained, although a detailed study of paleocurrent directions was beyond the scope of this investigation. Some exposures showed consistency of current direction for several metres vertically and for tens of metres laterally; others showed very rapid lateral and vertical changes with reversals through 180° occurring within tens of centimetres.

Any paleoenvironmental model of the Hinuera Formation must explain the deposition of four major lithotypes, the variations in current direction, the high degree of variability of the sediments in detail, and the regional uniformity of the formation.

Texture

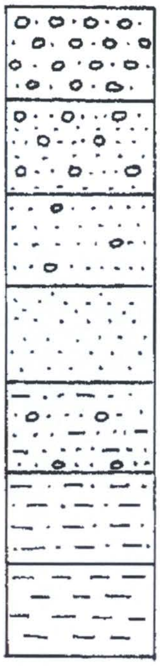

Sandy gravel

Gravelly sand

Slightly gravelly sand

Sand

Gravelly muddy sand

Sandy silt

Silt

Sedimentary Structures

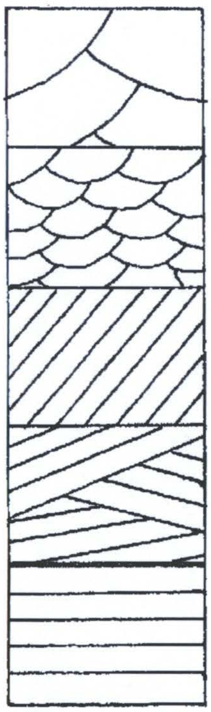

Rho cross-stratification (Rho X-strat)

Nu cross-stratification (Nu X-strat)

Epsilon cross-stratification (Epsilon X-strat)

Sigma cross-stratification (Sigma X-strat)

Horizontal stratification (H-strat)

Peat

Gradational boundary

Fig. 2. Stratigraphic Section Symbols

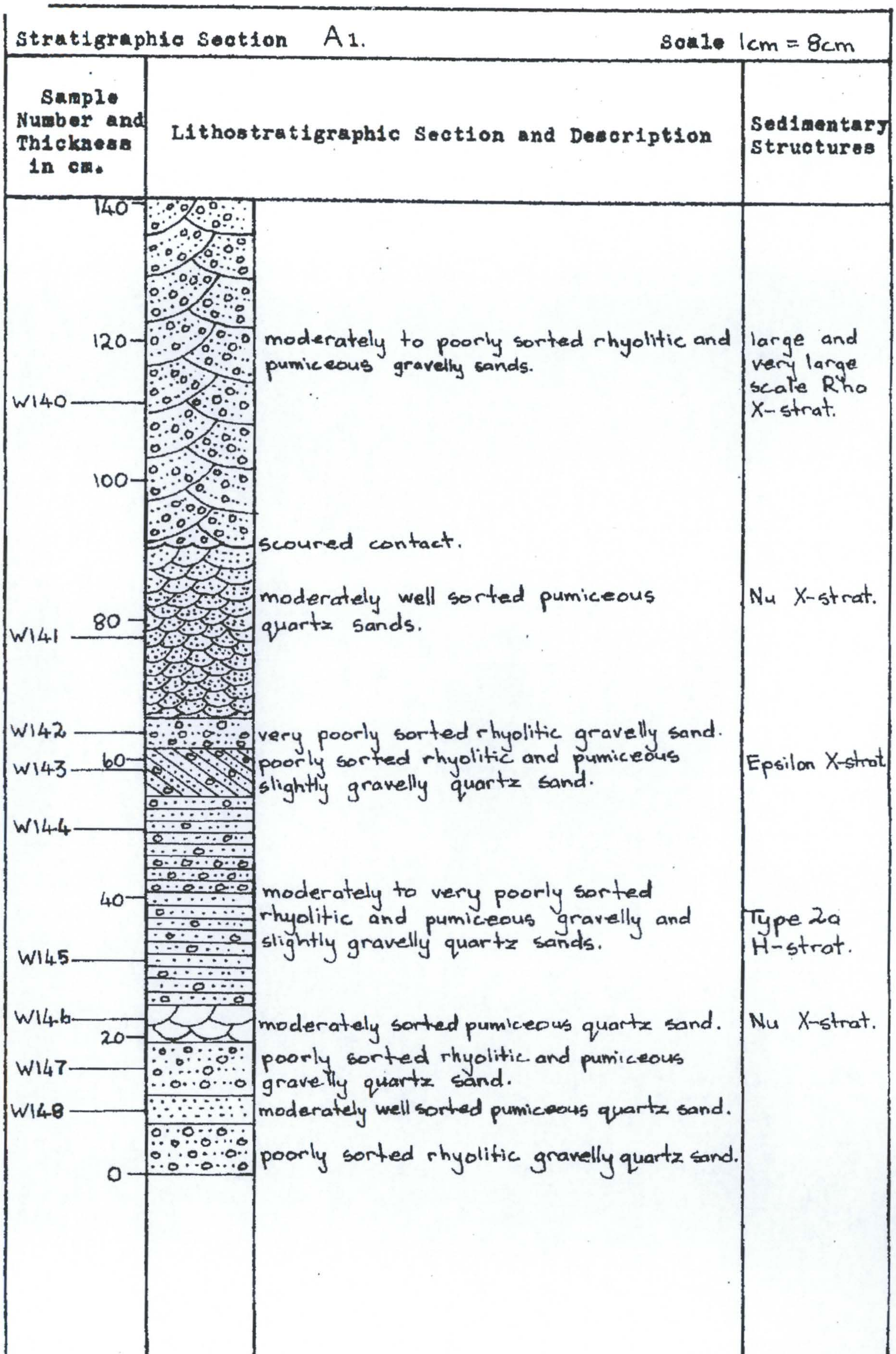
Stratigraphic Section A1.
Scale 1cm = 8cm
Sample Number and Thickness in cm.
Lithostratigraphic Section and Description
Sedimentary Structures
140
120
W140
100
80
W141
W142
W143
60
W144
40
W145
W146
20
W147
W148
0
moderately to poorly sorted rhyolitic and pumiceous gravelly sands.
large and very large scale Rho X-strat.
scoured contact.
moderately well sorted pumiceous quartz sands.
Nu X-strat.
very poorly sorted rhyolitic gravelly sand.
poorly sorted rhyolitic and pumiceous slightly gravelly quartz sand.
Epsilon X-strat.
moderately to very poorly sorted rhyolitic and pumiceous gravelly and slightly gravelly quartz sands.
Type 2a H-strat.
moderately sorted pumiceous quartz sand.
Nu X-strat.
poorly sorted rhyolitic and pumiceous gravelly quartz sand.
moderately well sorted pumiceous quartz sand.
poorly sorted rhyolitic gravelly quartz sand.

Fig. 2.3

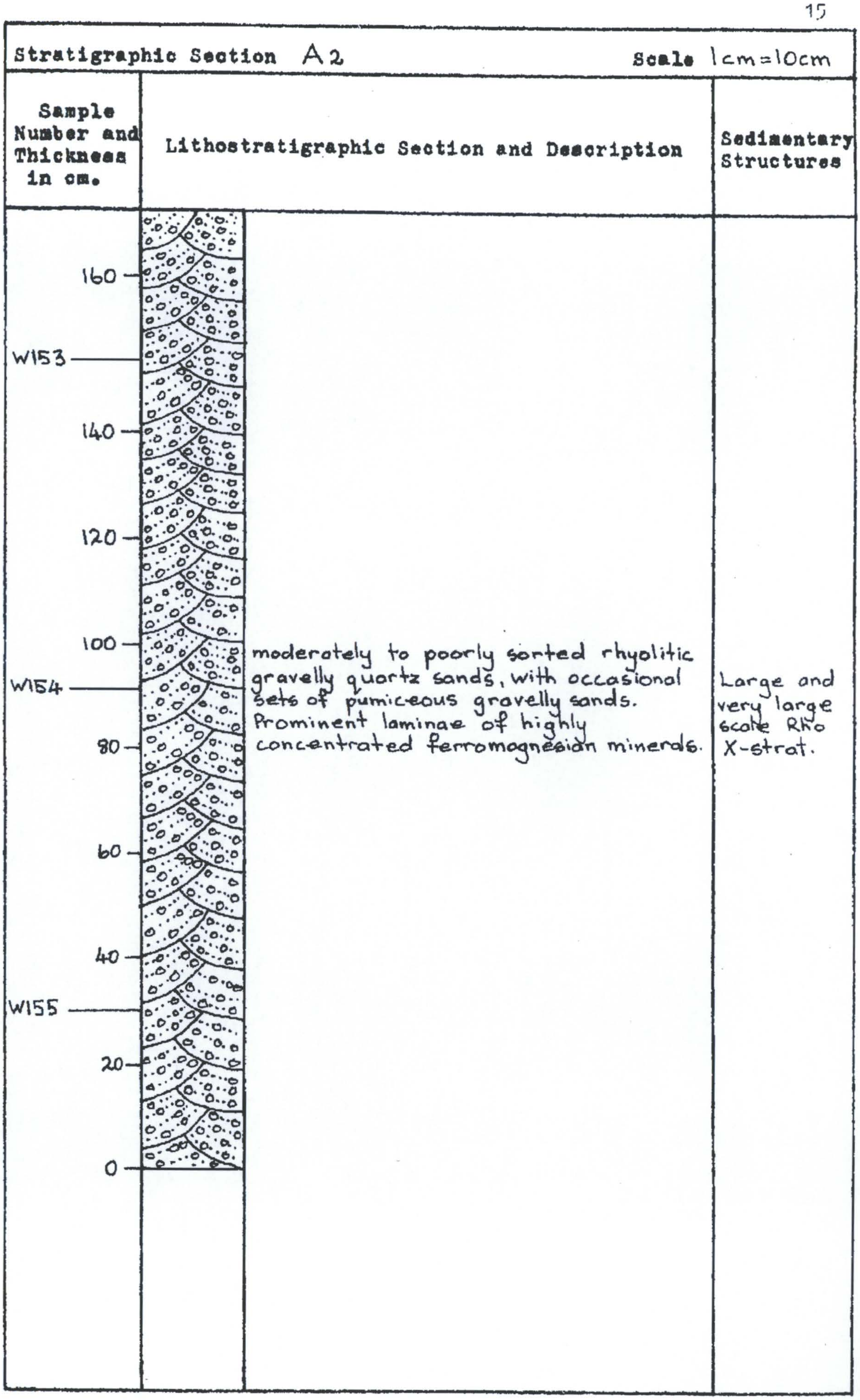
Stratigraphic Section A2
Scale 1cm=10cm
Sample Number and Thickness in cm.
Lithostratigraphic Section and Description
Sedimentary Structures
160
W153
140
120
100
W154
80
60
40
W155
20
0
moderately to poorly sorted rhyolitic gravelly quartz sands, with occasional sets of pumiceous gravelly sands. Prominent laminae of highly concentrated ferromagnesian minerals.
Large and very large scale RHo X-strat.

Fig. 2.4

Stratigraphic Section A3. **Scale** 1cm = 20cm

Sample Number and Thickness in cm.	Lithostratigraphic Section and Description	Sedimentary Structures
300 – 250	moderately to poorly sorted rhyolitic and pumiceous gravelly and slightly gravelly quartz sands.	Rho X-strat.
W156 200	moderately to moderately well sorted highly pumiceous slightly gravelly quartz sands.	Nu X-strat.
W157		
150		
W158		
W159	moderately to poorly sorted rhyolitic and pumiceous slightly gravelly and gravelly quartz sands, and muddy sandy gravels.	Rho X-strat.
100		
W160		
50		very large scale Rho X-strat.
W161		
W162	moderately well sorted to poorly sorted pumiceous, slightly gravelly quartz sands.	Nu X-strat.
0		

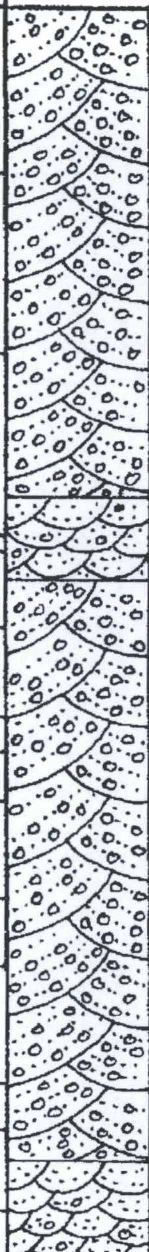

Fig. 2.5

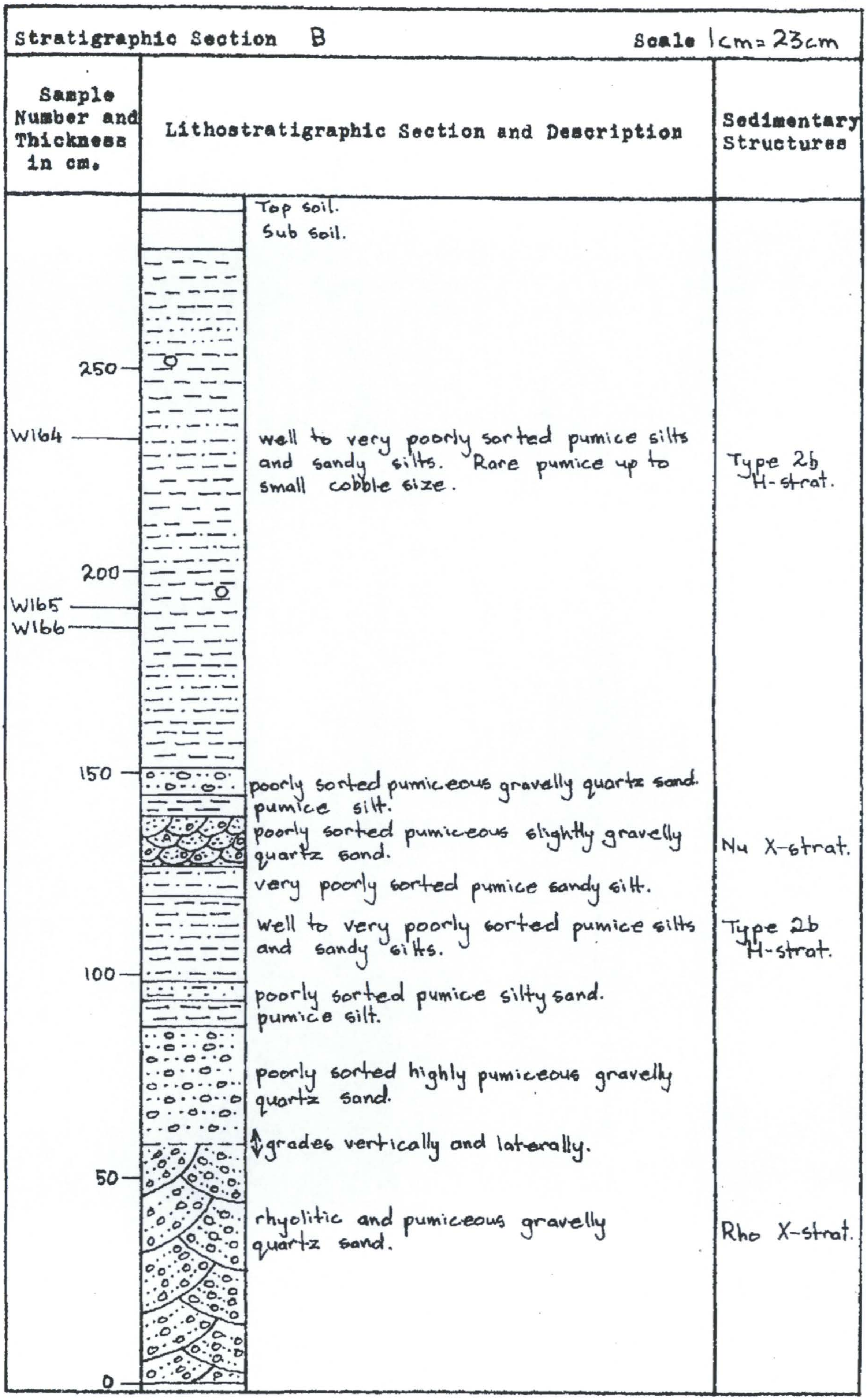
Stratigraphic Section B
Scale 1cm = 23cm
Sample Number and Thickness in cm.
Lithostratigraphic Section and Description
Sedimentary Structures
250
200
150
100
50
0
W164
W165
W166
Top soil.
Sub soil.
well to very poorly sorted pumice silts and sandy silts. Rare pumice up to small cobble size.
Type 2b H-strat.
poorly sorted pumiceous gravelly quartz sand.
pumice silt.
poorly sorted pumiceous slightly gravelly quartz sand.
Nu X-strat.
very poorly sorted pumice sandy silt.
Well to very poorly sorted pumice silts and sandy silts.
Type 2b H-strat.
poorly sorted pumice silty sand.
pumice silt.
poorly sorted highly pumiceous gravelly quartz sand.
grades vertically and laterally.
rhyolitic and pumiceous gravelly quartz sand.
Rho X-strat.

Fig. 2.6

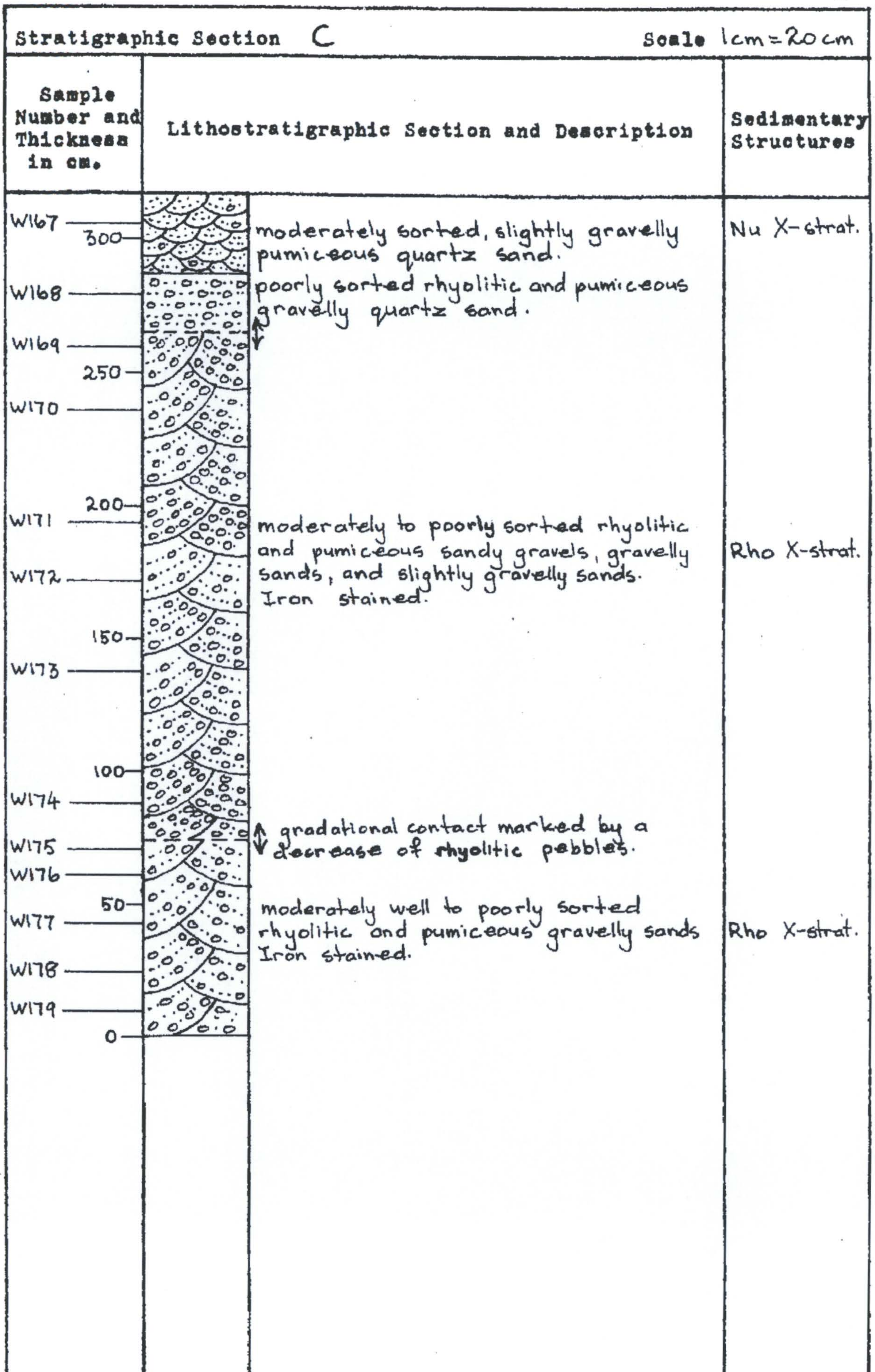
Stratigraphic Section C
Scale 1cm=20cm
Sample Number and Thickness in cm.
Lithostratigraphic Section and Description
Sedimentary Structures
W167
300
W168
W169
250
W170
200
W171
W172
150
W173
100
W174
W175
W176
50
W177
W178
W179
0
moderately sorted, slightly gravelly pumiceous quartz sand.
Nu X-strat.
poorly sorted rhyolitic and pumiceous gravelly quartz sand.
moderately to poorly sorted rhyolitic and pumiceous sandy gravels, gravelly sands, and slightly gravelly sands. Iron stained.
Rho X-strat.
gradational contact marked by a decrease of rhyolitic pebbles.
moderately well to poorly sorted rhyolitic and pumiceous gravelly sands Iron stained.
Rho X-strat.

Fig. 2.7

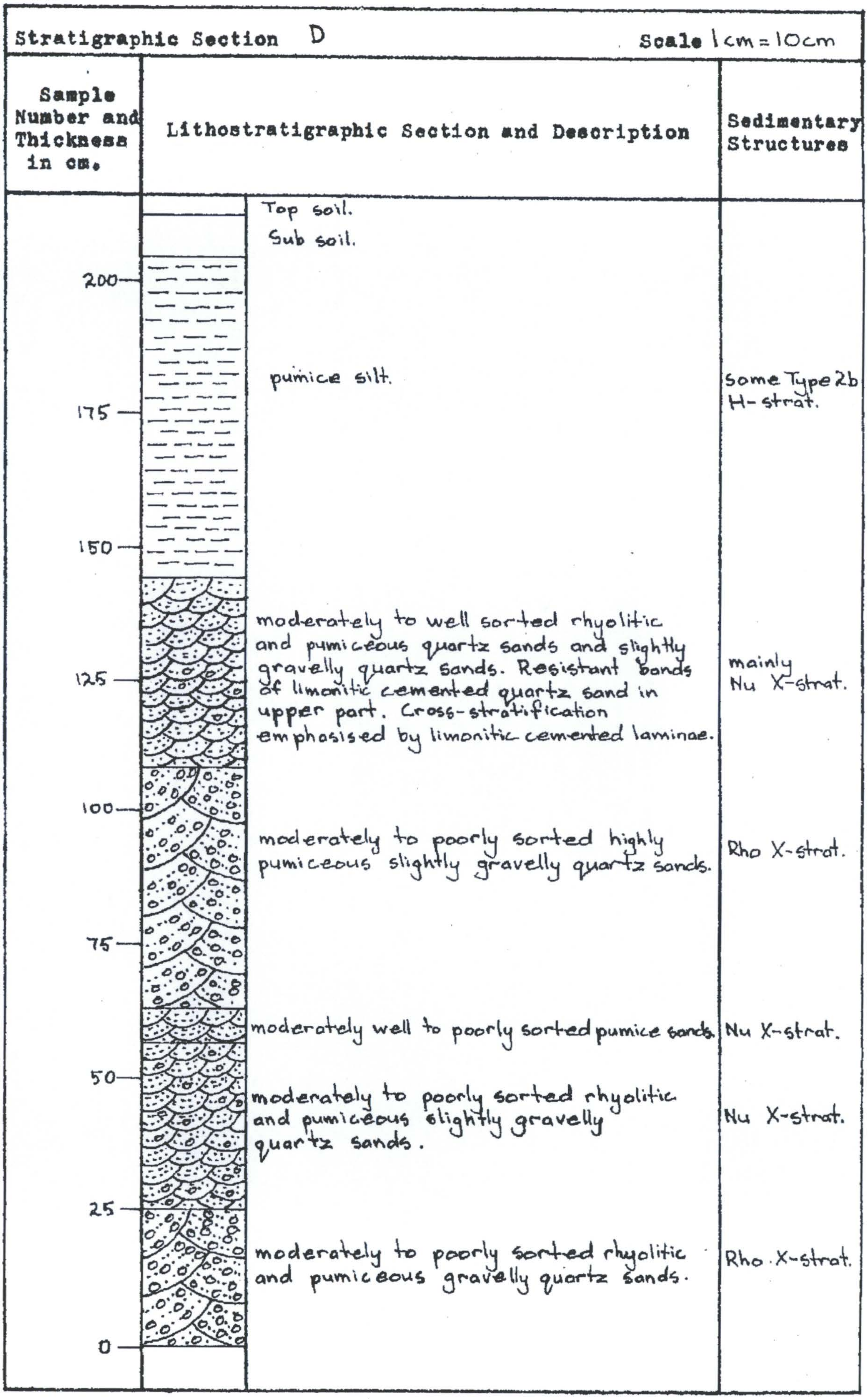
Stratigraphic Section D
Scale 1cm = 10cm
Sample Number and Thickness in cm.
Lithostratigraphic Section and Description
Sedimentary Structures
200
175
150
125
100
75
50
25
0
Top soil.
Sub soil.
pumice silt.
Some Type 2b H-strat.
moderately to well sorted rhyolitic and pumiceous quartz sands and slightly gravelly quartz sands. Resistant bands of limonitic cemented quartz sand in upper part. Cross-stratification emphasised by limonitic cemented laminae.
mainly Nu X-strat.
moderately to poorly sorted highly pumiceous slightly gravelly quartz sands.
Rho X-strat.
moderately well to poorly sorted pumice sands.
Nu X-strat.
moderately to poorly sorted rhyolitic and pumiceous slightly gravelly quartz sands.
Nu X-strat.
moderately to poorly sorted rhyolitic and pumiceous gravelly quartz sands.
Rho X-strat.

Fig. 2.8

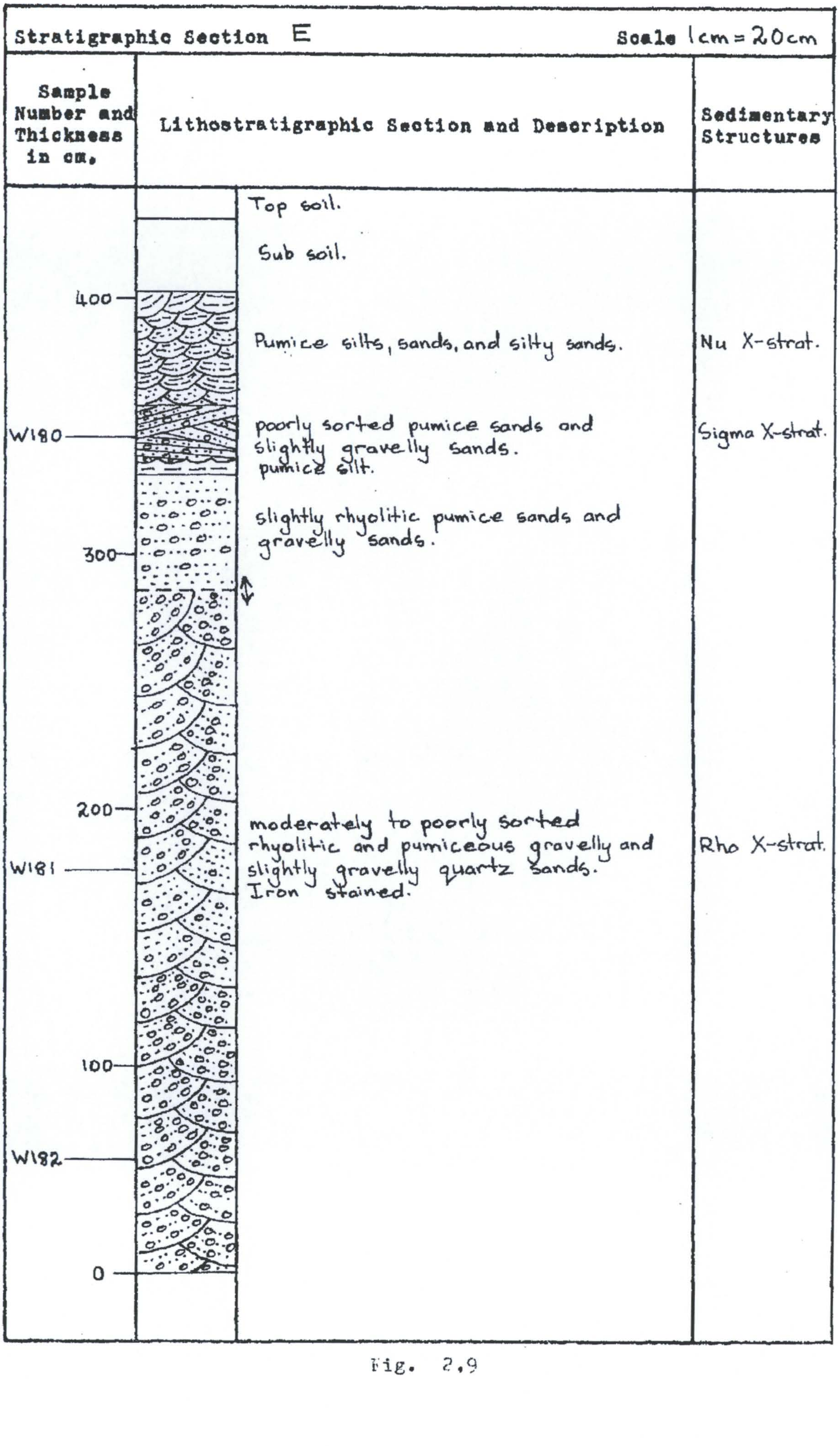
Stratigraphic Section E
Scale 1cm = 20cm
Sample Number and Thickness in cm.
Lithostratigraphic Section and Description
Sedimentary Structures
Top soil.
Sub soil.
400
Pumice silts, sands, and silty sands.
Nu X-strat.
W180
poorly sorted pumice sands and slightly gravelly sands.
pumice silt.
Sigma X-strat.
slightly rhyolitic pumice sands and gravelly sands.
300
200
moderately to poorly sorted rhyolitic and pumiceous gravelly and slightly gravelly quartz sands. Iron stained.
Rho X-strat.
W181
100
W182
0

Fig. 2.9

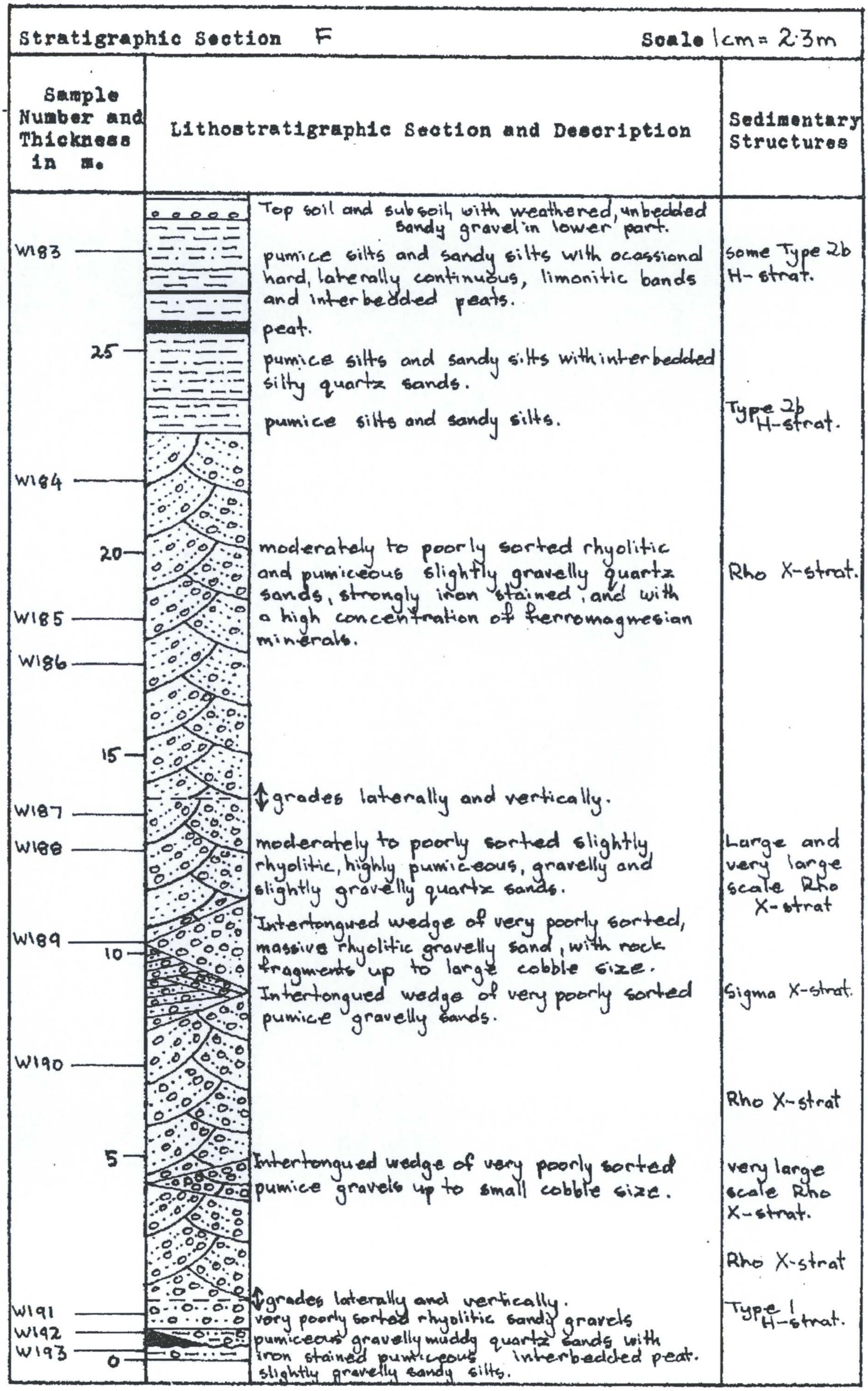
Stratigraphic Section F
Scale 1cm = 2·3m
Sample Number and Thickness in m.
Lithostratigraphic Section and Description
Sedimentary Structures
W183
25
W184
20
W185
W186
15
W187
W188
W189
10
W190
5
W191
W192
W193
0
Top soil and subsoil with weathered, unbedded sandy gravel in lower part.
pumice silts and sandy silts with ocassional hard, laterally continuous, limonitic bands and interbedded peats.
peat.
pumice silts and sandy silts with interbedded silty quartz sands.
pumice silts and sandy silts.
moderately to poorly sorted rhyolitic and pumiceous slightly gravelly quartz sands, strongly iron stained, and with a high concentration of ferromagnesian minerals.
grades laterally and vertically.
moderately to poorly sorted slightly rhyolitic, highly pumiceous, gravelly and slightly gravelly quartz sands.
Intertongued wedge of very poorly sorted, massive rhyolitic gravelly sand, with rock fragments up to large cobble size.
Intertongued wedge of very poorly sorted pumice gravelly sands.
Intertongued wedge of very poorly sorted pumice gravels up to small cobble size.
grades laterally and vertically.
very poorly sorted rhyolitic sandy gravels
pumiceous gravelly muddy quartz sands with iron stained pumiceous interbedded peat.
slightly gravelly sandy silts.
some Type 2b H-strat.
Type 2b H-strat.
Rho X-strat.
Large and very large scale Rho X-strat
Sigma X-strat.
Rho X-strat
very large scale Rho X-strat.
Rho X-strat
Type 1 H-strat.

Fig. 2.10

Stratigraphic Section G **Scale** 1cm=50cm

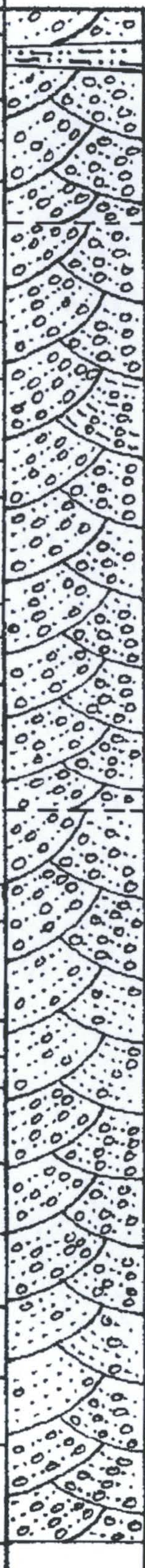

Sample Number and Thickness in m.	Lithostratigraphic Section and Description	Sedimentary Structures
11		
W194	moderately to poorly sorted slightly pumiceous rhyolitic gravelly quartz sands with interbedded lenses of muddy sand in upper part.	Rho X-strat.
W195, W196		
10	↕ grades laterally and vertically.	
9		
W197		
8	moderately to poorly sorted rhyolitic gravelly quartz sands, pumiceous rhyolitic gravelly quartz sands, and highly pumiceous gravelly sands and gravelly muddy sands.	Rho X-strat.
W198		
7		
W199		
W200		
6	↕ grades laterally and vertically.	
5		
W201		
4		
W202	moderately to poorly sorted slightly gravelly quartz sands, rhyolitic and pumiceous gravelly quartz sands and highly pumiceous gravelly sands.	Large and very large scale Rho X-strat.
W203		
3		
W204		
2		
W205		
1		
0		

Fig. 2.11

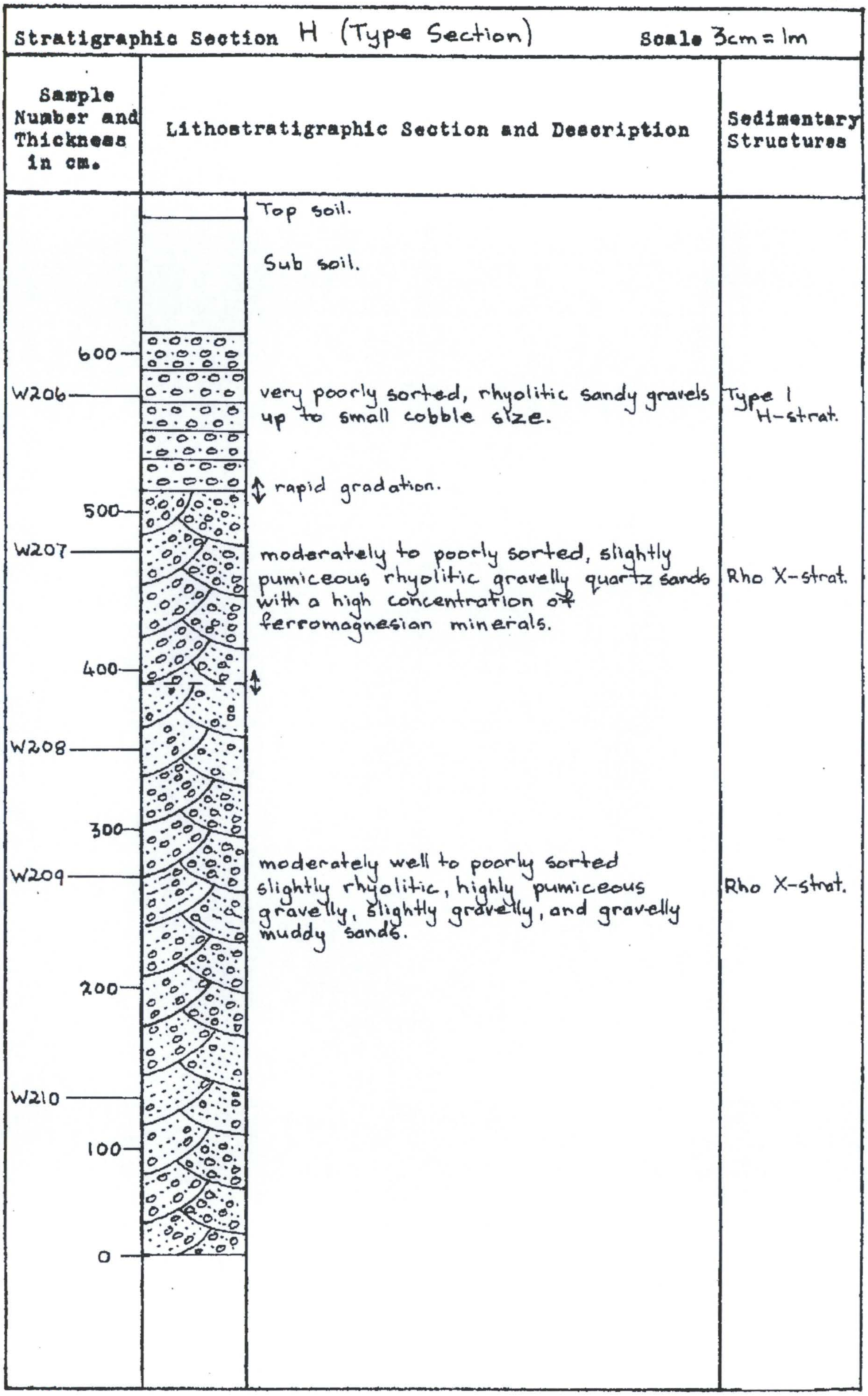
Stratigraphic Section H (Type Section)
Scale 3cm = 1m
Sample Number and Thickness in cm.
Lithostratigraphic Section and Description
Sedimentary Structures
Top soil.
Sub soil.
600
W206
very poorly sorted, rhyolitic sandy gravels up to small cobble size.
Type 1 H-strat.
rapid gradation.
500
W207
moderately to poorly sorted, slightly pumiceous rhyolitic gravelly quartz sands with a high concentration of ferromagnesian minerals.
Rho X-strat.
400
W208
300
W209
moderately well to poorly sorted slightly rhyolitic, highly pumiceous gravelly, slightly gravelly, and gravelly muddy sands.
Rho X-strat.
200
W210
100
0

Fig. 2.12

CHAPTER THREE

S E D I M E N T A R Y   S T R U C T U R E S

The primary sedimentary structures of the Hinuera Formation are dominated by cross-stratification, with less common types of horizontal stratification. A variety of post-depositional structures are present, although of limited occurrence. Each of these sedimentary structures is discussed in turn.

3.1 CROSS-STRATIFICATION

Cross-stratification is almost ubiquitous throughout the Hinuera Formation and is the most obvious features seen in exposures of the sediments. A detailed description and interpretation of the sedimentary structures was not the primary aim of this study, but an attempt is made to rationalise the observations made in the field with reference to recent literature on the subject. The terminology of McKee and Weir (1953) is followed for description, but not classification, of the cross-stratification.

Random measurements were made of the length and maximum height of 142 sets of cross-strata. An effort was made to keep the number of measurements of the different types of cross-strata in proportion to their occurrence to prevent introduction of a sampling bias, but otherwise no statistical controls were used.

Length was plotted as a function of height on semi-log paper for ease of presentation (Fig. 3.1). The two parameters are roughly proportional, with a length to height ratio of 6:1, increasing to about 8:1 when length dimensions are in the order of metres. The maximum and minimum height of a set measured was 70cm and 4mm respectively; the maximum and minimum length measured was 6.42mm and 1.8cm respectively. Histograms were plotted to show the frequency of cross-bedded sets as a function of length (Fig. 3.2) to height (Figs. 3.3 and 3.4). In Fig. 3.3, the scale of the abscissa is reduced by one tenth for lengths over one metre for ease of presentation, and does not erroneously affect the distribution pattern.

Fig. 3.2 shows a marked deviation from a normal distribution of set lengths, with a marked deficiency of sets of 40 to 50cm, and from 80 to 100cm in length. It is possible that the trimodal pattern of set lengths is simply a result of insufficient measurements. There does not appear to be any relationship between the modal values indicated and the lithology or texture of the cross-beds concerned, and work to date does not suggest any explanation.

Fig. 3.3 shows that sets up to 10cm in height are most abundant in the Hinuera Formation. To determine whether or not a trimodal distribution in the scale of cross-stratification exists for the heigh parameter, a histogram of occurrence as a function of height was plotted on a larger scale than Fig. 3.3 for heights between 0 and 20cm (Fig. 3.4). Although generalisations drawn from such limited data can be at best only tentative, cross-strata with set heights between 4 and 5cm, 9 and 12cm and 13 and 18cm appear to be uncommon. In proportion to the length to height ratio observed (Fig. 3.1), the lack of heights between 9 and 12cm and 13 and 18cm correspond to the lack of lengths of sets between 40 and 50cm and 80 and 100cm respectively. The scarcity of heights between 4 and 5cm corresponds to the division between small and large scale cross-stratified units made by Allen (1963a).

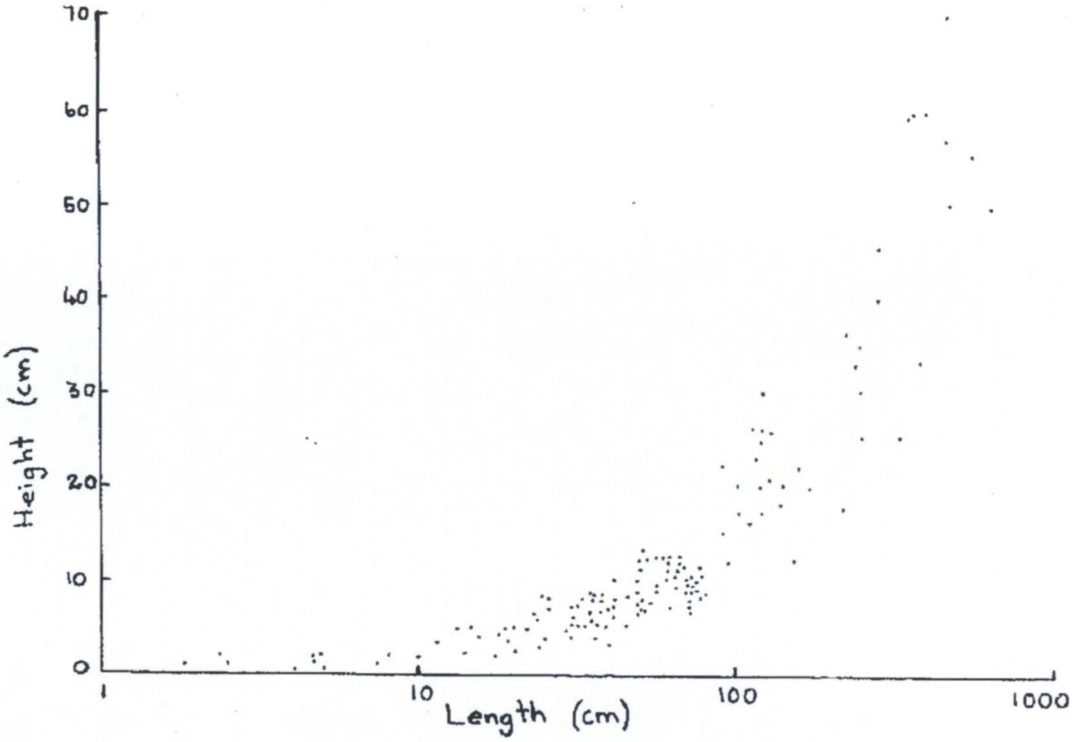

Fig. 3.1 Length of cross-stratified sets plotted as a function of height.

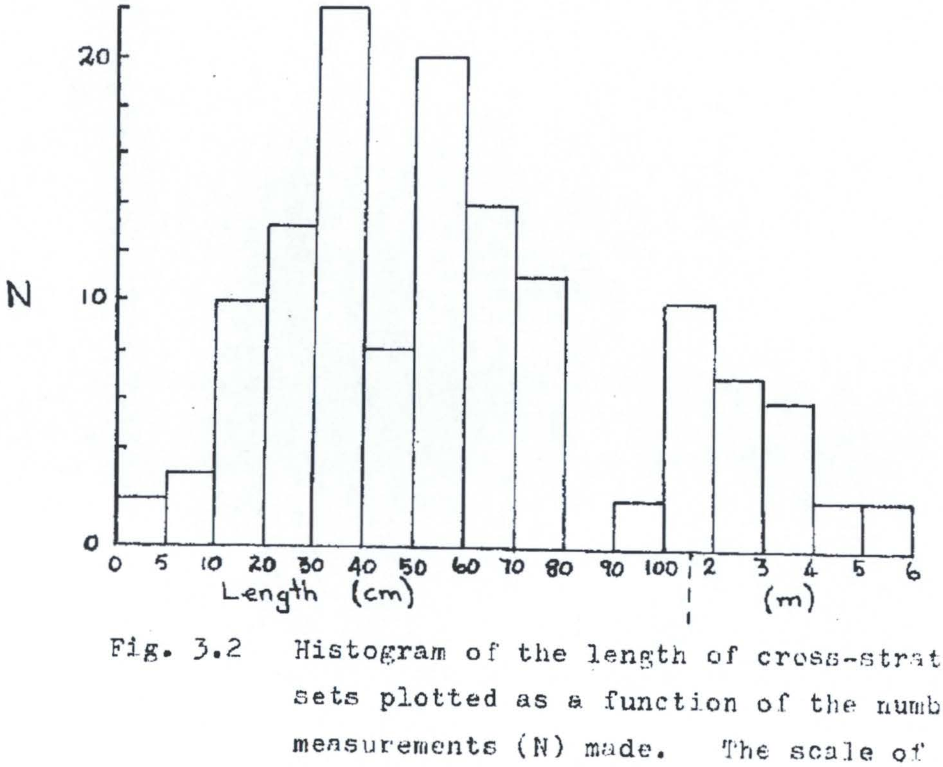

Fig. 3.2 Histogram of the length of cross-stratified sets plotted as a function of the number of measurements (N) made. The scale of the abscissa is reduced by one tenth for lengths over one metre.

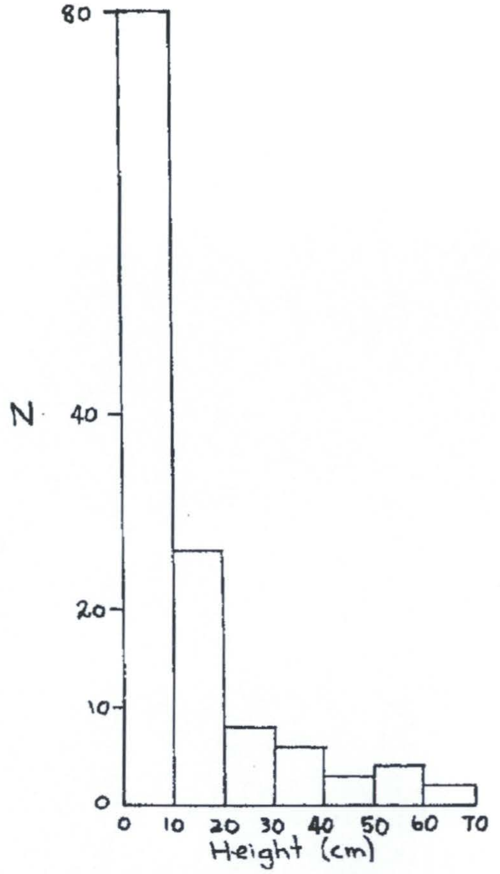

Fig. 3.3 Histogram of the height of cross-stratified sets plotted as a function of the number of measurements (N) made.

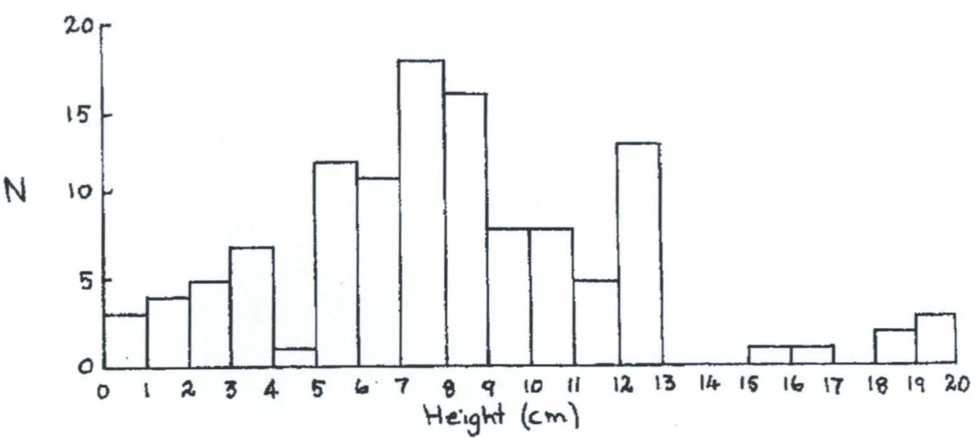

Fig. 3.4 Histogram of the height of cross-stratified sets between 0 and 20cm plotted as a function of the number of measurements (N) made.

Thus there appears to be a marked trimodal distribution of cross-stratified set dimensions with corresponding modes for height and length parameters in their observed ratio (Fig. 3.1). On the basis of the above, cross-stratified units of the Hinuera Formation are here tentatively classified with respect to scale for ease of description, using the height parameter (Table 3.1).

Scale of Cross-Stratification	Height of Cross-Stratification
Small scale	Less than 5cms
Large scale	5-15 cms
Very large scale	Greater than 15cms

Table 3.1 Classification of the cross-stratified sets in the Hinuera Formation on the basis of scale.

Four types of cross-stratification were observed in the Hinuera Formation (Fig. 3.5). These are described using Allen's (1963a) six criteria for classification of cross-stratified units (Table 3.2).

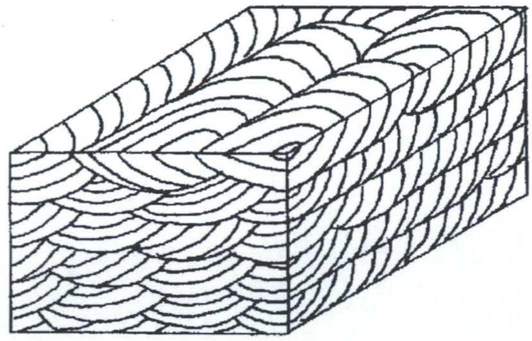

Type 1 Nu cross-stratification

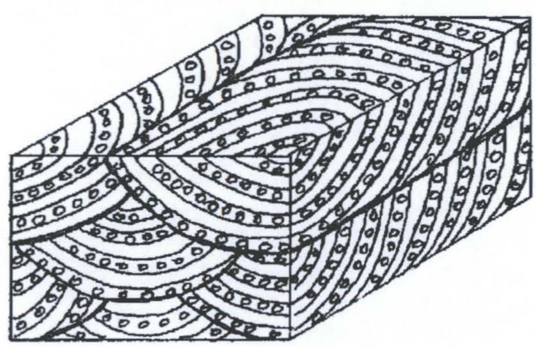

Type 2 Rho cross-stratification

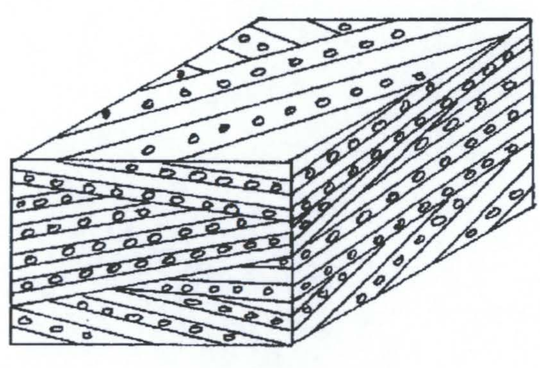

Type 3 Sigma cross-stratification

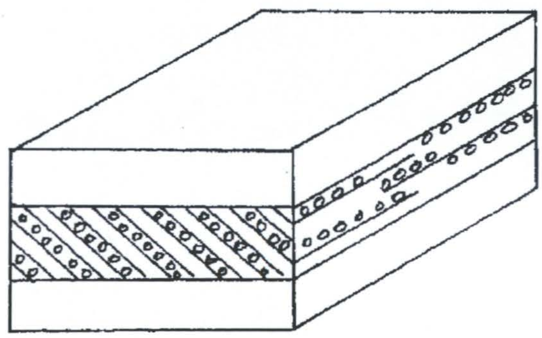

Type 4 Epsilon cross-stratification

Fig. 3.5 Schematic block diagrams illustrating the varieties of cross-stratification occurring in the Hinuera Formation.

Criteria	Type 1	Type 2	Type 3	Type 4
Grouping	Grouped	Grouped	Grouped	Solitary
Magnitude	Small scale	Large scale	Large scale	Large scale
Character of Lower Bounding Surface	Erosional	Erosional	Erosional	Erosional
Shape of Lower Bounding Surface	Scoop-shaped	Scoop-shaped	Planar	Planar
Angular Relation of Cross-strata to lower bounding surface	Discordant	Discordant	Concordant	Discordant
Lithology	Homogenous	Heterogenous	Heterogenous	Heterogenous

Table 3.2 Description of the cross-stratified sets in the Hinuera Formation using Allen's (1963a) criteria.

Types 1 and 2 cross-stratification correspond to McKee and Weir's (1953) trough cross-stratification, and both frequently display the "festoon" variety first described by Knight (1929). Types 3 and 4 correspond to McKee and Weir's planar cross-stratification. This nomenclature, combined with the classification presented on the basis of scale (Table 3.1), is adequate to describe the cross-stratification of the Hinuera Formation for the purposes of this study. However, a more recent and sophisticated classification scheme is available (Allen, 1963a). Using the six descriptive criteria as presented in Table 3.2, Allen recognised 15 cross-stratification types which he named using letters of the Greek alphabet.

Type 1 is identical to Allen's Nu cross-stratification (Fig. 3.6). Type 2 is similar to Pi cross-stratification, differing only in the lithological heterogenity of the cross-strata. Type 3 most closely resembles Xi cross-stratification, but is fundamentally different in that each set is underlain by an erosional surface, and that the cross-strata of the set appear to be concordant to the lower bounding surfaces. The cross-strata are also lithologically heterogenous. Type 4 is identical to Allen's Epsilon cross-stratification (Fig. 3.9).

In accordance with Allen's suggestion that the nomenclature be extended to include new types, type 2 is here tentatively called Rho cross-stratification (Figs. 3.7, 3.10 and 3.11), and type 3 is called Sigma cross-stratification (Fig. 3.8). Rho cross-stratification is by far the most abundant sedimentary structure in the Hinuera Formation, and is preserved in rhyolitic and pumiceous sandy gravels, gravelly sands, and slightly gravelly sands, and highly pumiceous gravelly muddy sands, muddy sandy gravels, gravelly sands, and slightly gravelly sands. (See Fig. 4.15 for textural classes.) Nu cross-stratification is common, and is preserved in pumiceous slightly gravelly quartz sands, highly pumiceous quartz sands, and quartz sands. Sigma cross-stratification is rare, and is preserved in highly pumiceous gravelly sands and rhyolitic pumiceous gravelly sands. Epsilon cross-stratification is also rare, and is preserved in pumiceous rhyolitic slightly gravelly sands.

Despite recent work, particularly by Allen (1963a, 1963b), a good deal of confusion remains as to the origin of different types of cross-stratification, although it is certain that there is no single simple explanation.

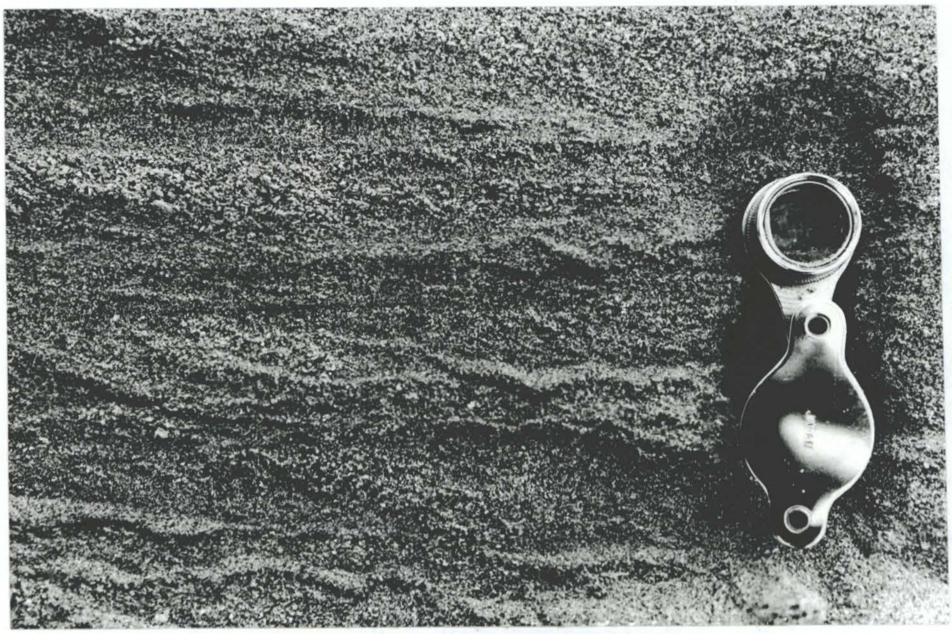

Fig. 3.6 Nu cross stratification in moderately well sorted pumiceous quartz sand. Micro-relief is the result of weakly limonitic cemented laminae. Grid Ref. N65/676427. Hand lens is 6cm long.

Fig. 3.7 Rho cross stratification in moderately well to very poorly sorted rhyolitic and pumiceous gravelly sands. Grid Ref. N66/193336 (Type section of Hinuera Formation). Scale in cm.

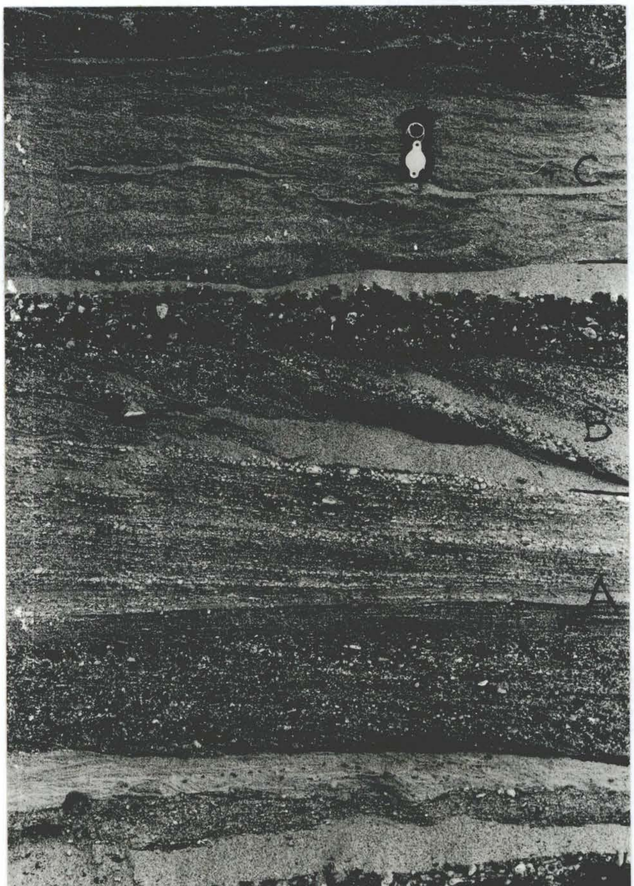
C
B
A

Fig. 3.8 Sigma cross stratification in poorly sorted pumiceous gravelly sands, showing cross-strata concordant to a planar, erosional lower bounding surface. Note overlying bed of very poorly sorted, structureless sandy gravels (see section 3.2). Grid Ref. N66/103275. Hammer is 33cm long.

Fig. 3.9 Epsilon cross-stratification (B), in poorly sorted rhyolitic and pumiceous slightly gravelly quartz sand. Also shown is Type 2a horizontal stratification (A), in moderately to very poorly sorted rhyolitic and pumiceous gravelly and slightly gravelly quartz sands, and Nu cross-stratification (C). Grid Ref. N65/676427. Hand lens is 6cm long.

It can be inferred from cosets of cross-strata that erosional and depositional processes have operated, the erosional processes accounting for the surfaces between sets, and the depositional processes for the growth of sets and the shapes and attitudes of cross-strata. Field evidence does not indicate whether or not the two processes acted simultaneously as a set was formed, nor does it indicate the vertical extent of erosion between sets. Basically, the migration of asymmetrical ripples leads to the formation of destructive types of cross-bedding (Allen, 1963b). The varying ability of sediment to settle from suspension onto the surface of a migrating ripple train advancing by stoss-side erosion and lee-side deposition is believed to control the accumulation of distinctive types of cross-bedding, depending on sediment supply and ripple size, geometry and velocity (Allen, 1063b).

Nu cross-stratification is believed to be formed by the migration of trains of linguoid small scale asymmetrical ripples (Allen, 1963a). Pi cross-stratification (Allen, 1963a) may be formed by the migration of lurate or linguoid large scale asymmetrical ripples. The heterogeneity of Rho cross-stratification is thought to be the result of fluctuations in sediment supply and current velocity, and it is suggested that it may form in the same way as Pi cross-stratification. In the absence of any comparative structure in the relevant literature, and the lack of experimental work, no mode of origin is suggested for Sigma cross-stratification. Epsilon cross-stratification is known to have formed by deposition on planar erosional surfaces of point bars.

A striking feature of the large scale forms of cross-stratification in the Hinuera Formation is their lithological heterogeneity. This was observed in some detail, and is illustrated by several of the figures in this work, and in particular by Figs. 3.10 and 3.11. Cross-strata range from 1mm to 5cm in thickness and are formed from alternating bands of a wide range of textures and lithologies, although dominated by three major associations: pumice or rhyolitic granules and small pebbles; concentrations of ferromagnesian minerals, sometimes iron-stained; and moderately sorted quartz sands. The dips of cross-strata vary from nearly horizontal to 45°, with the most common values between 15° and 30°. Pebbles show only moderate to weak imbrication. No relationship could be established between the dip or thickness of cross-strata and grain size or sorting.

Moss (1962) has shown that most natural sandy and gravelly sediments are deposited as composites, and not, as is commonly assumed in grain size analysis, as single homogenous particle populations. Moss used shape analysis of clastic particles to show that up to three distinct particle populations could occur in a single sedimentary lamina of any particular water-laid sandy and gravelly sediment. This conclusion has been supported by several workers (Tanner, 1964; Visher, 1965, 1969; and others), who have resolved cumulative grain size distribution curves into straight line segments, each representing a log normally distributed population of material deposited by a different physical process (see section 4.1). Moss

Fig. 3.11

Fig. 3.10 Rho cross stratification in moderately to poorly sorted pumiceous and rhyolitic gravelly sands, showing the heterogeneity of cross-strata in the Hinuera Formation. Grid Ref. N66/103275.

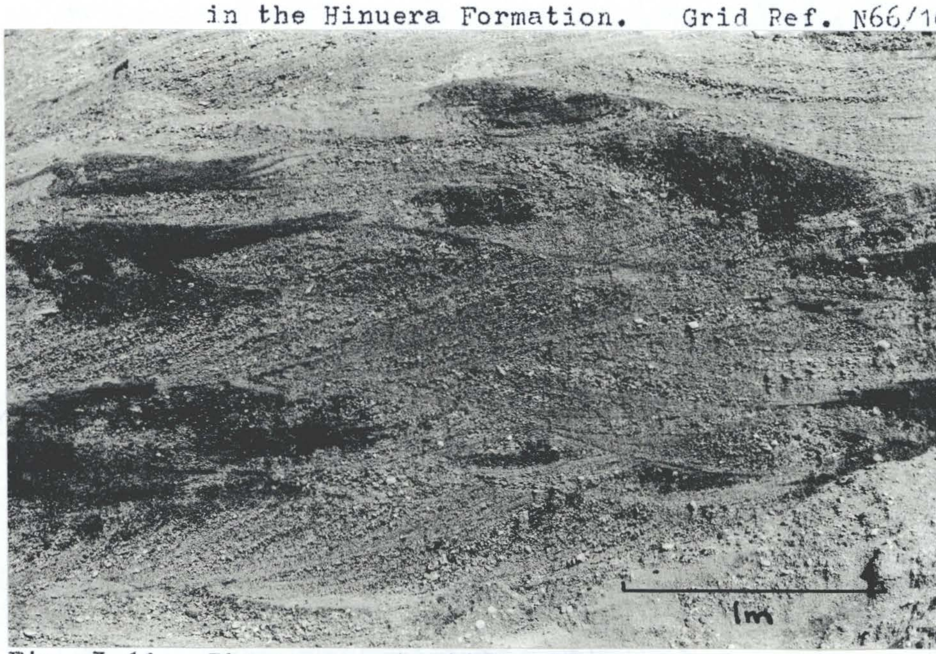

Fig. 3.11 Rho cross stratification in moderately to very poorly sorted highly pumiceous gravelly sands and sandy gravels. At the centre of the photograph is a pocket of structureless rhyolitic and pumiceous sandy gravel. Grid Ref. N66/103275. Hammer is 33cm long.

(1963) concluded that apart from "traction clog" deposits, all depositional sedimentary structures built of clean sandy and gravelly sediment are the result of traction carpet-saltation load interactions. Each sedimentary lamina making up these structures is apparently characterised by a single saltation population. The sudden textural change from one lamina to the next occurs because only certain saltation population particles are deposited until a critical stage is reached, whereupon a new saltation population is deposited (Moss, 1963). Hence, traction current bed load sediments are deposited in small "packets" or laminae, each with their own grain size distribution, the latter being dependant on the relationship between the transporting medium and the bed load.

A phenomenon commonly present in the cross-strata of the Hinuera Formation is the non-uniform distribution of grain sizes within individual laminae. Cross-stratified gravelly sands frequently showed a decrease in median grain size down the slope of the laminae, with resulting concentrations of pumice and rhyolitic pebbles and granules near the top of the set of cross-strata (Figs. 3.12 and 3.13a). This may be explained in terms of Bagnold's (1954) dispersive stress theory. The intergranular dispersive stress increases as the square of the particle diameter, and hence differential stress on the larger particles may be large enough to force them to the surface of the slip face where the dispersive stress is zero. Jopling (1965) used flume experiments to investigate grain size distributions of sedimentary laminae.

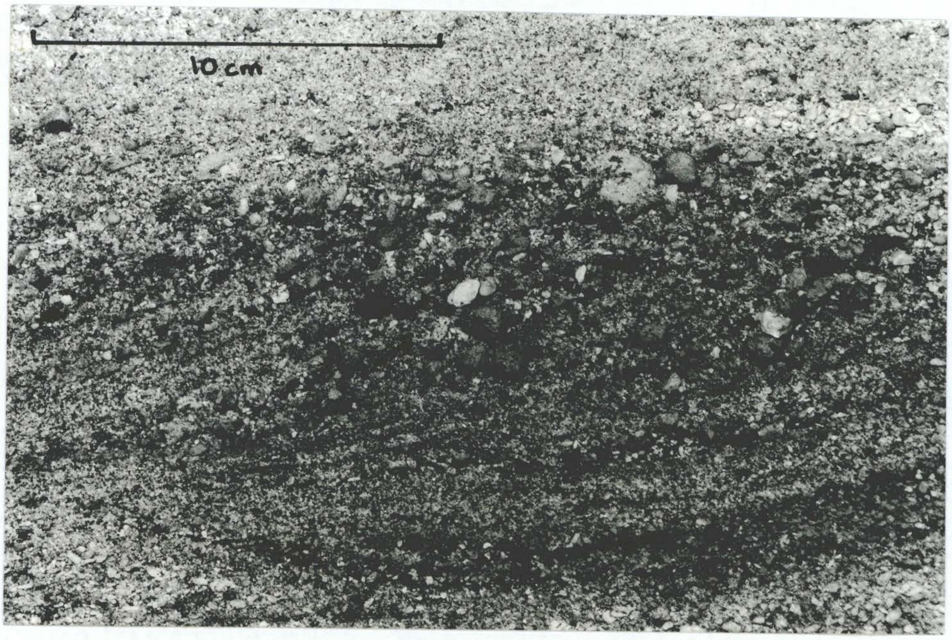

Fig. 3.12 Rho cross-stratification, showing a decrease in median grain size down the slope of the laminae. Granules and pebbles are rhyolitic rock fragments with some pumice; sand sized particles are quartz and ferromagnesian minerals. For explanation see text (pp. 37 to 40). Grid Ref. N65/812437.

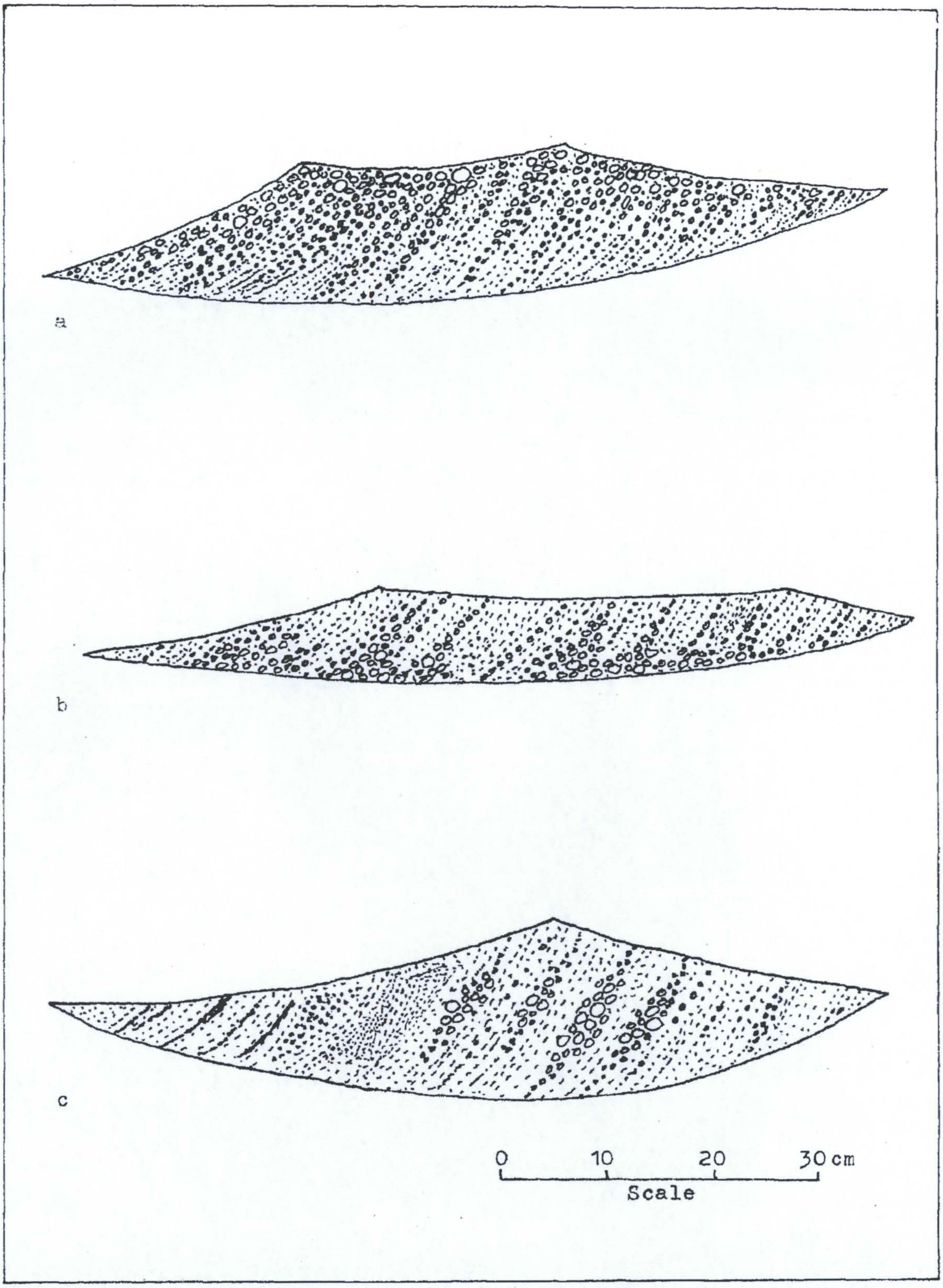

Fig. 3.13 Non-uniform grain size and lithology distribution in cross-stratified sets of Hinuera sediments. For explanation see text (pp.37-41). (a) rhyolitic gravelly quartz sand (b) highly pumiceous gravelly quartz sand (c) pumiceous gravelly quartz sand with concentration of ferromagnesian minerals.

For gravelly sands, the median grain size increased down the forest slope. The coarse fraction of the sediment load was deposited at the top of the forest slope, probably as the result of dispersive pressure caused by grain collisions, but a process of slip, or gravitational sliding, reversed this distribution in the downslope direction.

It is suggested that deposition of the sediments of the Hinuera Formation was commonly sufficiently rapid that the coarse fraction remained at the top of a sedimentary laminae and was preserved in this stage by deposition of the next lamina before appreciable slip-off could occur.

Many sets of cross-stratification are present in which the median grain size increased down the slope of the laminae. This occurred in rhyolitic sandy gravels, but was more common in highly pumiceous sandy gravels with pumice granules and small pebbles concentrated at the bottom of individual laminae (Fig. 3.13b), and may be explained by less rapid deposition enabling gravitational sliding to reverse the original grain size distribution.

Another uncommon phenomenon involving non-uniform grain size distribution of individual laminae is the preservation of "packets" or lersoid laminae of pumice granules and small pebbles, isolated from the upper and lower bounding surfaces of the set (Fig. 3.12c). These laminae of pure pumice alternated with, and were concordant with, laminae of well sorted quartz sand, occasionally showing a similar morphology, and laminae of highly concentrated ferromagnesian minerals. A progressive change in the lithology of laminae from one end of the set to the other is observed in some cases.

The above sediment distribution features cannot be explained in terms of dispersive stress theory and gravitational sliding alone. Other factors such as fall velocity and turbulent diffusion, which contributes to the sorting processes largely responsible for the formation of primary sedimentary structures (Brush, 1965), must be considered in any explanation of such complex sediment distributions.

An important factor in consideration of the sedimentary structures formed during the deposition of the Hinuera sediments is the extremely wide range of specific gravities involved in the different lithologies, from heavy ferromagnesian minerals (average density 4.3), through quartz (2.7) and rhyolitic rock fragments (1.88-2.15)*, to pumice (0.65-1.04)*. Possibly the most important, and as yet largely unknown factor, is the hydrodynamic behaviour of pumice, both when dry and when waterlogged. Without such experimentally derived information, the detailed interpretation of the cross-stratification in the Hinuera Formation in hydrodynamic terms is, at best, limited.

3.2 HORIZONTAL STRATIFICATION

Three distinct types of horizontal stratification are present in the Hinuera Formation, and are here classified according to thickness after McKee and Weir (1953) (Table 3.3).

---

* mean effective field densities (Oliver, 1969).

Beds	very thick-bedded
	100cm
	thick-bedded
	30cm
	medium-bedded
	10cm
	thin-bedded
	3cm
	very thin-bedded
	1cm
Laminae	laminated
	0.3cm
	thinly laminated

Table 3.3 Classification of stratification according to thickness. After McKee and Weir (1953) as modified by Ingram (1954).

(1) Type 1 : Thin to medium-bedded horizontal stratification. This refers to poorly defined horizontal or near horizontal strata, 4 to 25cm thick, preserved in very poorly sorted rhyolitic and pumiceous sandy gravels, and corresponding to the horizontal bedding described by Doeglas (1962). Thin to medium bedded horizontally stratified sediments are volumetrically unimportant, but physically distinctive units (Fig. 3.14), observed at only three exposures (B, F, and H). Lithologically similar deposits are occasionally structureless or massive (Fig. 3.8).

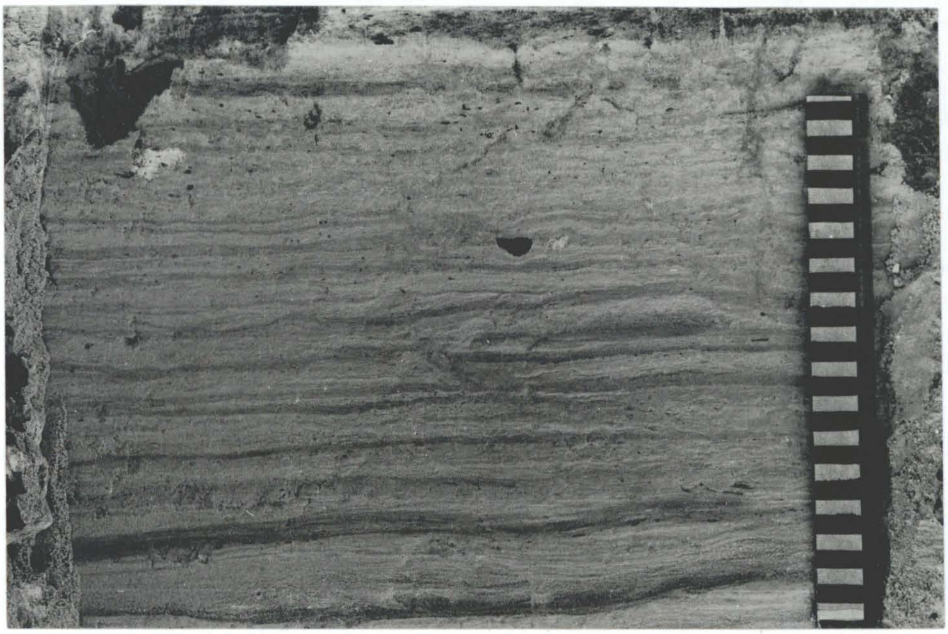

Fig. 3.14 Type 1 horizontal stratification in very poorly sorted rhyolitic and pumiceous sandy gravels. Grid Ref. N66/193336 (Type Section of Hinuera Formation). Scale in cm.

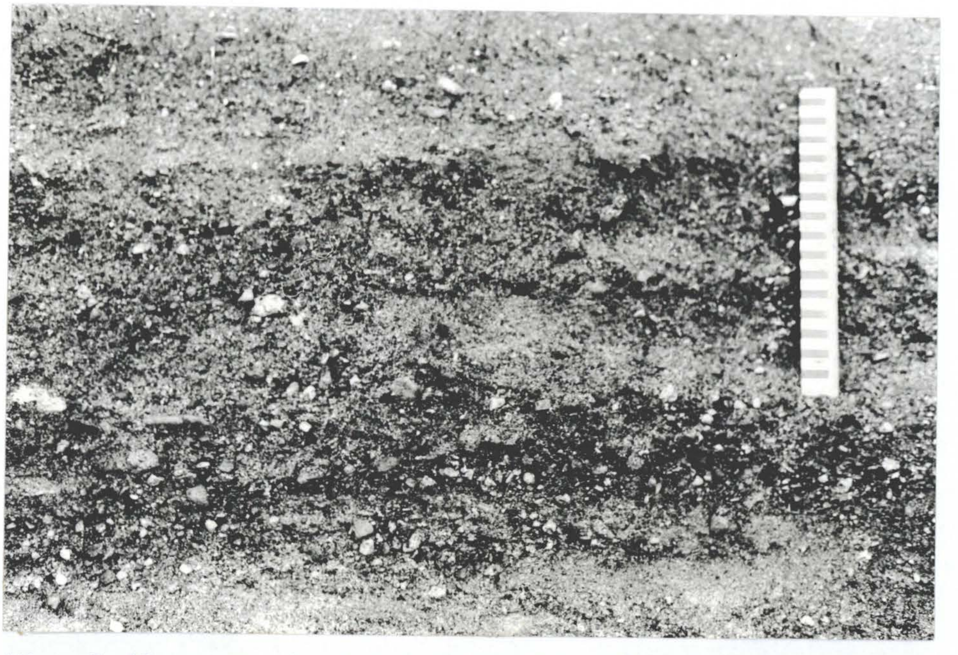

Fig. 3.15 Type 2b horizontal stratification in pumice silts and sandy silts, showing dark laminae of fine sediment alternating with lighter laminae of coarser sediment. Note occasional pebble sized pumice fragments (top left and upper right centre). Grid Ref. N56/795525. Scale in cm.

(2) Type 2 : Thinly laminated to laminated horizontal stratification, of two texturally distinct varieties.

Type 2a : This refers to horizontal or very gently dipping, laterally continuous sets of laminae, each only a few grains thick, preserved in moderately to very poorly sorted rhyolitic and pumiceous gravelly and slightly gravelly quartz sands (Fig. 3.9-A). This type corresponds to the horizontal stratification described by Harms and Fahnestock (1965), and was observed at only one exposure (N65/676427).

Type 2b : This refers to horizontal sets of laminae, 2 to 8mm thick, preserved in some pumice silts and sandy silts, consisting of alternating layers of fine and coarse sediments (Fig. 3.15). The structure corresponds to the parallel stratification described by Harms and Fahnestock (1965), and is particularly well developed in a large, lens-shaped deposit, approximately 60m across and up to 2m thick, at N56/795525. Many of the pumice silts and sandy silts in the Hinuera Formation show no horizontal stratification and appear massive.

3.5 POST-DEPOSITIONAL STRUCTURES

Several different post-depositional structures occur in the Hinuera Formation. They are not common, and most were observed at one exposure (N65/676427).

Liquefaction or partial liquefaction, resulting in a sudden increase in sediment mobility, appears to have played an important part in the formation of many of these post-depositional structures. Liquefaction originates in cohesionless sediment when the pore-water pressure increases to a value at which the shearing strength is zero. When the shearing strength is zero, the sediment behaves like a liquid (van der Lingen, 1969). Pore-water overpressure can be caused by shock, differential loading, or differences in ground-water level (Graff-Petersen, 1967). Sediments in the fine sand to silt range are the most susceptible to liquefaction (Williams, 1963); if liquefaction is in fact the mechanism causing post-depositional deformation in the Hinuera Formation, then the process has involved the mobilisation of sediment as coarse as medium and coarse sand.

Liquefaction appears to be restricted to certain beds in a sequence. In Fig. 3.16 the bed on which the hammer rests appears to have become liquefied. The resulting structures may be explained in terms of a mechanism outlined by Van der Lingen (1969) to explain the liquefaction structures in turbidites. Liquefaction commences at centres where packing is least dense (Williams, 1963), resulting in the development of irregular synclines and anticlines in the sediment. Sediment and water move towards the anticlines, and the confining layers yield to this distortion by plastic deformation. The liquefied sediment can act diapirically and may locally rupture the confining layers, forming an expulsion structure (above and to the left of the hammer in Fig. 3.16), or may inject into the confining layers forming a flame structure (right centre, Fig. 3.16). An alternative origin for the structures in Fig. 3.16 is that the broad dome-shaped structures are erosional features, and that the overlying beds were draped over the domes. This latter

Fig 3.17

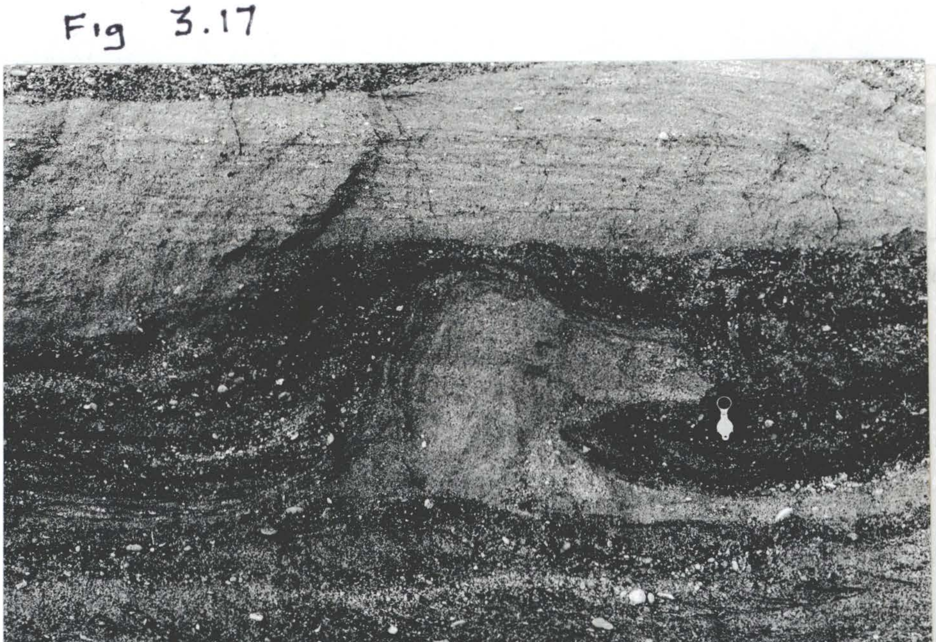

Fig. 3.16 Expulsion structure and flame structures resulting from post-depositional liquefaction. Also shows Nu and Epsilon cross-stratification and Type 2a horizontal stratification. Grid Ref. N65/676427. Hammer is 33cm long.

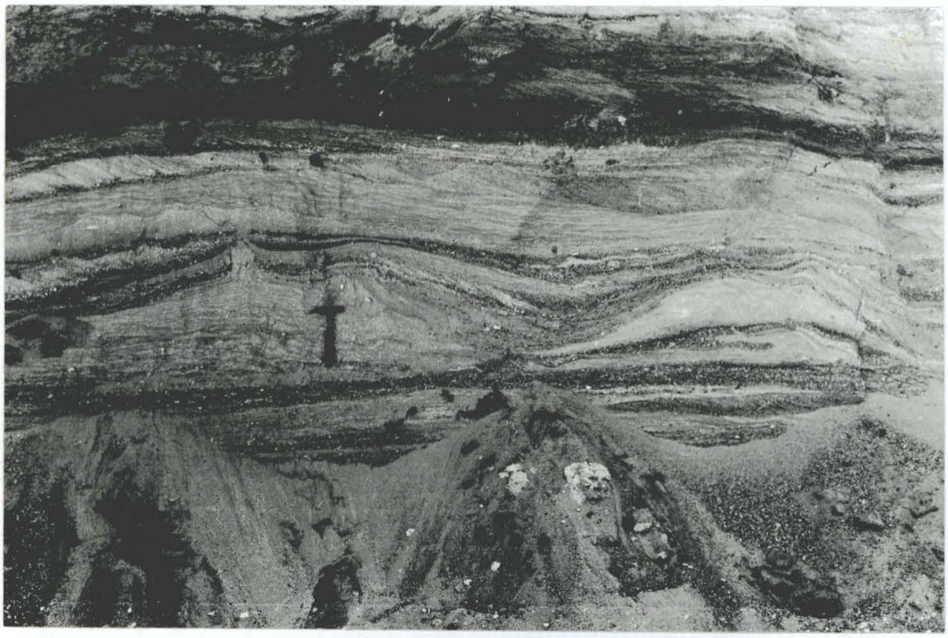

Fig. 3.17 "Injection" structure. Liquefied pumiceous sand has acted diapirically and distorted the overlying confining beds, which have subsequently been planed by erosion and Nu cross-stratified beds deposited above the erosional surface. Grid. Ref. N65/676427. Hand lens is 6cm long.

possibility is rejected because of the presence of expulsion structures (above left of hammer) and convolutions (immediately to the right of hammer), both of which were probably caused by liquefaction. Moreover, if the dome-shaped structures were erosional in origin, it is unlikely that they would have remained upstanding under the hydrodynamic energies necessary for the deposition of the overlying sandy gravels and gravelly sands. To the right and centre of Fig. 3.16 there is a small monoclinal structure which may have formed as a result of the withdrawal of the underlying liquefied bed during the formation of the dome-shaped structure below and to the left of the monocline.

Fig. 3.17 shows another "injection" structure, probably also the result of liquefaction. The pale pumiceous sand in the centre of the photograph liquefied to form an irregular anticline which diapirically distorted the overlying confining beds, but did not rupture them. Erosion subsequently planed the anticlinal form of the overlying beds, as evidenced by cut-off laminae, and Nu cross-stratified beds were deposited above the erosional surface.

Fig. 3.18 shows a small scale expulsion structure in which medium to coarse quartz sand has liquefied and ruptured the confining bed of pumiceous sandy gravel, and caused upward displacement of the overlying stratification.

Another post-depositional structure observed at only one locality (N65/676427) was a type of convolute lamination (Fig. 3.19), which probably also resulted from liquefaction. The laminations are emphasised by limonitic-cemented laminae of fine quartz sand. Only the fine grained laminae in the distorted interval show convolutions ; the coarser grained

Fig. 3.18 Expulsion structure. Pumiceous sand has ruptured the overlying confining beds and distorted the stratification above. Grid Ref. H56/795525. Scale in cm.

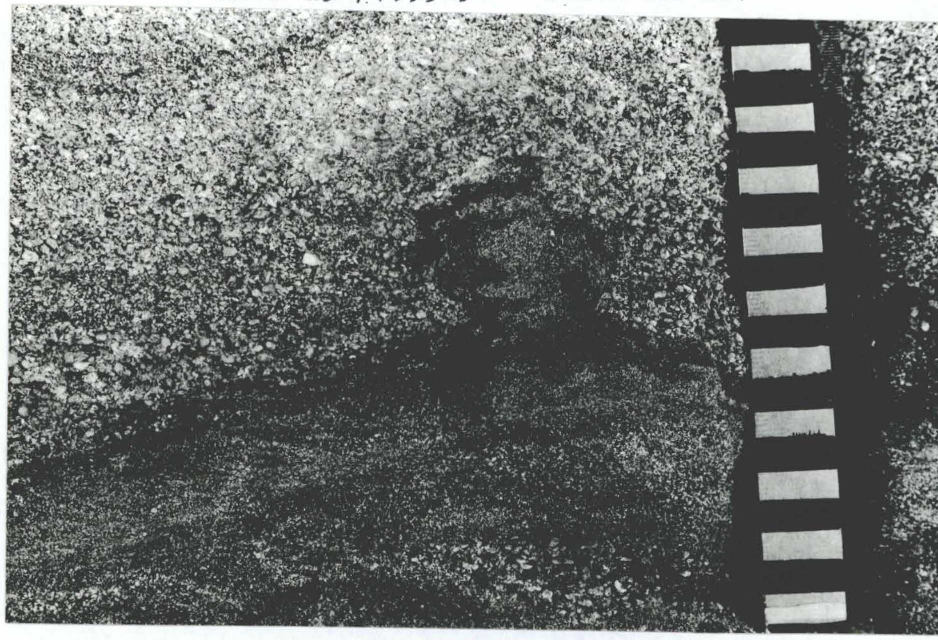

Fig. 3.19 Convolute lamination, emphasised by limonitic cemented laminae of fine quartz sand. Grid Ref. N65/676427. Hand lens is 6cm long.

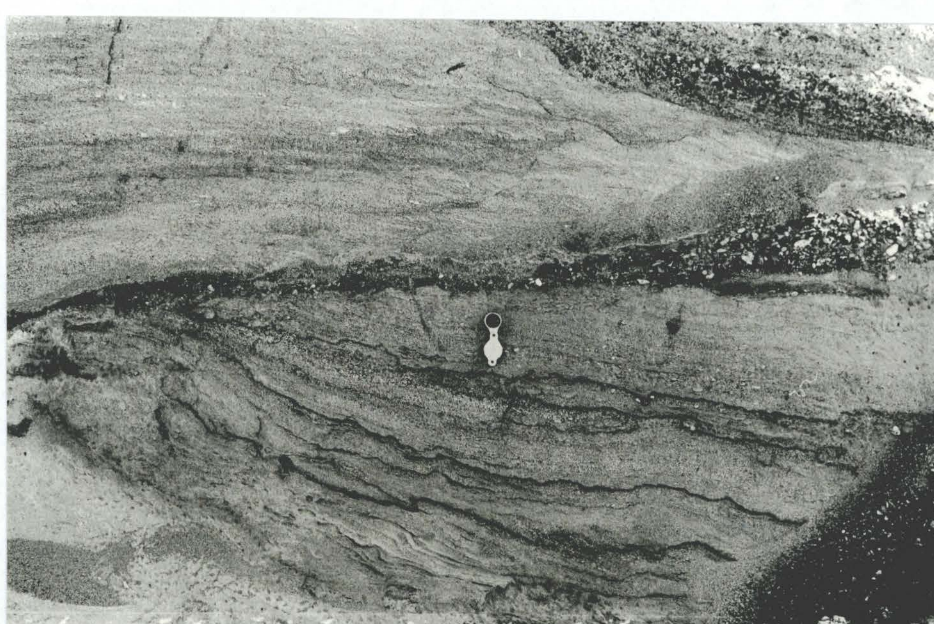

units are not convoluted. This is in agreement with the belief that convolute lamination is limited to fine sand and silt (Kingma, 1958; Dzulinski and Walton, 1965).

Fig. 3.20 shows the combined effects of liquefaction and post-depositional slumping, which has resulted in small scale intrastratal faulting. Beds of pumiceous and rhyolitic gravelly and slightly gravelly sands show displacements of up to 2cm along fault planes, indicating brittle deformation. Overlying these coarse sediments are laminated pumice silts. The silts appear to have liquefied and invaded the underlying sediments, as evidenced by the compressional convolutions of the laminae in the pumice silts. Where these thixotropic fine-grained sediments have punched into the coarser sediments, the latter exhibit plastic deformation. It is suggested that where brittle deformation has occurred, the water content of the sediments was insufficient to allow plastic deformation, and intrastratal faulting resulted, possibly from differential loading. The overlying liquefied sediments were able to punch into the coarse sediments only when the water content of the latter was sufficiently high to allow plastic deformation. There is no evidence to suggest that intrastratal faulting and liquefaction occurred other than simultaneously.

Fig. 3.21 shows large scale scour and post-depositional deformational structures. The predominant primary structure is horizontal stratification, and one bed is Epsilon cross-stratified. At least two cycles of scour, deposition and deformation are shown. The sequence of events producing the resulting complex structures is suggested to be as follows. A broad scour was eroded in a sequence of horizontally stratified beds and became partially filled with a further sequence of horizontally stratified beds, deposited concordant to the

Fig 3.21

Fig. 3.20 Small scale intrastratal faulting. For explanation see text (pp. 20.) Grid Ref. N56/795525. Scale in cm.

Fig. 3.21 Large scale scour and post depositional deformation of predominantly Type 2a horizontally stratified beds. The dark, massive bed at left centre is pumice sandy silt. For explanation see text (pp. 49 to 51). Grid Ref. N65/676427. Hammer is 33cm long.

erosional surface. The latter were subsequently deformed, possibly as a result of gravitational slumping due to overloading following abandonment of the adjacent channel. These post-depositional structures were then partially eroded, as shown by cut-off laminae. A very similar cycle of events followed, culminating in the formation of the large post-depositional contortion to the left of the centre of the large, massive body of pumice silt to the left of the photograph may have combined with gravity slumping to produce partial rotation of the originally horizontally laminated beds near the centre of this contortion. A sequence of Epsilon cross-stratified and horizontally stratified sandy gravels and Nu cross-stratified sands were then deposited, and further post-depositional deformation resulted from complete or partial liquefaction.

It would appear that under suitable conditions, the fine grained units of the Hinuera Formation are susceptible to post-depositional deformation. It is also apparent that fulfilment of these conditions is uncommon. On the evidence available, liquefaction is the most likely mechanism. The origin of the pore-water overpressure necessary for liquefaction may be differential loading, or differences in ground water level. It is suggested that these conditions may be met wherever rapid deposition in an alluvial environment is coupled with relatively major shifts of stream channels.

CHAPTER FOUR

T E X T U R E

4.1 GRAIN SIZE DISTRIBUTION CURVES

Grain size distribution curves were plotted for all samples on arithmetic probability paper with the abscissa scale in phi units, giving a log-probability plot. Other types of plots, such as arithmetic cumulative frequency plots and frequency histograms, are difficult to read and interpret, and changes in slope, amount of mixing, truncation points, and other parameters cannot be easily observed or compared. The striking aspect of the log-probability plot is that the tails of the simple "S" shaped arithmetic cumulative frequency curve appear as straight lines, and the curve usually exhibits two or three straight line segments indicating that grain size distributions do not follow a simple log-normal law. The consistency of the position of truncation points, slopes, and other characteristics for various depositional environments suggest that log-probability plots reflect meaningful relations (Visher, 1969). Spencer (1963) suggested that all clastic sediments consist of three or less log-normally distributed populations; and that sorting is a measure of the mixing of these populations. Each log-normal population has its own mean grain size and standard deviation value. The interpretation of straight line segments in log-probability plots is that each straight line represents a separate log-normal population (Visher, 1969).

The major problem in the study of grain size distributions of sediments is the relation of sedimentary processes to textural responses. Visher (1965, 1969) relates grain size distributions to modes of sediment transport, with each straight line segment of the log-probability plot representing material transported by a different physical process.

Sediment may be transported in alluvial channels by three mechanisms: by rolling or sliding over the stream bed, forming the contact load; by bounching along the bed in a diffuse layer immediately above the bed, forming the saltation load; and by turbulent suspension throughout the entire stream cross-section forming the suspension load. The contact load and the saltation load combine to form the bed load.

Visher's interpretation of the relation of the grain size distribution curve to sediment transporting mechanisms is shown in Fig. 4.1.

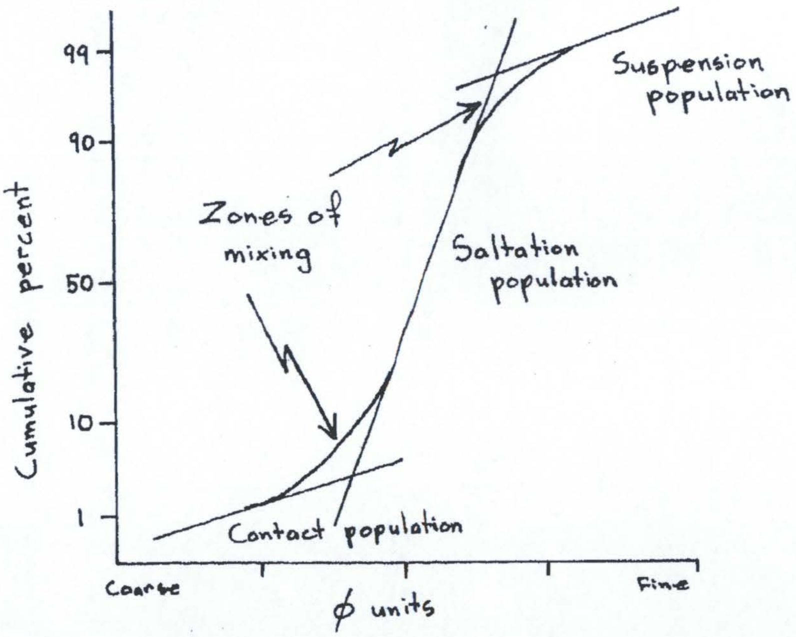

Fig. 4.1 Relation of sediment transport dynamics to populations and truncation points in a grain size distribution. (After Visher, 1969).

Grain size distributions may be characterised by the number, degree of mixing, size range, percentage, and degree of sorting of each log normal-population. If it is assumed that each transportation process is reflected in a single log-normal population within a single grain size distribution, the proportion of each population should be related to the relative importance of the corresponding process in the formation of the whole distribution. The sorting, size range, degree of mixing, and points of truncation of these populations may provide information on currents, rates of deposition and provenance.

Visher (1969) noted that the grain size distribution curves of modern fluvial sediments are characterised by:

(1) a well developed suspension population forming of up to 20 percent of the sample.

(2) a truncation point between suspension and saltation loads between 2.75 and 3.5Ø. This may represent the maximum particle size that vertical turbulence components can maintain in suspension.

(3) a truncation point between saltation and contact loads between 1.75 and 2.5Ø. This may represent the junction between the Stokes and Impact Law formulae (Fuller, 1961) which Visher interprets as the size where inertial forces cause rolling or sliding of particles rather than saltation.

(4) a slope of the saltation population straight line segment in the 60° to 65° range.

The 71 grain size distribution curves plotted for samples of the Hinuera Formation showed a high degree of variability. Approximately one third of the curves were of sigmoidal shape with the tails forming straight lines, giving three straight line segments (Fig. 4.2a) similar to Visher's pattern. These simple sigmoidal curves are characterised by:

(1) a poorly developed suspension population, usually less than 5 percent, but up to 20 percent of the sample.

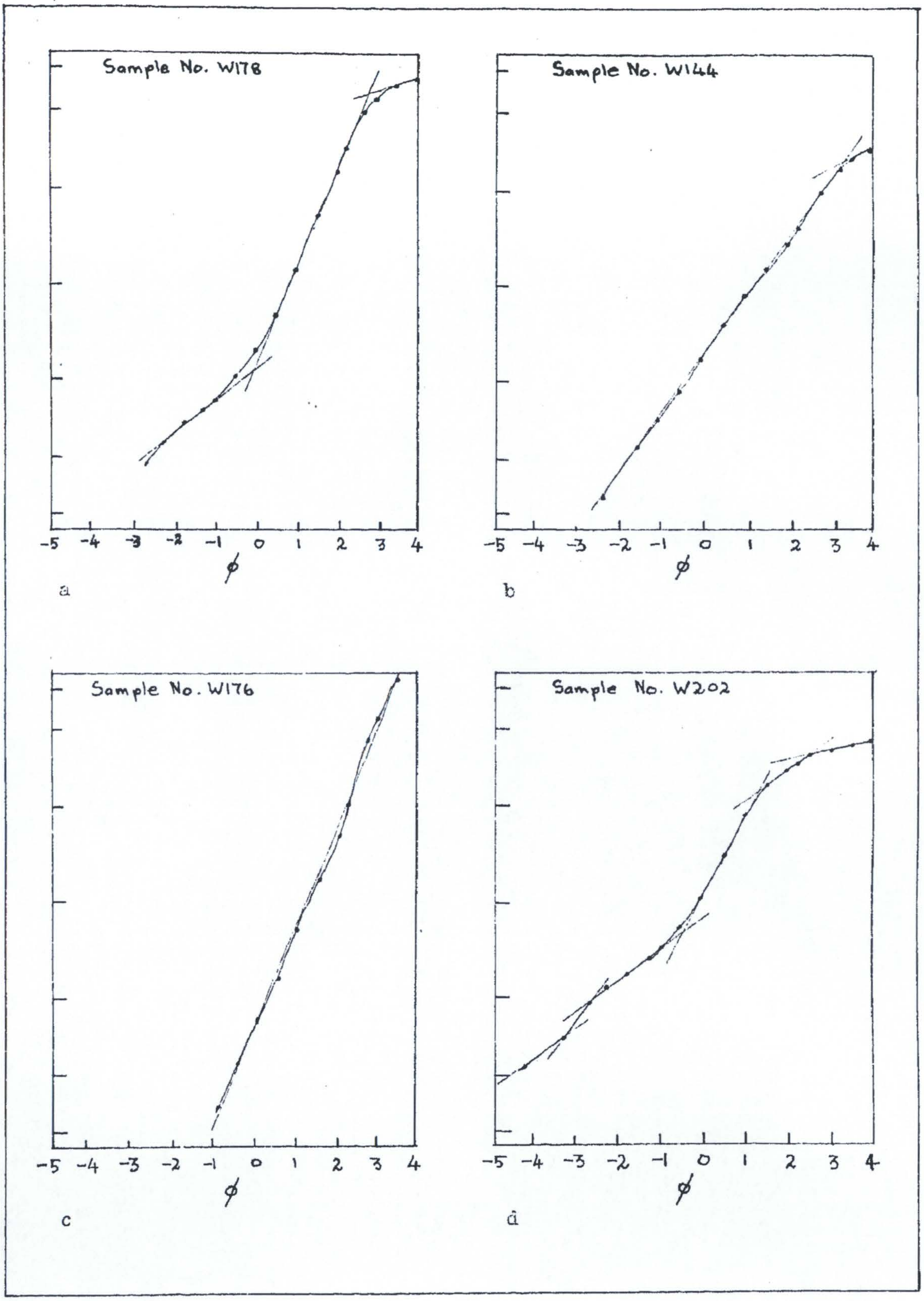

Fig. 4.2 Cumulative size frequency curves with straight line segments showing log-normally distributed populations.

(2) a truncation point between suspension and saltation loads between 2.2 and 3.5Ø.

(3) a truncation point between saltation and contact loads between -3.0 and 2.5Ø.

(4) a slope of the saltation population segment in the 55° to 70° range.

(5) a very well developed saltation population forming up to 90 percent of the sample.

The notable differences between these characteristics and those of Visher's distribution curves for fluvial sediments are the very coarse limit for the saltation population (-3.0Ø cf 1.75Ø), the greater range in the slope (sorting) of the saltation population segment, and the small suspension population (5% cf 20%). The curves for the Hinuera Formation samples suggest that in at least one instance, material of small pebble size (-3.0Ø) has been transported in saltation. The average truncation between saltation and contact load is at about -1.0Ø, which is very much coarser than Visher's truncation limit (1.75Ø), and indicates that very coarse sand has been transported in saltation. The coarse truncation point of the saltation population reflects the shear at the depositional interface (Visher, 1969), with high shear produced by high bed layer current velocities. If Visher's interpretation of this is correct, that the coarse truncation point is the particle size where inertial forces cause rolling or sliding rather than saltation, then a depositional environment of unusually high energy is indicated. This is supported by a coarse saltation suspension truncation point. The position of this fine truncation point may reflect turbulent energy at the depositional interface (Visher, 1969) and the fact that the fine truncation point for the saltation population of Hinuera sediments is commonly 0.5 phi greater than the limit indicated by Visher for fluvial sediments indicates a very high turbulent energy. The amount of the saltation population is partly dependent on the rate of deposition (Visher, 1969) and a saltation population of up to 90 percent in the Hinuera sediments indicates rapid deposition.

The suspension population reflects the conditions above the depositional interface. Sorting of this population and mixing with the saltation population appear to reflect turbulence in the overlying fluid and the presence of a boundary layer (Visher, 1969). The small, poorly sorted suspension population present in almost all the Hinuera sediment curves indicates that strong currents produced a boundary layer which restricted the amount and sorting of the suspension population included in the grain size distribution. Most curves show a moderate degree of mixing between the saltation and suspension populations (Fig. 4.1). In true suspension there is no variation of sediment concentration between the surface and the depositional interface, allowing some of this material to be deposited by interaction with coarser material at the sediment-water interface. Strong mixing between saltation and suspension populations appears to be related to highly variable energy conditions, which result in partial destruction of the boundary layer (Visher, 1969). The variation in the slope of the saltation population, which is a measure of sorting, also suggests highly variable energy conditions.

Some distribution curves for Hinuera sediments show a small suspension population, a well developed saltation population, and apparently no contact load population (Fig. 4.2b). Certain fluvial deposits do not show a contact load population (Visher, 1969). The reason for this is unknown, but Visher suggests that is is probably related to the removal of part of the coarsest fractions and to the strong shear at the depositional interface in deposits formed by continuous currents. An alternative explanation is that material of the appropriate grain size was not available at the time of deposition.

A few curves show a saltation population only (Fig. 4.2c) which may be the result of an extreme degree of mixing between suspension and saltation populations.

The remaining two thirds of the grain size distribution curves plotted for Hinuera sediments cannot be described and interpreted in terms of three or less straight line segments, but are most complex with commonly four and up to five or six straight line segments (Fig. 4.2d). The inference is that there are up to five or six log-normally distributed populations present. Two independant lines of reasoning may be pursued to explain this apparent anomaly: the first considers the mixing of two or more log-normally distributed populations in bimodal or polymodal sediments; the second considers the concept of the sedimentation unit and the effect of sampling procedures on grain size distribution curves.

Tanner (1964) noted that sediment size distributions commonly plot, on probability paper, as zig-zag lines. He showed that two or more log-normal distributions can be plotted on probability paper and then mixed in any desired proportions, a non-log-normal plot is obtained. If two distributions are combined by simple addition in equal proportions, the combined curve shows three straight line segments (Fig. 4.3). Variations in the characteristics of the combined curve depend on the number and proportions of the mixed populations.

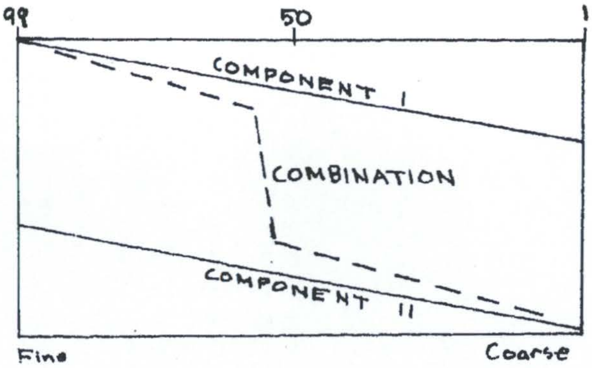

Fig. 4.3 Two components (1 and 11) with different means, mixed in equal proportions, and the combination obtained by simple mixing. Two inflection points appear. After Tanner (1964).

Dyer (1970) showed that when cumulative grain size distribution curves are plotted on arithmetic probability paper for bimodal sandy gravels, a zig-zag trend was obtained for most curves. Spencer (1963) considered the effects of sorting on bimodal grain size distributions and showed that all the Mississippi delta sediments may be adequately described by two separate log-normal grain size populations, or the two mixed together in various proportions as a result of sorting. Pettijohn (1957) drew attention to the fact that materials in the -1 to -2 phi and 3 to 5 phi range seem to be deficient in clastic sediments as a whole, and suggested that the process of rock disintegration may yield products of varying grain size and produce more of certain sizes and less of others. Three fundamental populations appear to exist in clastic sediments as a result of rock breakdown along joints or bedding planes yielding gravel sized particles, granual disintegration and abrasion yielding grains of sand size and chemical decomposition yielding clay. Spencer (1963) stated that all the grain size distribution curves he studied could be adequately described by either the three fundamental populations, mixtures of the three, the truncated form of any particular combination, or mixtures of truncated forms.

Very few Hinuera sediments are unimodal, most are bimodal or trimodal, and some were quadrimodal (See section 4.2.1). The greater the number of modes in any particular samples, the more complex is the grain size distribution curve for that sample.

It is suggested that the complex grain size distribution curves for polymodal Hinuera sediments are, in part at least, the result of mixing of up to four provenance dependant, log-normally distributed populations, each with its own mean grain size, in proportions determined by sorting processes.

Another factor in the consideration of grain size distribution curves is the interpretation of the sedimentation unit, which becomes critically important when dealing with sediments as heterogenous as the Hinuera Formation. Jopling (1964) discussed the concept of the sedimentation unit, and summarised the problem by stating that the precise definition of the sedimentation unit depends upon the scale factor, and upon the desired degree of resolution. Otto (1938) defined the sedimentation unit as "that thickness of sediment which was deposited under essentially constant physical conditions". A set of cross-strata (McKee and Weir, 1953) is generally accepted by field geologists as the basic sedimentation unit, and it was on this basis that all samples in this study were taken from single sets of cross-strata. However, as stated by Pettijohn (1957), cross-laminations record local and short-timed fluctuations in the velocity of the depositing current. Moss (1962) concluded that a sample from a single sedimentary lamina is usually a composite with up to three particle populations, and so a sample derived from, say, five laminae may contain up to 15 particle populations. For the purposes of environmental studies on the investigation of depositional processes, Moss believed that such a sample does not represent a discrete sedimentation unit. Jopling (1964) concluded that well-defined laminae can be deposited under a fairly wide range of flow conditions (including uniform conditions), and that until more refined interpretive techniques become available, theorising on the "essentially constant" conditions of deposition is not justified. Visher (1965, 1969) has since produced more adequate interpretive techniques with his recognition of log-normal populations within grain size distributions, dependant on modes of sediment transport, but appears to ignore the considerations discussed by Jopling. Because of this uncertainty, a set is here interpreted to lie within Otto's definition of a sedimentation unit. However, the composite nature of single laminae and the extreme heterogeneity of laminae within sets of the Hinuera Formation very probably contribute to the complexity of the grain size distribution curves obtained.

4.2 STATISTICAL PARAMETERS

Statistical parameters (Table 4.1, after Folk and Ward, 1957) were calculated for all samples. The verbal limits for these parameters, as suggested by Folk (1968), are included in Table 4.1. The results of analyses are presented in Appendix I. A grain size scale with verbal equivalents is presented in Table 4.2.

It should be noted that in the characterisation of size frequency distributions, standard deviation is a measure of the spread of phi units of the sample; negative or positive

Graphic Mean

$$M_z = \frac{\phi16 + \phi50 + \phi84}{3}$$

Inclusive Graphic Standard Deviation

$$\sigma_I = \frac{\phi84 - \phi16}{4} + \frac{\phi95 - \phi5}{6.6}$$

Verbal Classification:

σ_I under 0.35ϕ	very well sorted (vws)
0.35 to 0.50ϕ	well sorted (ws)
0.50 to 0.71ϕ	moderately well sorted (mws)
0.71 to 1.0ϕ	moderately sorted (ms)
1.0 to 2.0ϕ	poorly sorted (ps)
2.0 to 4.0ϕ	very poorly sorted (vps)
over 4.0ϕ	extremely poorly sorted (eps)

Inclusive Graphic Skewness

$$Sk_I = \frac{\phi16 + \phi84 - 2\phi50}{2(\phi84 - \phi16)} + \frac{\phi5 + \phi95 - 2\phi50}{2(\phi95 - \phi5)}$$

Verbal Classification:

Sk_I from +1.00 to +0.30	strongly fine-skewed (sfs)
+0.30 to +0.10	fine-skewed (fs)
+0.10 to -0.10	near-symmetrical (ns)
-0.10 to -0.30	coarse-skewed (cs)
-0.30 to -1.00	strongly coarse-skewed (scs)

Graphic Kurtosis

$$K_G = \frac{\phi95 - \phi5}{2.44(\phi75 - \phi25)}$$

Verbal classification:

K_G under 0.67	very platykurtic (vpk)
0.67 to 0.90	platykurtic (pk)
0.90 to 1.11	mesokurtic (mk)
1.11 to 1.50	leptokurtic (lk)
1.50 to 3.00	very leptokurtic (vlk)
over 3.00	extremely leptokurtic (elk)

Table 4.1 Statistical Parameters (after Folk and Ward, 1957).

MILLIMETERS	PHI (Ø)	WENTWORTH SIZE SCALE	
		BOULDER	GRAVEL
256	-8.0		
192	-7.5	LARGE COBBLE	
128	-7.0		
96	-6.5	SMALL COBBLE	
64	-6.0		
		VERY LARGE PEBBLE	
32	-5.0		
		LARGE PEBBLE	
16	-4.0		
		MEDIUM PEBBLE	
8	-3.0		
		SMALL PEBBLE	
4	-2.0		
		GRANULE	
2	-1.0		
		VERY COARSE SAND	SAND
1	0.0		
		COARSE SAND	
0.5	1.0		
		MEDIUM SAND	
0.25	2.0		
		FINE SAND	
0.125	3.0		
		VERY FINE SAND	
0.0625	4.0		
		SILT	MUD
0.0039	8.0		
		CLAY	

Table 4.2 Grain size scale for sediments

skewness indicates asymmetry towards the coarser or the finer fraction respectively; platykurtosis and leptokurtosis indicate a poorer and better sorting respectively in the central part of the distribution as compared with the tails.

4.2.1. Average Grain Size

Two measures of average grain size are used in this study; mean grain size and mode.

Mean size is a function of the size range of materials available, and the amount of energy imparted to the sediment which depends on current velocity or the turbulence of the transporting medium (Folk, 1968).

A histogram of mean grain sizes for the Hinuera Formation is presented in Fig. 4.4. The range of mean grain sizes is from -2.45Ø (small pebble) to 6.03Ø (medium silt).

The range and general coarseness of mean grain size indicates that a wide range of grain sizes was available and that this material was transported by currents of high velocity or turbulence. It is notable that there is no decrease in mean grain size in the sections studied between Cambridge and the Taupiri Gorge.

Important textural studies by Friedman (1961) and Sevon (1966) used grain size parameters to distinguish different environments of clastic sedimentation, but comparison with mean grain size or other parameters of Hinuera sediments cannot be made as only fine and medium sands were used by these authors.

Modal grain sizes for the Hinuera sediments samples were determined from sieve analysis data. Very few samples were unimodal, most were bimodal and trimodal, and some were quadrimodal. Fig. 4.5 is a histogram in which modal grain sizes are plotted as a function of the numerical occurrence of

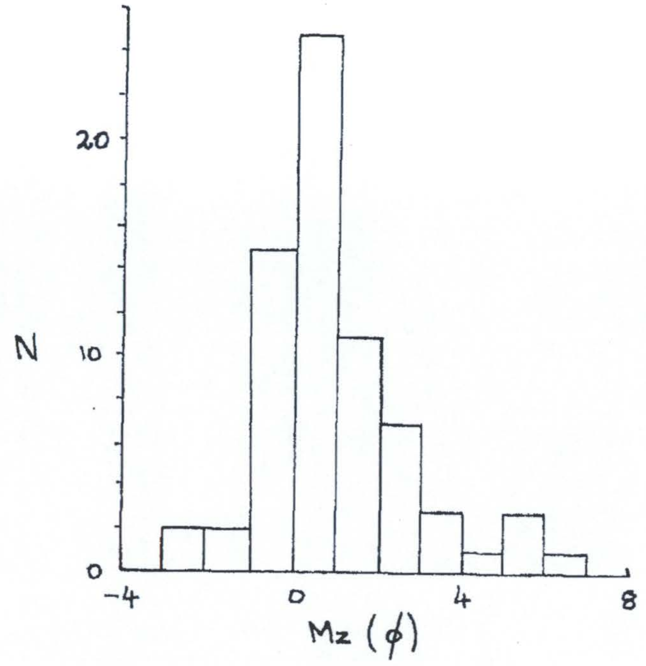

Fig. 4.4 Histogram of mean grain sizes (Mz) plotted as a function of their numerical occurrence (N).

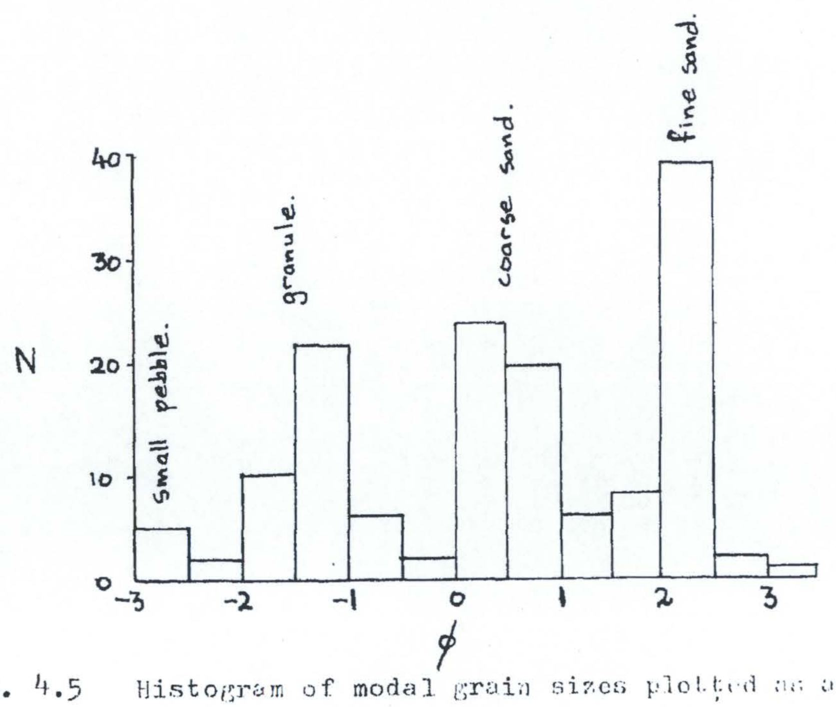

Fig. 4.5 Histogram of modal grain sizes plotted as a function of their numerical occurrence (N) in Hinuera sediments.

each mode. A quadrimodal grain size distribution for Hinuera sediments is shown, with gravel modes at -2.5 to -3.0Ø (small pebble) and -1.0 to -2.0Ø (granule), and sand modes at 0 to 1.0Ø (coarse sand) and 2.0 to 2.5Ø (fine sand). The mode at -1.0 to -2.0Ø is not in accordance with the widely recognised scarcity of particles of this size range in clastic sediments (Pettijohn, 1957). If is suggested that the two gravel modes are the result of physical disintegration of the source rocks, the two sand modes are the result of the release of mineral grains from the course rocks during this process.

The modes for each sample were related back to the straight line segments of their respective grain size distribution curves, and the transport mechanisms inferred from these segments (see section 4.1). In all but a few instances, the small pebble mode was transported as contact load. The granule mode was transported as bed load, either in saltation, or more commonly as contact load. The coarse sand mode was always transported as saltation load. The fine sand mode was usually coarser than the suspension-saltation truncation point, showing transport by saltation also. However, a moderate degree of mixing is shown by the latter two populations (see section 4.1) and the fine sand modal value is frequently within this zone of mixing.

4.2.2. Sorting

A histogram of sorting values is presented in Fig. 4.6. Samples ranged from very well sorted to very poorly sorted. Sorting is dependant on four major factors (Folk, 1968) (1) the size range of material supplied to the environment (2) the type of deposition (3) current characteristics and (4) the rate of supply of detritus compared with the efficiency of the sorting

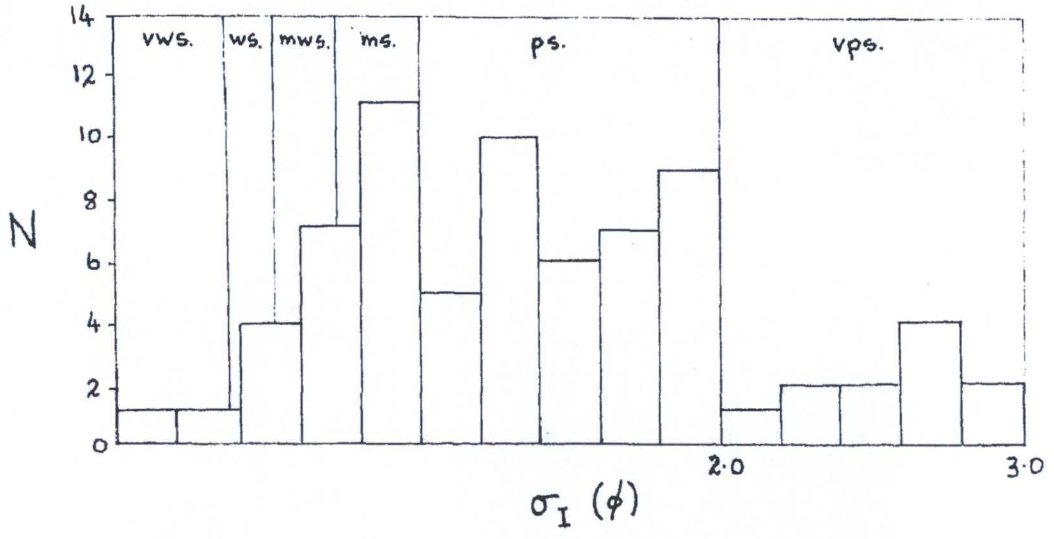

Fig. 4.6 Histogram of sorting values (σ_I) plotted as a function of their numerical occurrence (N).

agent. It has already been shown (section 4.2.1.) that a wide range of particle sizes was supplied to the depositional agent of the Hinuera Formation. The generally poorly sorted sediments indicate rapid deposition by strong, fluctuating currents and/or a rapid influx of sediment into the stream system.

Sorting is generally strongly dependant on grain size (Folk, 1966, 1968), and this trend can be evaluated by plotting mean size (mz) as a function of sorting (σ_I). A sinusoidal relationship between size and sorting is generally obtained (Folk, 1966, 1968) (Fig. 4.7). Folk (1966) believes that this sorting trend is caused by the high frequency of pebbles, sand and clay in nature, with a relative lack of granules and fine silt.

Fig. 4.8 is a scatter plot of mean size against sorting. A V- shaped trend is shown which fits onto the sinusoidal trend of Folk. As the mean grain size of the gravels increases however, they continue to become more poorly sorted rather than better sorted. This is probably a function of rapid deposition, preventing washing out finer sediments. The mode of granule sized material in Hinuera sediments does not appear to affect the sinusoidal relationship.

4.2.3 Skewness

Skewness is environmentally sensitive; kurtosis is not (Friedman, 1961). Awasthi (1970) used the sign of skewness to differentiate between environmental conditions of deposition of Recent sands of the Solani River system, Roorke, India, correlating positively skewed sediments irrespective of numerical value with a clam and steady environment of sedimentation, and negatively skewed sediments irrespective of numerical value with turbulent energy conditions of the depositing medium.

Friedman (1961) noted that coarse grained river sands and gravels had variable, unpredictable skewness characteristics and

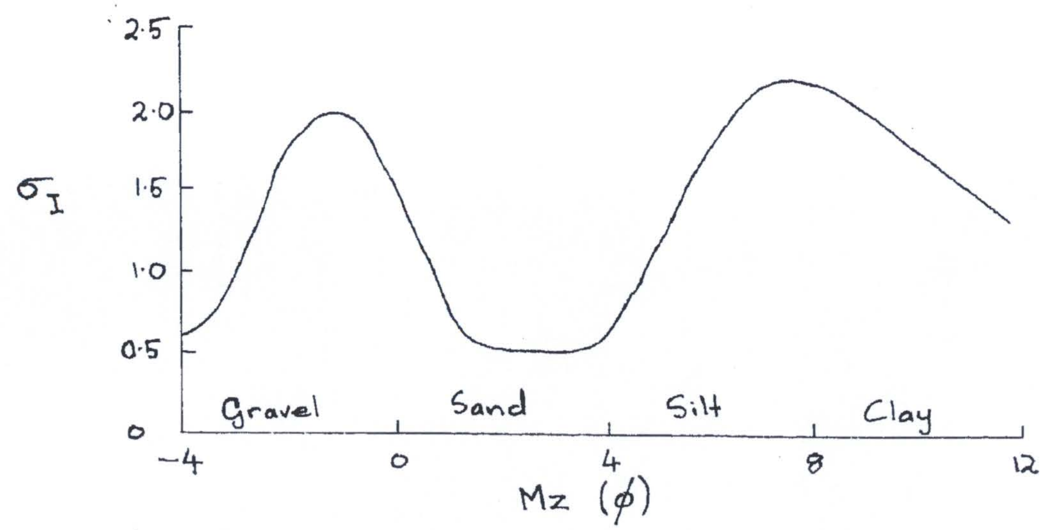

Fig. 4.7 General mean grain size (Mz) vs. sorting (σ_I) curve for clastic sediments showing sinusoidal relationship between these parameters. (After Folk, 1968).

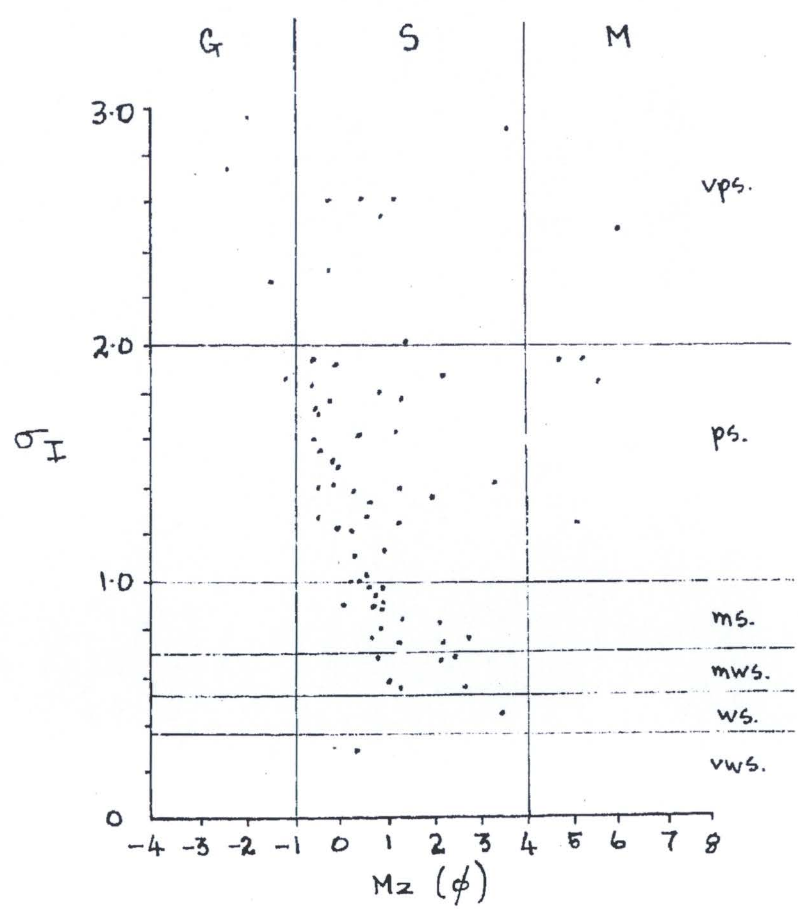

Fig. 4.8 Plot of sorting (σ_I) against mean grain size (Mz)

could not be employed as an indicator of the depositional environment. Only medium, fine, and very fine sands were used in Friedman's study, and these were generally positively skewed.

Skewness values between +0.77 and -0.75 were obtained for sediments of the Hinuera Formation. Distribution about zero is nearly symmetrical, with only a slight tendency towards positive skewness (Fig. 4.9).

When skewness is plotted as a function of mean grain size for Hinuera sediments (Fig. 4.10), a trend towards positive skewness with decreasing grain size is evident. All samples with a mean grain size finer than 1.5Ø (medium sand) are positively skewed. Positive skewness in medium and fine grained river sands is believed to be the result of the unidirectional flow of the depositing medium (Friedman, 1961), a relationship which does not hold for coarse grained sediments. It is suggested that rapid deposition, which prevents a washing out of fines, is an alternative explanation for positive skewness in fine grained Hinuera sediments. For coarser sediments, there is no relation between skewness and mean grain size, and samples from within a few metres, and even tens of centimetres, may show reversals in the sign of skewness. Two samples (W195, W196) from opposite ends of a single cross-stratified set were opposite in sign of skewness which may be an indication of rapid, short-lived fluctuations in the depositing medium of the coarse-grained Hinuera sediments (Awasthi, 1970). It is notable that the sign of skewness tends to be constant at any one locality (Appendix I), suggesting a relative consistency of energy throughout a depositional phase at any one place.

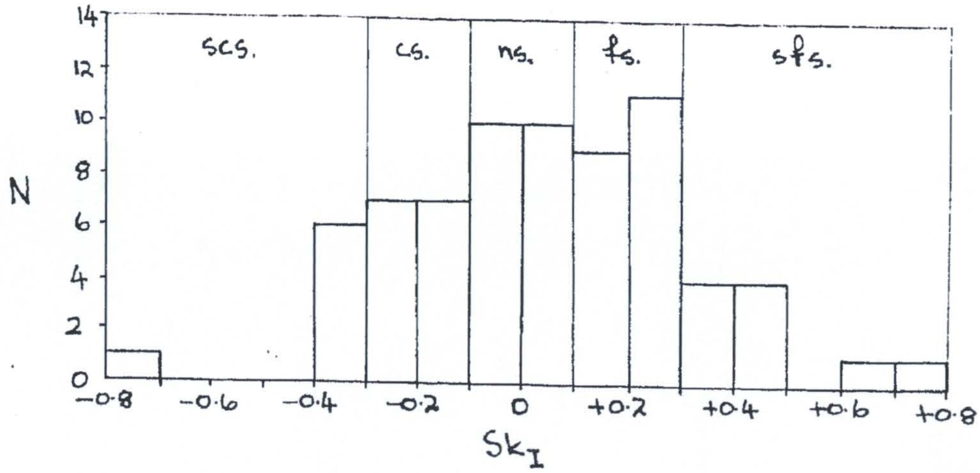

Fig. 4.9 Histogram of skewness balues (Sk_I) plotted as a function of their numerical occurrence (N).

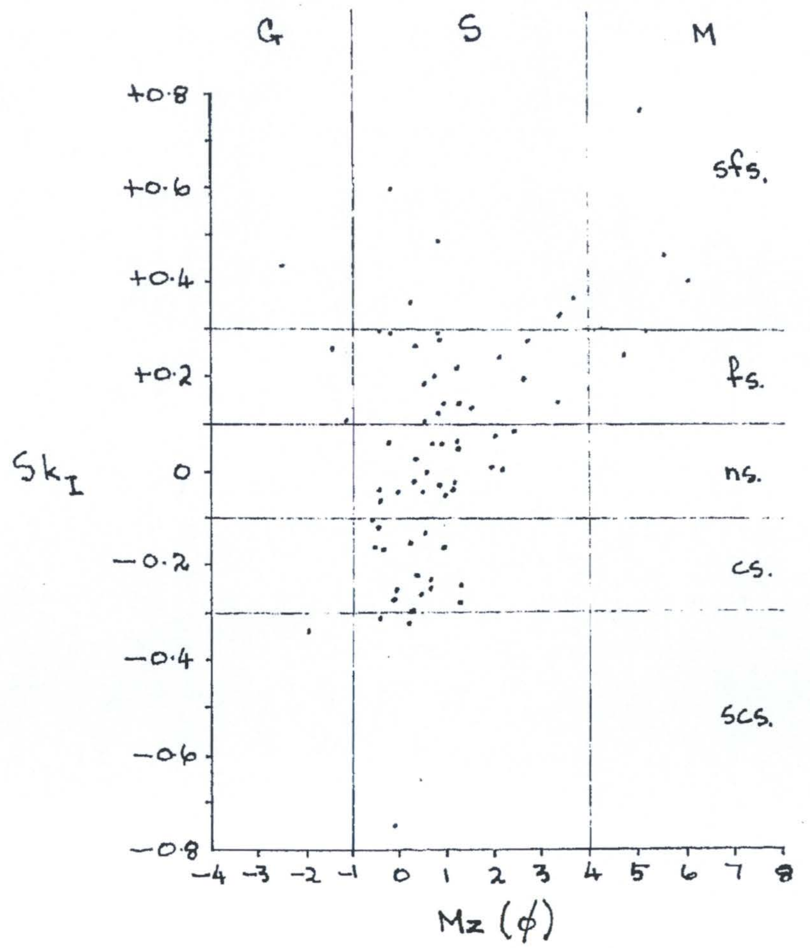

Fig. 4.10 Plot of skewness (Sk_I) against mean grain size (Mz).

4.2.4. Kurtosis

Samples ranged from very leptokurtic to very platykurtic (Fig. 4.11), with a slight tendency towards leptokurtic values. Kurtosis in itself is not environmentally diagnostic, but its relation to other grain size parameters is important. A plot of kurtosis (K_G) against mean grain size (Mz) (Fig. 4.12) shows a slight tendency towards platykurtosis with increasing grain size. With one exception, all platykurtic or very platykurtic samples have a mean grain size less than 0.5∅.

Folk and Ward (1957) found that when mean size, sorting, and skewness were coplotted in three dimensions, a helix resulted, with kurtosis varying along the helix (mean vs. sorting, sinuscidal; vean vs. skewness, sinusoidal; sorting vs. skewness, circular). Helical trends have since been found for many other distributions with two distinctly separated populations (e.g. Dyer, 1970). However, plots for sediments of the Hinuera Formation show a sinusoidal relation between mean grain size and sorting (Fig. 4.8), but no relation between skewness and kurtosis, (Fig. 4.13) or between sorting and skewness (Fig. 4.14). This is very probably the result of the polymodality and heterogeneity of the Hinuera Formation.

4.3 TEXTURAL PLOTS

The proportions of gravel (less than -1.0∅), sand (between -1.0 and 4.0∅), and mud (greater than 4.0∅ i.e. silt plus clay) were calculated for 75 samples from grain size analysis data. Dry material that passed through the 240 mesh (4.0∅) sieve after sieve analysis was added to the mud weight obtained by wet sieving and to the total sample weight. The results (Appendix II) are plotted on a triangular gravel-sand-mud diagram (Folk,

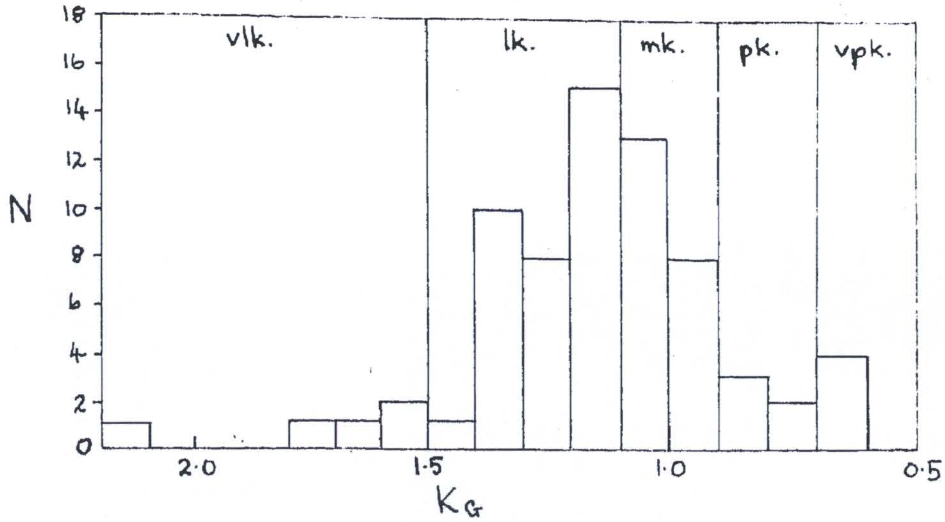

Fig. 4.11 Histogram of kurtosis values (K_G) plotted as a function of their numerical occurrence (N).

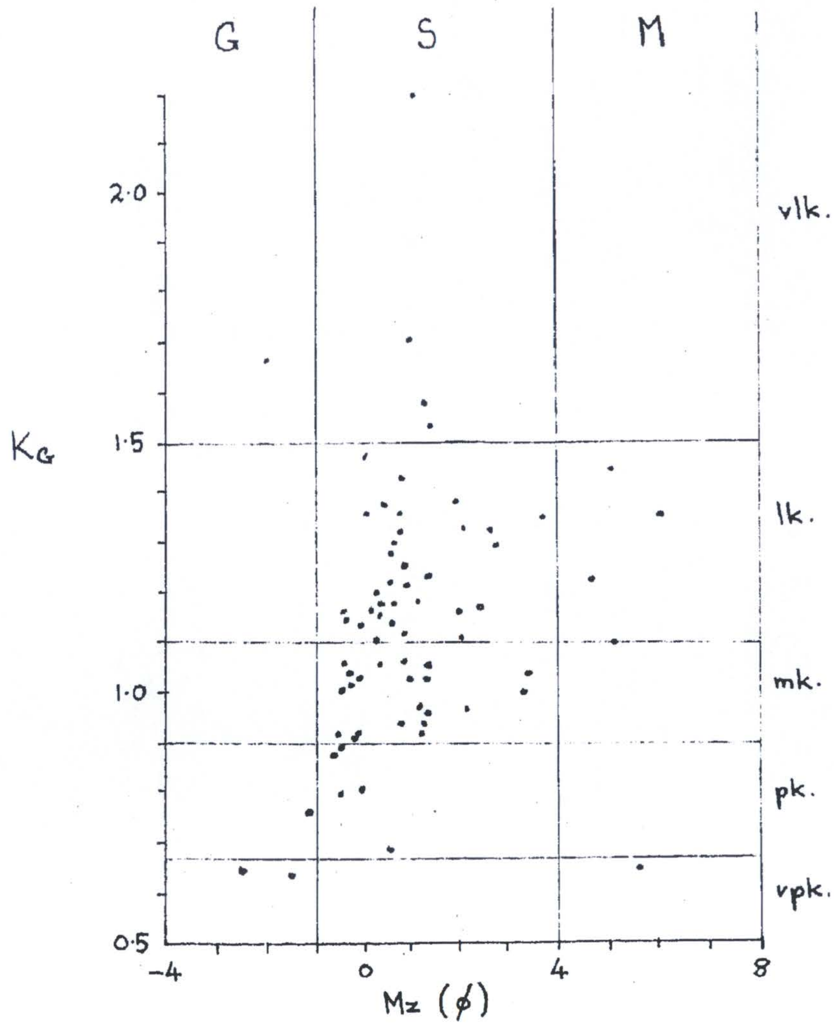

Fig. 4.12 Plot of kurtosis (K_G) against mean grain size (Mz).

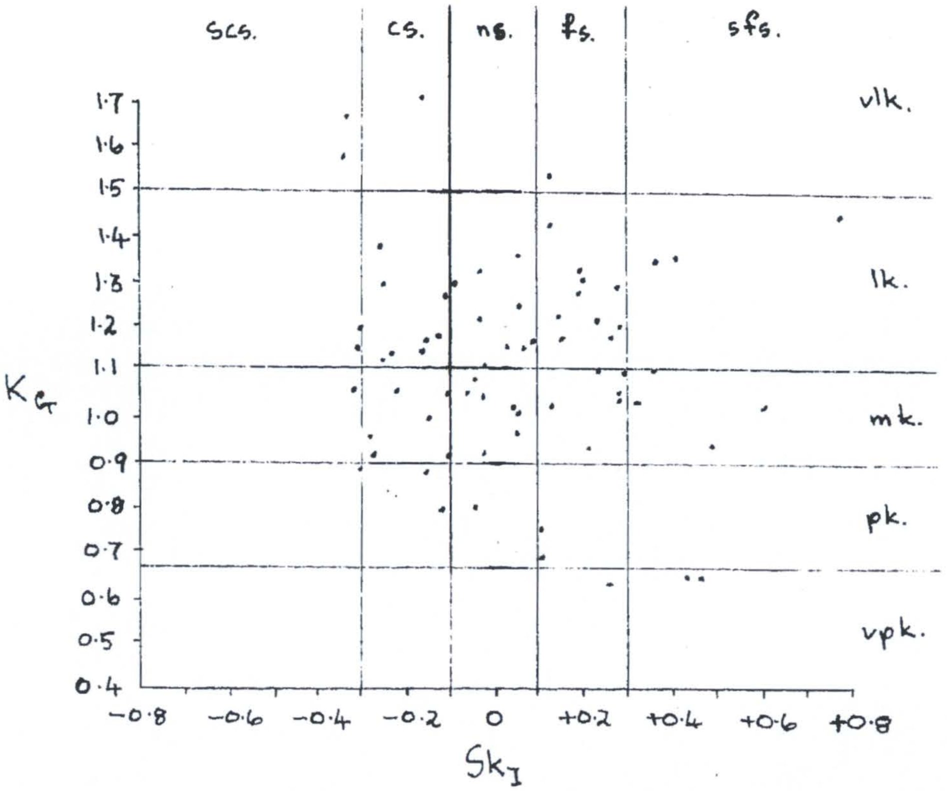

Fig. 4.13 Plot of kurtosis (K_G) against skewness (Sk_I).

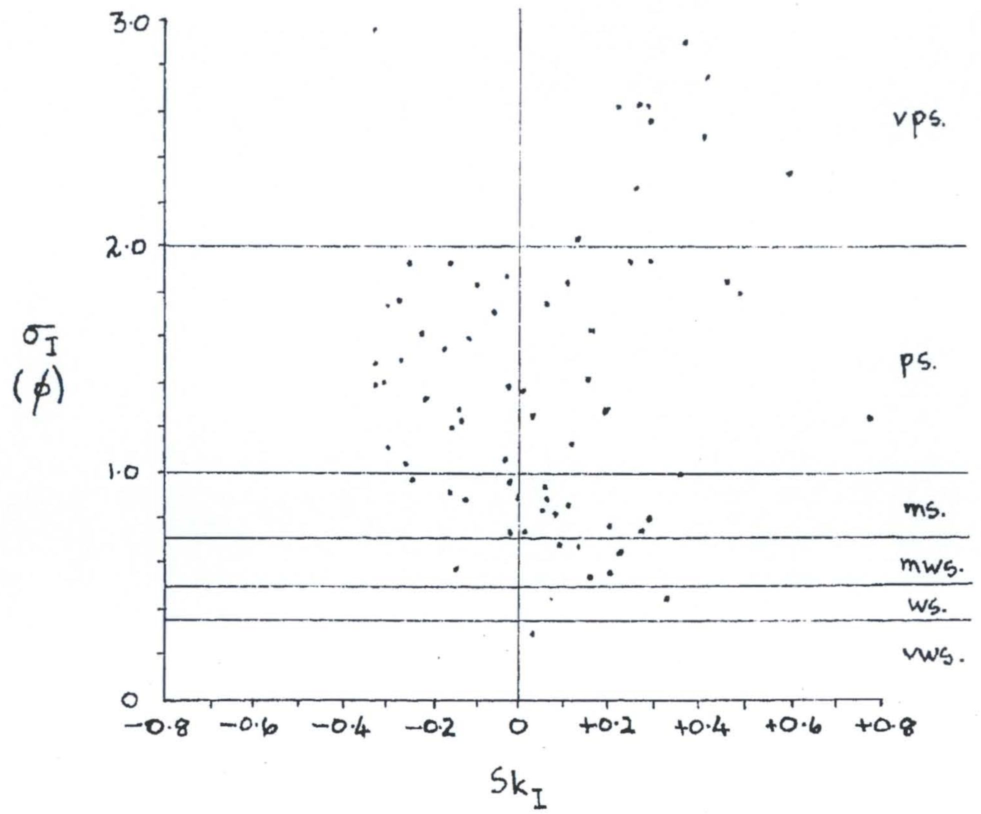

Fig. 4.14 Plot of sorting (σ_I) against skewness (Sk_I).

1968), enabling the samples to be placed in one of fifteen major textural groups (Fig. 4.15a). Folks divisions are used here with the exception that the sandy gravel/gravelly sand boundary is placed at 45 percent gravel instead of 30 percent gravel for the reason that a more natural division of samples is obtained. The natural breaks at 5 percent and 30 percent gravel reported by Folk, Andrews, and Lewis (1970) do not appear to exist in the sediments of the Hinuera Formation.

All the samples plot within 11 major textural groups (Fig. 4.15b). The most significant features to appear are that there are no true gravels and that the samples generally show a low content of mud : 77 percent of the samples contain less than 10 percent mud and 69 percent contain less than 5 percent mud. By far the most common textures are gravelly and slightly gravelly sands : 65 percent of the samples fall into these two groups. Nine percent of the samples are muds or sandy muds, and are clearly texturally distinct from the other samples. Because of their uniqueness the proportion of muds in the Hinuera Formation is probably exaggerated by a sampling bias. From pipette analysis data, five of these samples were plotted on a triangular sand-silt-clay diagram (after Folk, 1968) and classified according to Folk's textural divisions (Fig. 4.1b). None of the samples contained significant proportions of clay sized material, and are silts or sandy silts.

It is concluded that the currents that deposited the gravelly and slightly gravelly sands and associated sediments generally washed their deposits free from significant amounts of silt and clay, and had a sufficiently high degree of competence to more significant amounts of gravel. In contrast, the currents that deposited the silts and sandy silts had sufficient competence to move only small quantities of fine sand, although their deposits

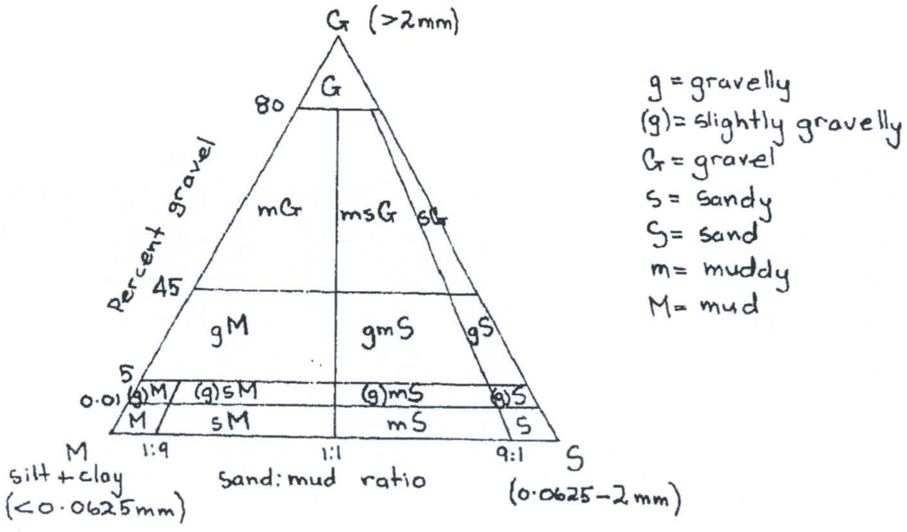

a

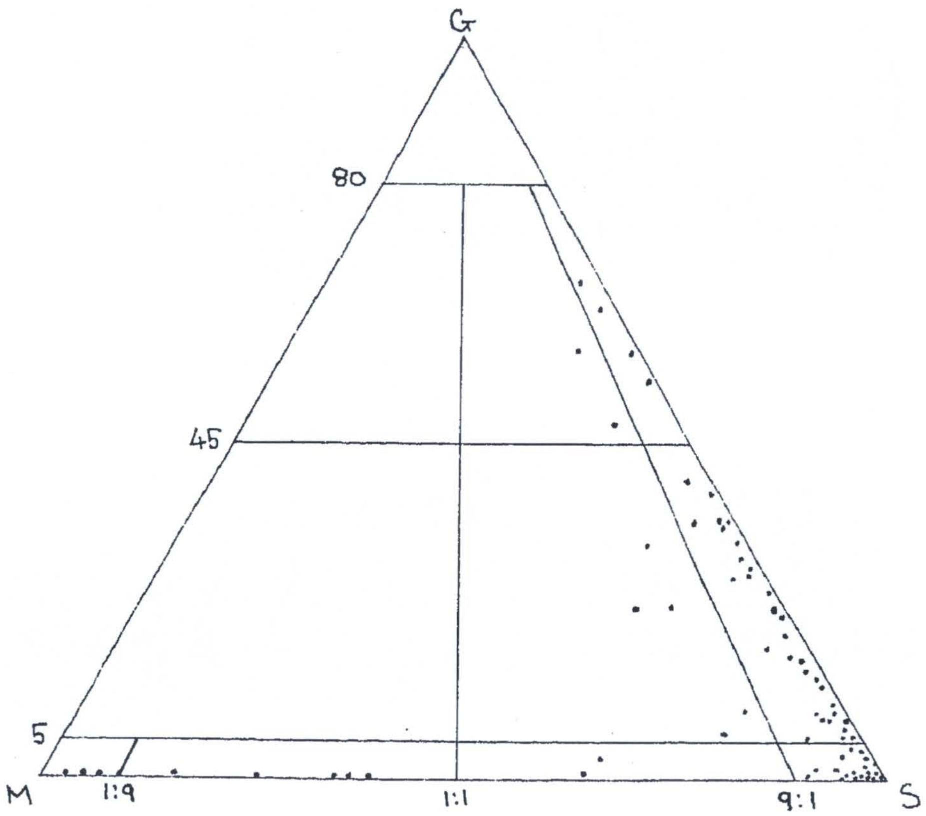

b

Fig. 4.15 (a) Textural divisions of gravelly sediments (After Folk, 1968).

(b) Textural plot of gravelly Hinuera sediments.

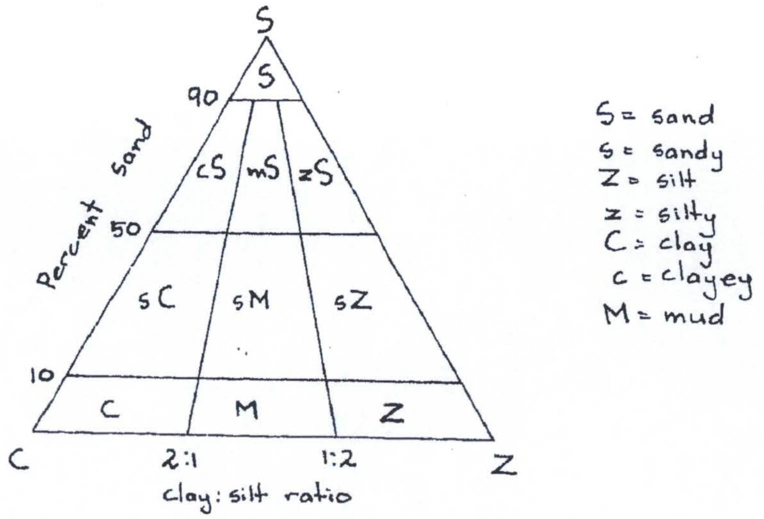

a

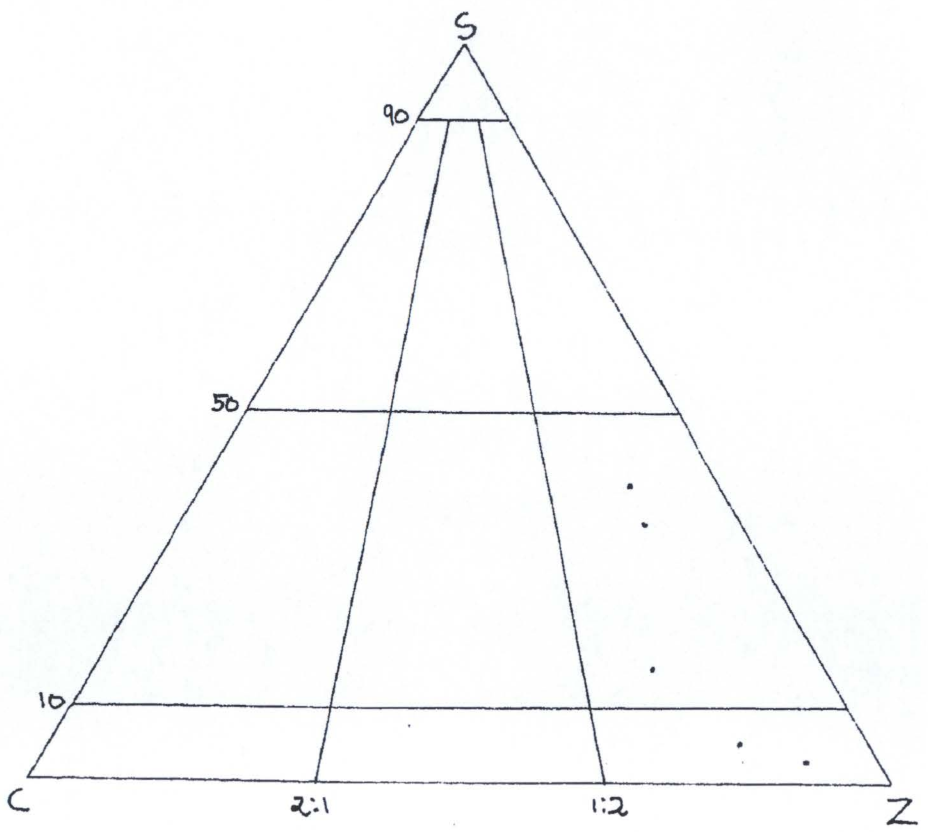

b

Fig. 4.16 (a) Textural divisions of muddy sediments (after Folk, 1968).

(b) Textural plot of muddy Hinuera sediments.

were washed free from significant clay sized material. Alternatively, the latter grain size may not have been supplied to the depositional agent.

4.4 C-M RELATIONS

Passega (1957, 1964) presented plots of samples from known environments using two grain size distribution parameters: C, the coarsest one percentile, and M, the median grain size. The value of C is representative of the minimum competence of the transporting agent, and M is a statistic characteristic of the total range of particle sizes undergoing transport by this agent. The value C=M constitutes a limit for the coordinates (C,M) and is approached for samples in which the coarse half of the sediment is well sorted, or when the first and fiftieth percentiles have nearly corresponding particle sizes. The relative displacement of plotted points from the line C=M, measured parallel to the M- axis and expressed in phi units is an index of sorting in the coarse half of the sediment samples.

Passega (1964) interpreted the composite CM pattern for river transported sediment in terms of transport modes. A tractive current (Passega, 1957) may transport its load in three ways (see section 4.1). In any river, all or none of these mechanisms may be present, or the contact load or the entire bed load may be absent. Transport by suspension only, or saltation and suspension is common under fluvial regines.

Passega (1964) established the relations between sediment textures and modes of transport for three environments of the Mississippi River (Fig. 4.17). The CM pattern for the Mississippi River is divisible into three segment (I, II and III of Fig. 4.17) which represent samples from the main channel, the

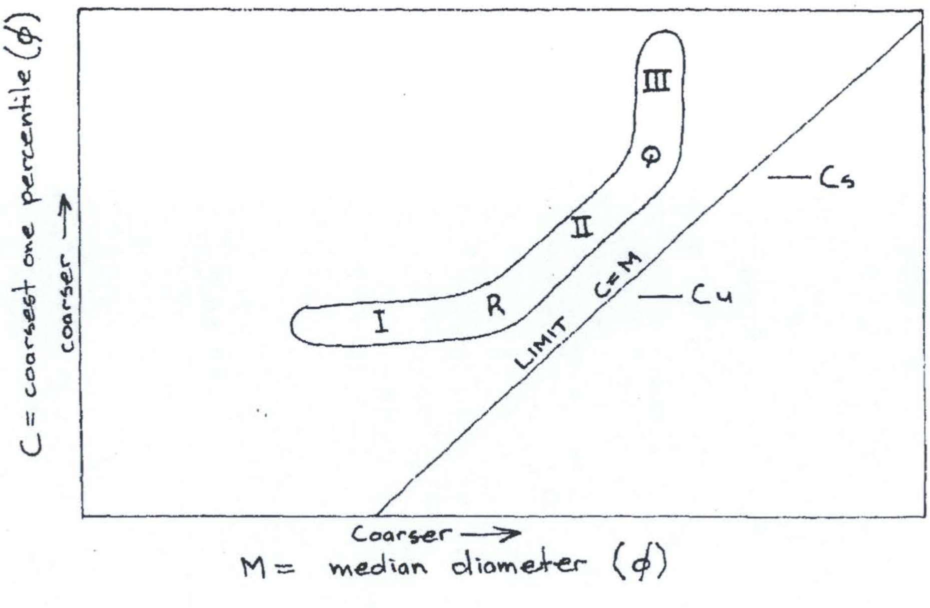

Fig. 4.17 Basic CM pattern for tractive currents (After Passega, 1957).

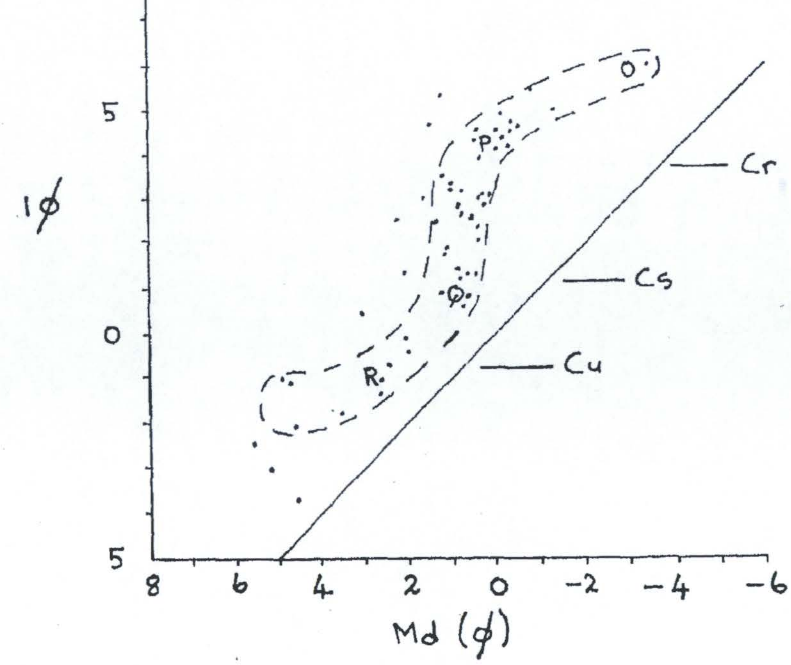

Fig. 4.18 CM pattern for sediments of the Hinuera Formation.

subaqueous bank and the protected backwater environments, with CM values corresponding to transport by traction, saltation and suspension respectively. The value of C at the point of inflection between segment II and III of the CM pattern (point Q of Fig. 4.17) is designated Cs and corresponds to the larges particle which can be transported in saltation. Similarly, the value Cu (point R of Fig. 4.17) is the coarsest particle which can be transported in suspension. Bull (1962) and Royse (1968) have successfully tested the application of the CM pattern in differentiating various depositional environments within alluvial deposits.

A CM pattern was constructed for the Hinuera Formation on arithmetic paper, plotting C, the first percentile, as a function of M, the median diameter, in Phi units (Fig. 4.18). The 71 sample shown represent the range of textures available and were taken from discrete sedimentatioh units (see section 4.1 pp. 60-61). The resulting pattern is similar to that established by Passega (1964) for tractive current deposits. There is, however, a considerable displacement of the inflection points of the CM pattern towards the coarse end of the first percentile (C) axis when compared to Passega's (1964) pattern, and the patterns established by Royse (1967, 1968).

The maximum diameter transported in suspension (Cu) is 0.9∅ or coarse sand. The maximum diameter transported in saltation (Cs) is -1.1∅ or granule size. Transport of such relatively coarse material in saltation and suspension necessitates considerable flow velocities. Knowing the grain size and mode of transport enables some indication of flow velocity to be obtained from grain size-flow velocity diagrams (Allen, 1965, after Sundborg, 1956). Plotting the above particle sizes in the appropriate fields of sediment transport indicates maximum flow velocities in the order of 80 to 100 cm/sec.

The curve OPQ in the bed load transported segment matches Passega's (1964) pattern, and is apparently the result of a gap in grain sizes between sediments that can be transported by saltation and these that are easiest to transport by rolling. Passega (1964) suggests that the value Cr, here -3.4ø or pebble size, corresponds to the optimum diameter at which grains are easiest to roll under the conditions of sedimentation, indicating a high energy environment.

The dispersion of points of the segments OPQR with values that are larger than normal for the value of M is probably due to rolling of individual particles on an earlier formed finer deposit, as suggested by Passega (1964). The dispersion of points of the segment RS with values of C that are smaller than normal for the value of M shows a lack of coarse particles in these samples, which are pumice silts, and indicates a lack of competence of the transporting agent.

4.5 RELATION OF TEXTURE TO SEDIMENTARY STRUCTURES

Incorporation of sedimentary structures into plots of textural parameters suggests that sedimentary structures are primarily dependant on grain size and to a lesser extent on sorting (Figs. 4.19 and 4.20), but are independant of skewness and kurtosis. Too few samples of Epsilon and Sigma cross-stratification and Type 2a horizontal stratification were analysed for any meaningful relations to be established.

Rho cross-stratification is preserved in moderately well to very poorly sorted sands, slightly gravelly muddy sands, slightly gravelly sands, gravelly muddy sands, and sandy

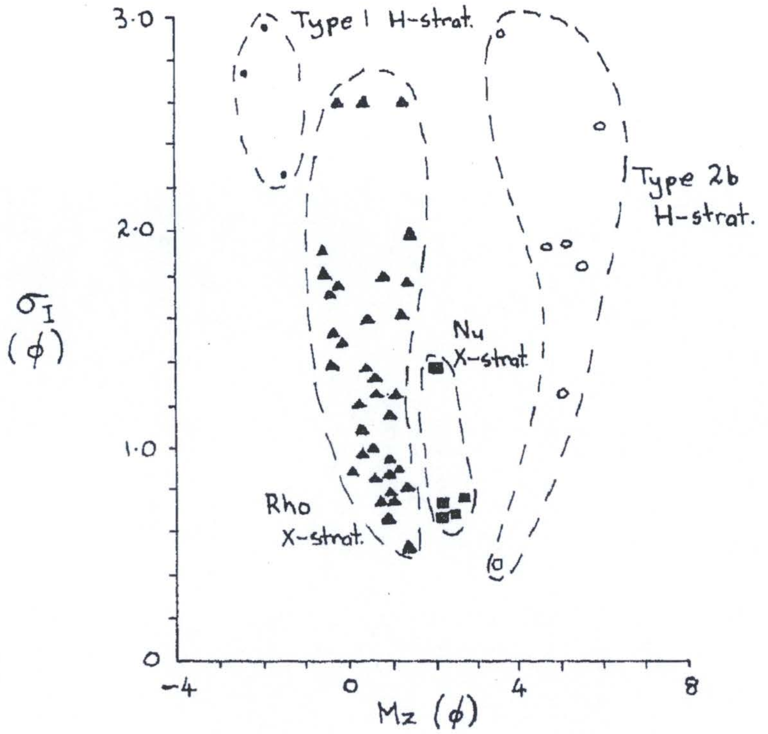

Fig. 4.19 Plot of sorting (σ_I) against mean grain size (Mz) showing the relation of sedimentary structures to these parameters.

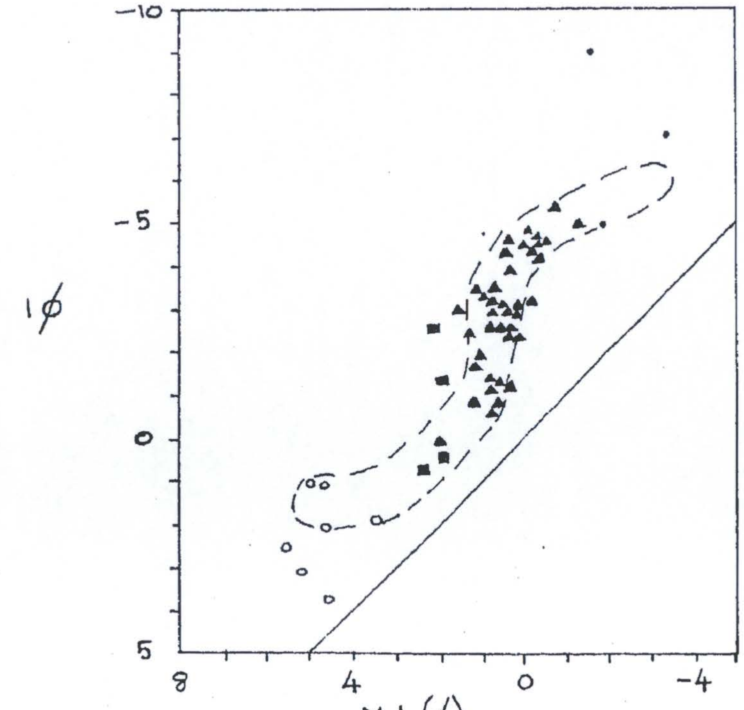

Fig. 4.20 The relation of sedimentary structures to the CM plot for Hinuera sediments. Symbols the same as for Fig. 4.19.

gravels, with a mean grain size of 1.5 to -0.75Ø (medium to very coarse sand).

Nu cross-stratification is preserved only in moderately well to poorly sorted sands with a mean grain size of 2.75 to 2.25Ø (fine sand).

Type 1 horizontal stratification is always in very poorly sorted sandy gravels with a mean grain size of -1.5Ø (granule) or greater. Rhyolitic rock fragments up to 10.3cm in diameter and pumice fragments up to 24.6cm in diameter were found in this structure at one locality (N66/164273).

Type 2b horizontal stratification is restricted to pumice silts and sandy silts with a mean grain size between 3.25 and 6.03Ø (very fine sand to medium silt). Samples were analysed from both fine and coarse laminae of this structure. Fine laminae (W164, W165) have a mean grain size between 4.75 and 5.5Ø (medium to coarse silt) and are poorly to very poorly sorted. Coarse laminae (W166) have a mean grain size around 3.5Ø (very fine sand) and are well sorted. This suggests a difference in the energy of the transporting agents which deposited the coarse and fine lamine of Type 2b horizontal stratification. The coarse laminae appear to have been deposited by low energy currents, and the fine lamine by settling out of suspension in a tranquil environment. Pumice fragments up to 3cm in diameter were found within the laminae of Type 2b horizontal stratification. These have obviously been transported by some mechanism other than that which deposited the laminae. It is apparent that these large pumice particles have floated into the depositional environment and have been deposited either after recession of the transporting medium or after becoming water-logged.

Incorporation of sedimentary structures into the CM plot shows a separation of structures dependant on mean grain size, and a less well defined separation dependant on the first percentile (Fig. 4.21). Comparison with Passega's (1957) tractive-current pattern indicates that Type 2b horizontal stratification is formed from suspension load sediments, Nu cross-stratification is formed from saltation load sediments, and Rho cross-stratification is formed largely from contact load sediments. Type 1 horizontal stratification appears to be very coarse contact load sediment deposited by currents with a high degree of competence.

An attempt was made to relate sedimentary structures to the shape of grain size distribution curves, as similar sedimentary structures should result from similar sedimentary processes. The curves of samples of each type of sedimentary structure were superimposed on each other, as were the curves of samples from each stratigraphic section. Apart from a separation of curves for Types 1 and 2b horizontal stratification, which is largely a function of mean grain size, sedimentary structures could not be characterised by the shape of their grain size distribution curves. However, curves from samples of the same structure from the same stratigraphic section often had similar shapes. Fig. 4.22 shows the grain size distribution curves for one stratigraphic section (F), and their relations to sedimentary structures.

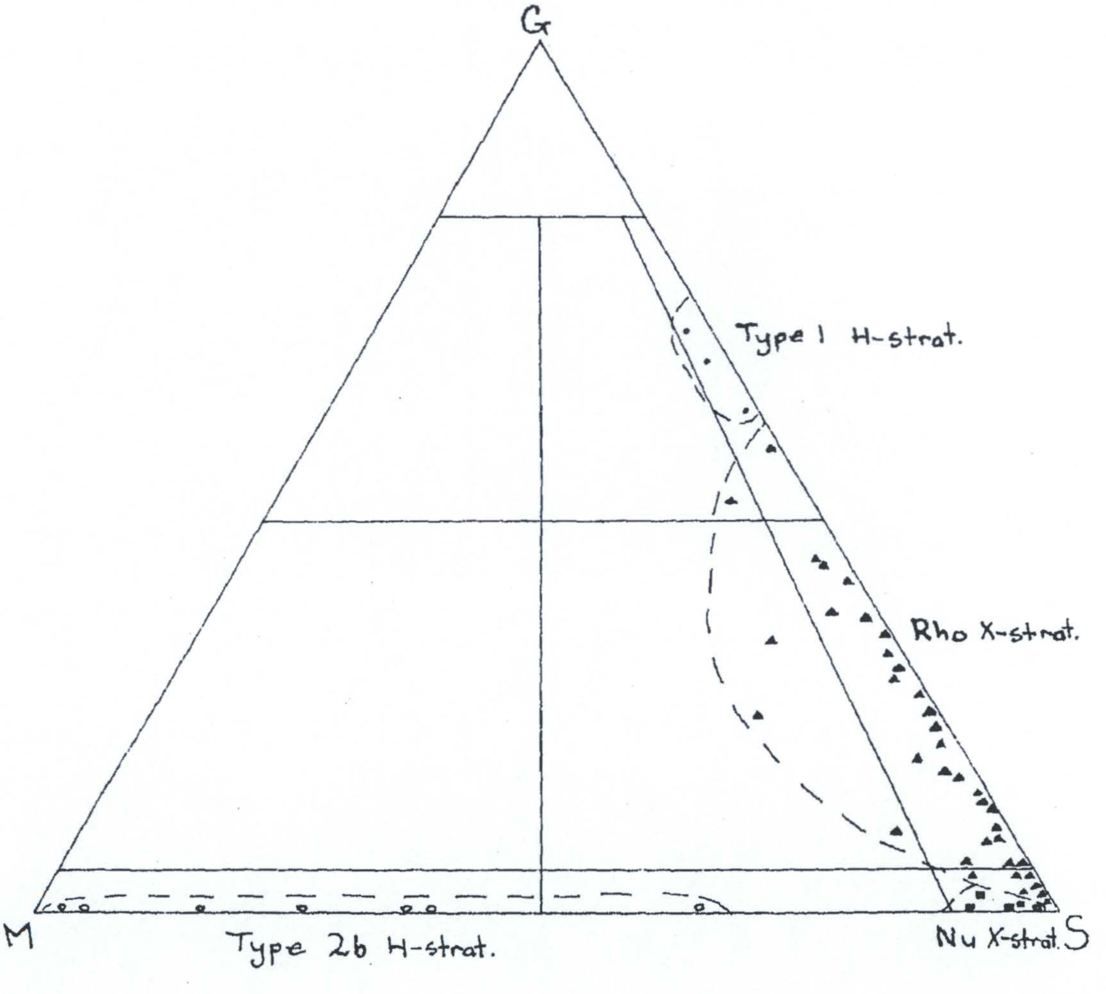

Fig. 4.20 Textural plot showing the relation of sedimentary structures to the ratio of sand-gravel-mud.

Fig. 4.22 Grain size distribution curves from one locality, section F, (N66/103275) showing the relation of the sedimentary structures present to the shape of the curves.

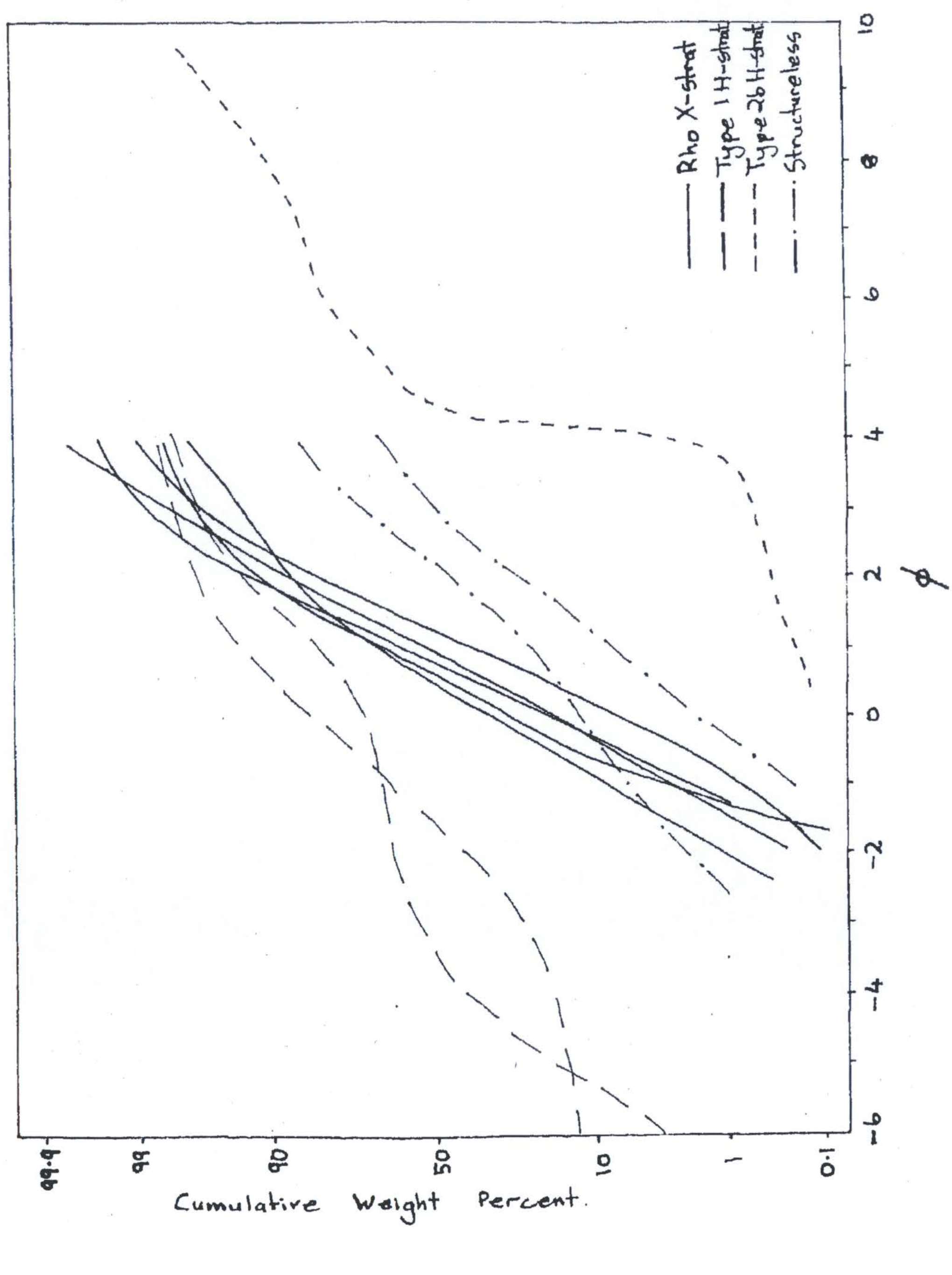

CHAPTER FIVE

I N T E R P R E T A T I O N

5.1 FACIES

The sediments of the Hinuera Formation are relatively uniform over wide areas. However, detailed stratigraphic sections show that textures, lithologies and sedimentary structures are variable, and that rapid changes of current direction took place during deposition of the sediments. Four major lithotypes are present: (1) cross-stratified, moderately to poorly sorted, rhyolitic and pumiceous gravelly and slightly gravelly quartz sand, (2) cross-stratified moderately to well sorted quartz sands, (3) laminated pumice silts, and (4) very poorly sorted, poorly stratified rhyolitic sandy gravels. Cross-stratification is restricted to the first two lithotypes and is of four types. Rho cross-stratification is dominant, and occurs mainly in pumiceous and rhyolitic moderately to poorly sorted gravelly sands. Nu cross-stratification is common and is preserved mainly in moderately well sorted quartz sands. Epsilon and Sigma cross-stratification are uncommon and occur in the same lithologies as Rho cross-stratification. Three distinct types of horizontal stratification are present. Type 2a is found in pumiceous and rhyolitic moderately to poorly sorted gravelly sands. The other two varieties are found in the two less important lithotypes; Type 1 in the very poorly sorted sandy gravels, and Type 2b in pumice silts.

A very wide range of grain sizes (large cobbles to clay) was supplied to the river system which deposited the Hinuera Formation, although there is a notable paucity of clay sized material. Textural evidence indicates deposition of the first lithotype under rapidly fluctuating and highly variable energy conditions by currents of generally high velocity and with a high turbulent energy. The very poorly sorted Type 1 horizontally stratified sandy gravels were deposited by currents of even greater competence, and the Type 2b horizontally stratified silts deposited in a much lower energy environment. The relation of sedimentary structures to the CM plot shows that Rho cross-stratification is deposited mainly from contact load sediments. Epsilon cross-stratification and Type 2a horizontal stratification occur in sediments having the same grain size range as Rho cross-stratified deposits and are probably also contact load sediments. Nu cross-stratification is formed from saltation load sediments. Type 1 horizontal stratification is formed from contact load sediment under very high energy conditions; Type 2b horizontal stratification is formed from suspension load sediments in a relatively tranquil environment.

Harms and Fahnestock (1965) related bed forms and the resulting forms of stratification in the deposits of the Rio Grande to flow regime. Large scale trough cross-stratification (Rho cross-stratification) forms by dune migration in the upper part of the lower flow regine. Small scale trough cross-stratification (Nu cross-stratification) forms by ripple migration in the lower part of the lower flow regine. Tabular cross-stratification (Epsilon cross-stratification) is formed at point bar margins or by bar migration in shallow channels in the upper or lower flow regine. Horizontal stratification (Type 2a horizontal stratification) is the product of plane bed transport in the lower part of the upper flow regime.

On the converging lines of lithological, structural, and textural evidence of the previous three chapters, six facies, related to flow regime, are erected for the Hinuera Formation.

<u>Facies A1.</u> Rho cross-stratified, moderately to poorly sorted rhyolitic and pumiceous gravelly and slightly gravelly quartz sands, formed in the upper part of the lower flow regime. This facies constitutes the bulk of the Hinuera Formation.

<u>Facies A2.</u> Epsilon cross-stratified gravelly sands showing the same textures and lithologies are facies A1, formed in the upper or lower flow regimes.

<u>Facies B.</u> Nu cross-stratified, moderately to well sorted quartz sands, formed in the lower part of the lower flow regime.

<u>Facies C1.</u> Type 1 horizontally stratified, very poorly sorted rhyolitic sandy gravels, formed in the upper flow regime.

<u>Facies C2.</u> Type 2a horizontally stratified, moderately to poorly sorted gravelly sands, formed in the upper flow regime.

<u>Facies D.</u> Type 2b horizontally stratified pumice silts formed mainly by deposition of suspension load from low energy currents, and so is not related to the flow regime concept involving transport of bed load material.

In the following section an attempt is made to incorporate the six facies into a paleoenvironmental model of the Hinuera Formation.

5.2 <u>PALEOENVIRONMENT</u>

The geomorphological form of the Hinuera Formation in the Hamilton Basin is that of a very low angle (less than 0.1°) alluvial fan, its apex with the Maungatautiri Gorge forming the apex, and its toe abutting against the ranges of Mesozoic rocks to the north and northwest, through which the Waikato River now flows via the Taupiri Gorge. Sediments eroded from a hinterland of dominantly rhyolitic provenance were transported in a channelled river to the Hamilton Basin, where the river was forced to deposit its load because of the sudden decrease in slope. Continued sediment supply formed a large aggradational fan. The Hinuera Formation in the Hauraki Lowland has a broadly similar fan shape, with the Hinuera valley forming the apex. The Hinuera fan is unusual in two aspects. The stratigraphic sections in the restricted area of this study show no decrease in mean grain size from the apex towards the toe of the fan, and calculations from topographical contours on the fan (Schofield, 1965) show that the slope near the apex is about 0°06', and less than 0°03' on the main body of the fan. Slopes of this order are more characteristic of flood plains than alluvial fans (Blissenbach, 1954).

Deposition of the Hinuera Formation between 10 to 12,000 and 20,000 years B.P. (Schofield, 1965) occurred during a cold period corresponding to the Otiran Glaciation. Aggradational processes forming the Hinuera fan were under three possible controls at this time: climate, volcanism, and base level changes. The cold climate probably increased the extent of the snowline in the North Island (Willet, 1950), but the effect of the lowered snowline on the area of vegetation is not known. However, the climate and the time was both cold and wet, giving at least a greater potential erosive capacity than during interglacial times. Perhaps the most important control on the deposition of the Hinuera Formation was the influence of volcanic activity. Deposition was contemporaneous with a period of intense volcanic activity in the Central Volcanic Region (Grindley, 1960) which had two major effects. The first was a great increase in the supply of dominantly rhyolitic material to rivers draining the region. The second was the destruction of large areas of vegetation, which combined with the prevailing wet climate, lead to accelerated erosion and the supply of even greater amounts of sediment to local river systems. Base level control of sedimentation was probably only local. Ultimate base level (sea level), was low during the time of deposition, and affected sedimentation north of the Taupiri Gorge. However, sedimentation within the Hamilton Basin was probably under the control of local base level determined by the Taupiri Gorge, and deposition of the Hinuera Formation was under continental controls only, independant of the effects of glacio-eustatic sea level changes.

Deposition of the Hinuera Formation ceased when climatic warming, coincident with a lowering of volcanic activity in the Central Volcanic Region, resulted in less erosion and a drastic reduction in the amount of sediment supplied to the local river systems. As a consequence, the ancient Waikato River had greater erosional competence, and was able to entrench itself in its own deposits.

The fan-like form, and the lithologies, textures, and sedimentary structures of the sediments of the Hinuera Formation, indicate deposition in a braided river system. Williams and Rust (1969) described very similar textures and sedimentary structures from the deposits of the braided Donjek River, Yukon, Canada. There is a striking similarity in the grain size distribution curves, the curves from the Donjek River sediments showing the same range of straight line segment combinations and truncation points as those for sediments of the Hinuera Formation. The major lithotypes of the Donjek River sediments correspond to those described from the Hinuera Formation. and there are similarities in the facies relationships of the two groups of sediments. Large and small scale trough cross-stratification (Rho and Nu cross-stratification respectively) are reported as being common, and the lithological heterogeneity which characterises Rho cross-stratification in the Hinuera Formation is also described from the equivalent structure in the Donjek River sediments.

Doeglas (1962) described the sedimentary structures of two braided rivers in France, the Durance and the Ardeche. Festoon cross bedding (Rho cross-stratification) is again the most common structure, and laminated silts and stratified gravels are also described. An important feature described by Doeglas from braided rivers is low, natural levees of coarse sediments (cobbles and pebbles), built up by primary channels. Doeglas summarised characteristic sedimentary structures and textures of braided rivers, which correspond very closely to those of the Hinuera Formation.

A range of sedimentary structures similar to those of the Hinuera Formation is described from the Rio Grande by Harms and Fahneshock (1965). Large and small scale trough cross-stratification (Rho and Nu cross-stratification respectively) are again the most common sedimentary structures. Parallel stratified beds (Type 2b horizontal stratification) deposited from suspension are also reported.

Further evidence for the deposition of Hinuera Formation by a braided river is the similarity of the CM plot to a pattern described by Bull (1962) for braided stream deposits of alluvial fans. However, Bull's pattern does not contain the suspension deposits found in the Hinuera Formation.

In the above studies of the deposits of braided rivers, the authors were able to relate sedimentary structures, textures and lithologies to bed forms and stream morphology. The paleoenvironmental interpretation of ancient sediments can only be based on the sedimentological record preserved in the deposits, and this then compared to studies of present-day environments. Because of the close similarity of the sedimentary structures, lithclogies and textures of the sediments in this study to the braided river deposits described in the literature, a physiographic model of the Hinuera Formation can be erected with some degree of confidence.

Bars are the most important morphological features of braided rivers (Doeglas, 1962; Allen, 1965; Harms and Fahneshack, 1965; Williams and Rust, 1969; Smith, 1971; and others). There are three types of bars; longditudinal, transverse, and point bars. Point bars are uncommon in braided rivers (Williams and Rust, 1969). Longditudinal bars are common in streams with gravel and sandy gravel beds, while transverse bars are typical of braided streams with well sorted sandy beds (Smith, 1971). The sedimentary structures and the lithologies and textures of the Hinuera Formation may be explained by the variable activities of these bars dependant on flow regime as related to stream discharge, and a physiographic model of the Hinuera Formation is suggested on this basis.

Normal discharge during the deposition of the Hinuera Formation was probably relatively high, largely as a result of the prevailing wet climate. Whether or not a river is meandering or braided is governed mainly by the relation between slope and discharge, and the very low angle on the Hinuera surface implies that the braided river that deposited the formation had a very high discharge, although it is likely that the initial slope of the fan was greater than present, perhaps up to 5°. A high normal discharge is a possible explanation for the high turbulent energy indicated by the textural characteristics of the Hinuera Formation.

On the basis of the above, the six facies described in the previous section are incorporated into a suggested physiographic model of the Hinuera Formation. Facies A1, which forms the bulk of the Formation, was deposited either by the migration of dunes on longditudinal bars or by the migration of longditudinal bar avalanche face topography, or a combination of both, during normal discharge. Facies A2 formed from longditudinal bar migration in narrow, shallow channels under the same conditions. Facies C1 was formed during periods of high discharge by movement of cobbles and pebbles down avalanche faces of longditudinal bars into adjacent shallow channels. Low, linear, mid-channel mounds were constructed, which become exposed as the flood waters receded. These correspond to the natural levees of braided streams described by Doeglas (1962). Facies C2 formed by plane bed movement on the surface of longditudinal bars at high discharges. During flood periods, the river covered its floodplain, and on falling discharge, sandy silts were deposited as a thin veneer in areas beyond the main channels. On returning to normal discharge, suspension laden water was trapped in abandoned channels and other topographic lows, and silts were deposited from suspension in backswamp-like environment. Overbank deposition resulted in the formation of facies D. At low discharge periods, only sand was transported by the stream, and transverse bars were formed. The migration of small scale ripples over these bars formed facies E.

This physiographic model is summarised in Fig. 5.1 and is in part illustrated in Fig. 5.2. The model supports the conclusions of Wolman and Leopold (1957) on the relation of vertical to horizontal acretion and the construction of flood plains. The bulk of the Hinuera Formation is formed from in-channel sedimentation, and overbank deposits (facies D) constitute only a minor proportion of its sediments. This is largely the result of reworking of stream deposits by the migratory action of channels across the entire width of the floodplain. Overbank deposits of appreciable thickness are found only at the top of stratigraphic sections; elsewhere they have been completely eroded or reduced to thin intercalations.

The present micro-topography of the Hinuera surface, consisting of low amplitude ridges and swales is also explained by the above physiographic model. The ridges are low, linear, mid-channel mounds constructed during flood discharge (facies D1). Overbank **silts** and occasional peats accumulated in abandoned channels adjacent to these channel bars. This relationship is illustrated in Fig. 5.2.

The sedimentological characteristics of the six facies of the Hinuera Formation are summarised in Table 5.1

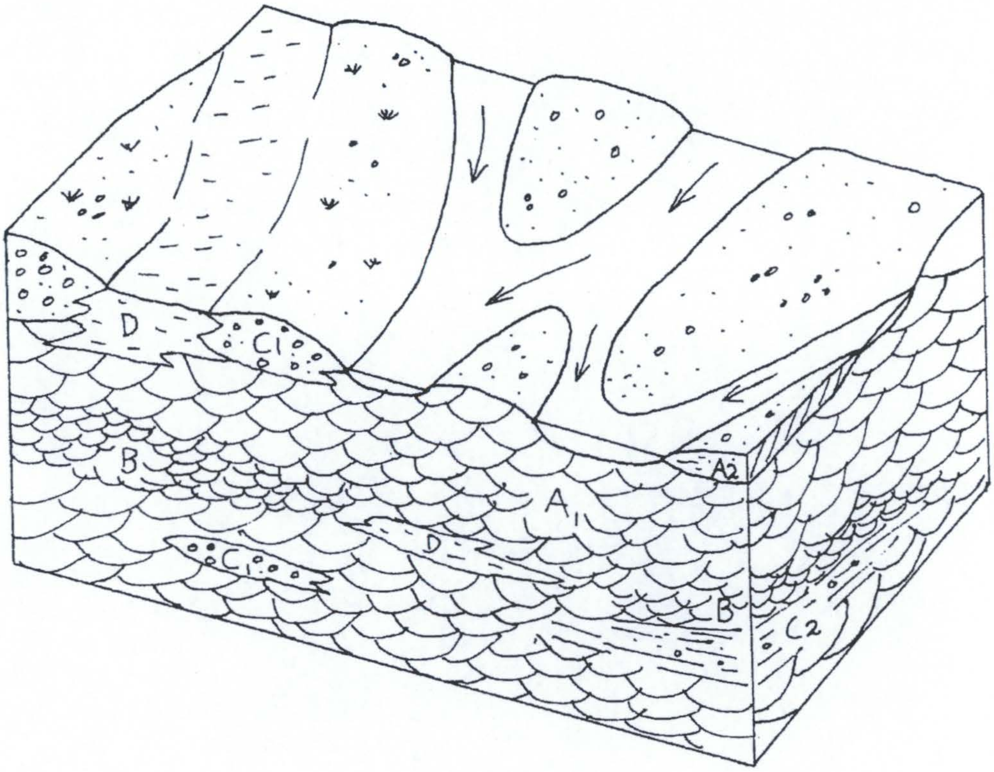

Fig. 5.1 Physiographic model showing facies relationships in the Hinuera Formation.

Fig. 5.2 Relationships of three facies of the Hinuera Formation, showing ridge and swale topography. Linear channel bars of rhyolitic sandy gravels (Facies C1) form low amplitude ridges. Pumice silts (facies D) accumulate in swales formed by abandoned channels. Rho cross-stratified rhyolitic and pumiceous gravelly sands (facies A1) underlie both. Grid Ref. N56/795525. Hammer near centre of photograph is 33 cm long.

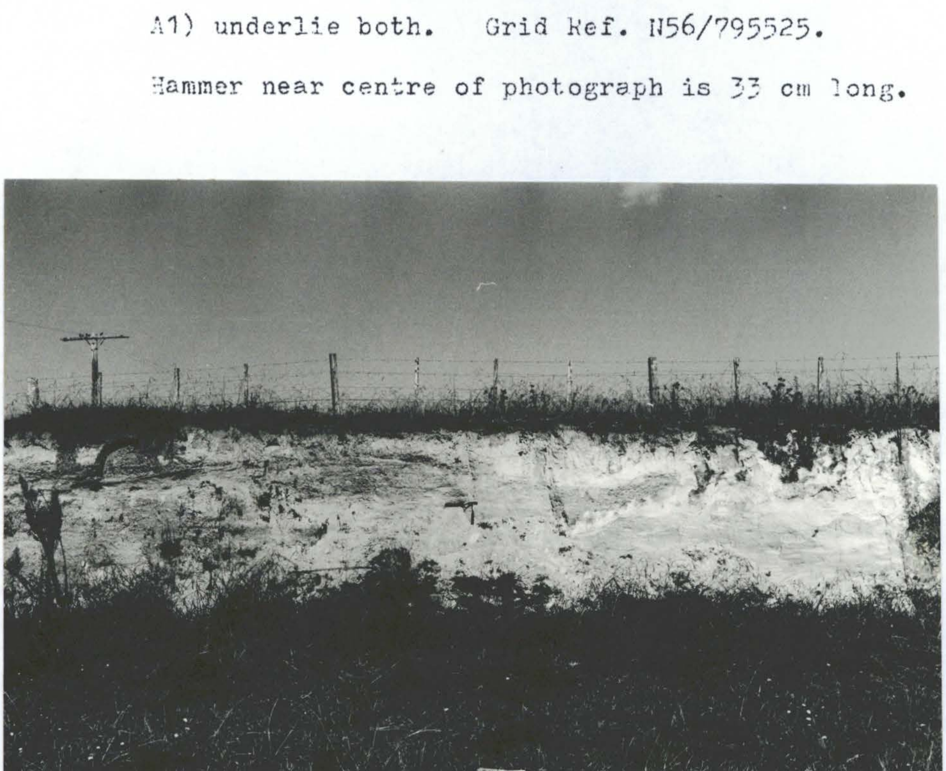

Facies	Dominant Lithology (Field Determination)	Dominant Textural Group	Sorting	Sedimentary Structure	Flow Regime	Depositional Environment
A1	rhyolite and pumice	gravelly sand	moderate to poor	Rho cross-stratif-ication	upper lower	
A2	rhyolite and pumice	gravelly sand	moderate to poor	Epsilon cross-stratif-ication	upper or lower	
B	quartz	sand	moderate to good	Nu cross-stratif-ication	lower lower	Channel Deposits
C1	rhyolite	sandy gravelly	very poor	Type 1 horizon-tal stratifica-tion	upper	
C2	rhyolite and pumice	gravelly sand	moderate to poor	Type 2a horizon-tal stratifica-tion	upper	
D	pumice	silt	poor to good	Type 2b horizon-tal stratifica-tion	deposition from sus-pension	Overbank deposits

Table 5.1 Sedimentological characteristics of the six facies of the Hinuera Formation.

REFERENCES

Allen, J.R.L., 1963a: The classification of cross-stratified units with notes on their origin. <u>Sed.</u> 12(12): 93-114.

------ 1963b: Asymmetrical ripple marks and the origin of water laid cosets of cross-strata. <u>Lppol. Manchr. Geol. Jl.</u>: 3(2): 187-236.

------ 1965: A review of the origin and characteristics of recent alluvial sediments. Sed. V.5: 89-191. Special Issue.

Awasthi, A.K., 1970: Skewness as an environmental indicator in the Solani River system, Roorkee, India. <u>Sed. Geol.</u>: 4(2): 177-183.

Bagnold, R.A., 1954: Experiments on a gravity-free dispersion of large solid spheres in a Newtonian fluid under shear. <u>Roy. Soc. lond. Proc.</u>: Sher. A, V. 255: 49-63.

Blissonbach, E., 1954: Geology of alluvial fans in semiarid regions. <u>Geol. Soc. Am. Bull.</u>: V.65: 175-190.

Brush, L.M., 1965: Sediment sorting in alluvial channels. <u>in</u> Middleton, G.V. (ed); Primary Sedimentary Structures and their Hydrodynamic Interpretation: S.E.P.M. Spec. Pub. 12.

Bull, W.B., 1962: Relation of textural (CM) patterns to depositional environments of alluvial fan deposits. <u>J. Sed. Pet.</u>: 32(2): 211-216.

Cussen, L., 1889: Notes on the Waikato River Basins. <u>Trans. N.Z. Inst.</u>: 21: 406-167.

------ 1894: Notes on the Piako and Waikato River Basins. <u>Trans. N.Z. Inst.</u>: 26: 398-407.

Doeglas, D.J., 1962: The structure of sedimentary deposits of braided rivers. <u>Sed.</u>: 1(3): 167-190.

Dyer, K.R., 1970: Grain size parameters for sandy gravels. J. Sed. Pet.: 40(2): 616-620.

Folk, R.L., 1966: A review of grain size parameters. Sed.: V.6: 73-93.

----- 1968: Petrology of Sedimentary Rocks. 170pp. Hempills, Austin, Texas.

Folk, R.L., Andrews, P.B., and Lewis, D.W., 1970: Detrital sedimentary rock classification and nomenclature for use in N.Z. N.Z. Jl. Geol. Geophys.: 13(4): 937-968.

Folk, R.L., and Ward. W.C., 1957: Brazos River Bar: a study in the significance of grain size parameters. J. Sed. Pet.: 27(1): 3-26.

Friedman, G.M., 1961: Distinction between dune, beach, and river sands from their textural characteristics. J. Sed. Pet.: 31(4): 514-529.

Fuller, A.O., 1961: Size characteristics of shallow marine sands from Cape of Good Hope, South Africa, J. Sed. Pet.: 31: 256-261.

Graff-Petersen, P., 1967: Intraformational deformations and pore-water hydrodynamics. Abstr. 7th Int. Congr. Sediment., England.

Grindley, G.W., 1960: Sheet 8 - Taupo (1st ed.). "Geological Map of N.Z., 1:250,000." N.Z.D.S.I.R.

Harms, J.C., and Fahnestock, R.K., 1965: Stratification, bed forms, and flow phenomena (with an example from the Rio Grande) in Middleton, G.V. (ed): Primary Sedimentary Structures and their Hydrodynamic Interpretation: S.E.P.M. Spec. Pub. 12.

Healy, J., 1946: Geology of the Karapiro District, Cambridge. N.Z. Jl. Sci. Tech.: B27: 199-217.

Healy, J., Schofield, J.C., and Thompson, B.N., Sheet 5 - Rotorua (1st ed.). "Geological Map of N.Z., 1:250,000." N.Z.D.S.I.R.

Henderson, J., 1913: The geology of the Aroha Subdivision, Hauraki, Auckland. N.Z. Geol. Surv. Bull. 16.

Henderson, J., and Grange, L.I., 1926: The geology of the Huntly-Kawhia Subdivision, Pirongia and Hauraki Divisions. N.Z. Geol. Surv. Bull. 28.

Hochstetter, F. von., 1867: New Zealand.

Jopling, A.V., 1964: Interpreting the concept of the sedimentation unit. J. Sed. Pet.: 34(1): 165-172.

----- 1965: Laboratory study of the distribution of grain sizes in cross-bedded deposits. in Middleton, G.V. (ed.): Primary Sedimentary Structures and their Hydrodynamic Interpretation: S.E.P.M. Spec. Pub. 12.

Kear, D., 1960: Sheet 4 - Hamilton (1st ed.) "Geological Map of N.Z., 1:250,000". N.Z.D.S.I.R.

Kear, D., and Schofield, J.C., 1964: Stratigraphic Summary, Nguawhahia. N.Z. Jl. Geol. Geophys.: 7(4): 892-893.

Kear, D., and Schofield, J.C., in press: Geology of the Nguawhahia Subdivision. N.Z. Geol. Surv. Bull.

Knight, S.H., 1929: The Fountain and Casper Formations of the Laramie Basin. Univ. Wyo. Pub. Sci., Geol.: V.1: 1-82.

McCraw, J.D., 1967: The surface features and soil pattern of the Hamilton Bason. Earth Sc. Jl.: 1(1): 59-74.

McKee, E.D., and Weir, G.W., 1953: Terminology for stratification and cross-stratification in sedimentary rocks. Bull. Geol. Soc. Am.: 64(4): 381-390.

Moss, A.J., 1962: The physical nature of common sandy and pebbly deposits. Part 1. Am. J. Sci.: V.260: 337-373.

----- 1963: The physical nature of common sandy and pebbly deposits. Part II. Am. J. Sci.: V.261: 297-343.

Oliver, T.I., 1969: Scarp initiation and retreat in an area of pumice lithology near Whakamaru. Unpublished thesis, University

Otto, G.H., 1938: The sedimentation unit and its use in field sampling. Jour. Geol.: V.46: 569-582.

Passega, R., 1957: Texture as characteristic of clastic deposition. B.A.A.P.G.: 41(9): 1952-1984.

----- 1964: Grain size representation by CM patterns as a geological tool. J. Sed. Pet.: 34(4): 830-847.

Pettijohn, F.J., 1957: Sedimentary Rocks. (2nd ed.) Harper and Row. 718pp.

Royse, C.F., 1968: Recognition of fluvial environments by particle-size characteristics. J. Sed. Pet.: 38(4): 1171-1178.

Schofield, J.C., 1965: The Hinuera Formation and associated Quaternary events. N.Z. Jl. Geol. Geophys.: 8(5): 772-791.

Schofield, J.C., 1967: Sheet 3 - Auckland (1st ed.) "Geological Map of N.Z., 1:250,000". N.Z.D.S.I.R.

Sevon, W.D., 1966: Distinction of N.Z. beach, dune, and river sands by their grain size characteristics. N.Z. Jl. Geol. Geophys.: 9(3): 212-223.

Smith, N.D., 1971: Transverse bars and braiding in the Lower Platte River, Nebraska. Geol. Soc. Am. Bull.: 82(12): 3407-3420.

Spencer, D.W., 1963: The interpretation of grain size distribution curves of clastic sediments. J. Sed. Pet.: 33(1): 180-190.

Tanner, W.F., 1964: Modification of sediment size distributions. J. Sed. Pet.: 34(1): 156-164.

Thompson, B.H., 1958: The geology of the Atiamuri dam site. N.Z. Jl. Geol. Geophys.: 1(2): 275-306.

Van der Lingen, G.J., 1969: The turbidite problem. N.Z. Jl. Geol. Geophys.: 12(1): 7-50.

Visher, G.S., 1965: Fluvial processes as interpreted from ancient and recent fluvial deposits. in Middleton, G.V. (ed.): Primary sedimentary structures and their hydrodynamic interpretation, S.E.P.M., Spec. pub. 12.

----- 1969: Grain size distributions and depositional processes. J. Sed. Pet.: 3a(3): 1074-1106.

Willett, R.W., 1950: The New Zealand Pleistocene snow line, climatic conditions, and suggested biological effects. N.Z. J. Sci. Tech.: B.32: 18-48.

Williams, E., 1963: Convolute folds and movement in water-logged granular sediments. in Carey, S.W. (convener): "Syntaphral Tectonics and Diagenisis. A Symposium." Geology Department, University of Tasmania, Hobart.

Williams, P.F., and Rust, B.R., 1969: The sedimentology of a braided river. J. Geol. Pet.: 39(2): 649-679.

Wolman, M.G., and Leopold, L.B., 1957: River flood plains: some observations on their formation. U.S.G.S. Prof. Papers: 282C: 87-107.

Appendix I

Sample No.	Mz	$\sigma_I(\phi)$	Sk_I	K_G	Grid. Ref.
W140	0.84	1.80	+0.49	0.94	N65/676427
W141	2.12	0.67	+0.24	1.11	"
W142	-0.43	1.71	-0.06	1.06	"
W143	0.95	1.13	+0.14	1.03	"
W144	1.22	1.25	+0.06	0.97	"
W145	0.35	0.29	+0.03	1.16	"
W146	2.77	0.75	+0.28	1.29	"
W147	1.28	1.39	-0.34	1.58	"
W148	-0.21	2.32	+0.60	1.03	"
W149	0.85	2.55	+0.29	1.06	"
W150	2.65	0.56	+0.20	1.32	"
W151	2.04	0.83	+0.08	1.16	"
W152	5.13	1.94	+0.30	1.10	"
W153	0.06	0.90	0.00	1.36	"
W154	0.25	1.11	-0.30	1.20	"
W155	0.50	1.05	-0.03	1.22	"
W156	2.43	0.68	+0.09	1.17	"
W157	0.38	1.62	-0.22	1.06	"
W158	1.16	1.63	+0.16	1.18	"
W159	1.39	2.03	+0.13	1.54	"
W160	-0.29	2.62	+0.29	1.04	"
W161	-0.27	1.77	+0.06	1.02	"
W162	1.94	1.36	+0.01	1.38	"
W163	6.03	2.49	+0.41	1.36	N56/795525
W164	4.74	1.94	+0.25	1.22	"
W165	5.63	1.85	+0.46	0.65	"
W166	3.41	0.44	+0.33	1.04	"
W167	2.16	0.74	+0.01	0.97	N65/812437

Appendix I (continued)

Sample No.	Mz	$\sigma_I(\phi)$	Sk_I	K_G	Grid. Ref.
W168	-0.10	1.92	-0.25	1.13	N65/812437
W169	-0.50	1.60	-0.12	0.80	"
W170	0.45	1.04	-0.26	1.38	"
W171	-1.15	1.84	+0.11	0.76	"
W172	1.00	0.58	-0.05	2.20	"
W173	-0.08	1.23	-0.04	0.81	"
W174	0.02	1.48	-0.32	1.06	"
W175	-0.14	1.41	-0.75	0.92	"
W176	1.21	0.74	-0.02	0.93	"
W177	-0.43	1.28	-0.04	1.09	"
W178	0.64	0.97	-0.25	1.30	"
W179	0.63	0.88	-0.13	1.18	"
W180	3.33	1.42	+0.15	1.00	N66/001337
W181	0.86	0.89	+0.06	1.25	"
W182	0.61	1.33	-0.23	1.14	"
W183	5.09	1.25	+0.77	1.45	N66/103275
W184	0.51	0.87	+0.11	0.69	"
W185	0.86	0.97	-0.02	1.12	"
W186	0.78	0.94	+0.06	1.36	"
W187	0.26	1.00	+0.36	1.11	"
W188	0.53	1.27	+0.19	1.28	"
W189	1.27	0.84	+0.05	1.03	"
W190	-2.45	2.75	+0.44	0.65	"
W191	-2.00	2.96	-0.33	1.67	"
W192	2.17	1.87	-0.03	1.33	"
W193	3.70	2.92	+0.37	1.35	"
W194	-0.59	1.83	-0.10	0.92	N66/164273
W195	-0.48	1.73	-0.30	0.89	"

Appendix I (continued)

Sample No.	Mz	$\sigma_I(\phi)$	Sk_I	K_G	Grid. Ref.
W196	0.80	0.68	+0.13	1.43	N66/164273
W197	0.22	1.21	-0.15	1.17	"
W198	0.37	2.62	+0.27	1.18	"
W199	0.91	0.91	-0.16	1.71	"
W200	-0.15	1.50	-0.27	0.92	"
W201	-0.63	1.93	-0.16	0.88	"
W202	-0.43	1.40	-0.31	1.16	"
W203	0.69	0.77	+0.20	1.32	"
W204	0.89	0.80	+0.29	1.21	"
W205	-0.40	1.54	-0.17	1.15	"
W206	-1.49	2.25	+0.26	0.64	N66/193336
W207	1.27	1.77	-0.28	0.96	"
W208	1.28	0.55	+0.15	1.23	"
W209	0.30	1.38	-0.02	1.05	"
W210	1.23	2.62	+0.22	0.94	"

Appendix II

Sample No.	Mud %	Sand %	Gravel %	Textural Class
W140	4.76	77.75	17.50	gS
W142	1.05	63.56	35.39	gS
W141	4.03	95.97	0	S
W143	1.49	94.17	4.34	(g)S
W144	3.28	93.33	3.39	(g)S
W145	1.90	82.36	15.74	gS
W146	8.83	91.17	0	S
W147	3.03	88.07	8.90	gS
W148	7.34	34.78	57.88	msG
W149	13.37	63.46	23.17	gmS
W150	4.63	95.37	0	S
W151	4.30	95.70	0	S
W152	64.83	35.17	0	sM
W153	1.33	89.83	8.84	gS
W154	0.85	85.93	13.22	gS
W155	1.77	89.65	8.57	gS
W156	3.42	96.51	0.07	(g)S
W157	1.36	79.36	19.28	gS
W158	5.74	88.46	5.80	gS
W159	11.30	79.67	9.03	gmS
W160	7.76	44.97	47.27	msG
W161	4.41	60.94	34.75	gS
W162	7.14	91.29	1.57	(g)S
W163	84.44	15.56	0	sM
W164	61.22	38.78	0	sM
W165	95.17	4.83	0	M
W166	4.76	95.24	0	S
W167	3.89	95.95	0.16	(g)S
W168	3.23	69.23	27.54	gS

Appendix II (continued)

Sample No.	Mud %	Sand %	Gravel %	Textural Class
W169	0.71	60.66	38.64	gS
W170	0.58	89.07	10.03	gS
W171	0.80	45.87	53.88	sG
W172	0.15	99.15	0.70	(g)S
W173	0.22	74.48	25.30	gS
W174	0.84	76.41	22.75	gS
W175	0.62	67.21	32.17	gS
W176	0	99.58	0.42	(g)S
W177	0	72.44	27.56	gS
W178	0.21	92.59	7.20	gS
W179	0.55	93.67	5.78	gS
W180	34.84	64.53	0.63	(g)mS
W181	0.31	95.66	4.03	(g)S
W182	0.60	86.01	13.39	gS
W183	97.70	2.30	0	M
W184	1.57	94.35	4.08	(g)S
W185	0.20	96.73	3.07	(g)S
W186	0.40	97.58	2.02	(g)S
W187	0.38	87.74	11.88	gS
W188	2.89	89.06	8.05	gS
W189	1.07	98.11	0.82	(g)S
W190	2.14	30.77	67.09	sG
W191	1.59	34.78	63.62	sG
W192	15.33	78.47	6.20	gmS
W193	34.20	65.54	0.26	(g)sM
W194	2.61	57.34	40.06	gS
W195	1.41	64.57	34.02	gS
W196	1.61	96.81	1.58	(g)S

Appendix II (continued)

Sample No.	Mud %	Sand %	Gravel %	Textural Class
W197	1.28	83.66	15.07	gS
W198	11.95	56.81	31.24	gmS
W199	1.55	92.88	5.57	gS
W200	1.60	70.59	27.82	gS
W201	2.49	56.68	40.83	gS
W202	1.22	70.93	27.84	gS
W203	1.36	96.97	1.67	(g)S
W204	2.44	96.86	0.72	(g)S
W205	1.74	68.69	29.58	gS
W206	0.93	41.51	57.56	sG
W207	0.94	77.54	22.47	gS
W208	2.30	97.50	0.20	(g)S
W209	2.03	81.33	16.65	gS
W210	17.50	59.38	23.12	gmS